Using Radionuclides ^{7}Be, ^{210}Pb and ^{137}Cs to Estimate Soil Erosion in the Khlong U-Tapao Catchment and Accumulated Sedimentation Rate in the Outer Songkhla Lagoon

Santi Raksawong

A Thesis Submitted in Fulfillment of the Requirements for the Degree of Doctor of Philosophy in Physics

Prince of Songkla University

2017

Thesis Title	Using radionuclides ^{7}Be, ^{210}Pb and ^{137}Cs to estimate soil erosion in the Khlong U-Tapao catchment and accumulated sedimentation rate in the outer Songkhla lagoon
Author	Mr. Santi Raksawong
Major Program	Physics

Major Supervisor

…….

(Assoc. Prof. Dr. Tripob Bhongsuwan)

Examining Committee:

……..…..Chairperson
(Assoc. Prof. Dr. Thawat Chittrakarn)

…….Committee
(Assoc. Prof. Dr. Tripob Bhongsuwan)

…….Committee
(Asst. Prof. Dr. Prasong Kessaratikoon)

…….Committee
(Dr. Kamhaeng Wattanasen)

The Graduate School, Prince of Songkla University, has approved this thesis as partial fulfillment of the requirements for the Degree of Doctor of Philosophy in Physics.

……..…….
(Assoc. Prof. Dr. Teerapol Srichana)
Dean of Graduate School

This is to certify that the work here submitted is the result of the candidate's own investigations. Due acknowledgement has been made of any assistance received.

……Signature
(Assoc. Prof. Dr. Tripob Bhongsuwan)
Major Supervisor

……Signature
(Mr. Santi Raksawong)
Candidate

I hereby certify that this work has not been accepted in substance for any degree, and is not being currently submitted in candidature for any degree.

……Signature

(Mr. Santi Raksawong)

Candidate

ชื่อวิทยานิพนธ์	การใช้ประโยชน์จากนิวไคลด์กัมมันตรังสี เบริลเลี่ยม-7 ตะกั่ว-210 และซีเซียม-137 เพื่อประเมินการชะล้างหน้าดินในพื้นที่ลุ่มน้ำคลองอู่ตะเภาและอัตราการสะสมตัวของตะกอนในทะเลสาบสงขลาตอนนอก
ผู้เขียน	นายสันติ รักษาวงศ์
สาขาวิชา	ฟิสิกส์
ปีการศึกษา	2559

บทคัดย่อ

ปัญหามลภาวะในบริเวณลุ่มน้ำและทะเลสาบสงขลามีสภาพเสื่อมโทรมลงอย่างมาก อันเป็นผลมาจากปัจจัยต่างๆ ไม่ว่าจะเป็นมาจากการชะล้างของหน้าดินที่เป็นผลมาจากเปลี่ยนสภาพการใช้ประโยชน์ที่ดินในพื้นที่ลุ่มน้ำ ปัญหาคุณภาพน้ำ ปัญหาสารพิษหรือธาตุอาหารในดินปนเปื้อนในน้ำ และปัญหาการตื้นเขินของทะเลสาบ จากกรณีปัญหาดังกล่าวนี้การศึกษาปัญหาการชะล้างของหน้าดินในเขตลุ่มน้ำ อัตราการสะสมตัวของตะกอนหรือลักษณะทางพลวัตในทะเลสาบสงขลาจะทำให้เข้าใจปัญหาและนำข้อมูลที่ศึกษานี้มาบริหารจัดการในเรื่องการใช้ประโยชน์ที่ดินอย่างยั่งยืนและปกป้องรักษาระบบนิเวศในทะเลสาบสงขลาอีกทางหนึ่งได้ ดังนั้นการศึกษาวิจัยในครั้งนี้จึงประกอบด้วยการศึกษาฟลักซ์ของเบริลเลี่ยม-7 ซึ่งวัดได้จาก 3 สถานีในพื้นที่ลุ่มน้ำคลองอู่ตะเภา จังหวัดสงขลา พบว่าฟลักซ์ของเบริลเลี่ยม-7 ขึ้นอยู่กับอิทธิพลของฤดูกาลและการชะล้างรวมทั้งการตกร่วมกันของ เบริลเลี่ยม-7 กับน้ำฝน และความสัมพันธ์ระหว่างฟลักซ์ของเบริลเลี่ยม-7 กับปริมาณน้ำฝนรายวัน รายเดือนมีความสัมพันธ์กันอย่างมีนัยสำคัญ รวมทั้งเมื่อแยกพิจารณาเป็นฤดูกาล เช่น ฤดูมรสุมตะวันออกเฉียงเหนือ ตะวันตกเฉียงใต้ และในฤดูร้อน พบว่าอิทธิพลการตกของเบริลเลี่ยม-7 กับปริมาณน้ำฝนในพื้นที่ศึกษามีความสัมพันธ์กัน นอกจากนั้นยังศึกษาค่าอ้างอิงของการสะสมตัวคงเหลือและความลึกเชิงมวลของเบริลเลี่ยม-7 ในดินเพื่อนำไปคำนวณการชะล้างของหน้าดิน ศึกษาการกระจายตัวและความลึกมากที่สุดของเบริลเลี่ยม-7 ในตะกอนท้องน้ำทะเลสาบสงขลาเพื่อช่วยประเมินการสะสมตัวของตะกอนในบริเวณต่างๆ และยัง ศึกษากระบวนการแลกเปลี่ยนอนุภาคที่เกิดจากการรบกวนของสิ่งมีชีวิตหน้าดินในทะเลสาบ พบว่าอัตราการรบกวนของตะกอนโดยการวิเคราะห์จากค่ากัมมันตภาพรังสีของตะกั่ว-210 และเบริลเลี่ยม-7 ตามความลึก รวมทั้งการกระจายตัวเชิงพื้นที่ของอัตราการรบกวน และสุดท้ายของการวิจัยนี้คือศึกษาอัตราการทับถมของตะกอนท้องน้ำ โดยใช้การวิเคราะห์จากค่ากัมมันตภาพรังสีของตะกั่ว-210 และซีเซียม-137 โดยเลือกใช้วิธีการวัดตะกั่ว-210 ซึ่งประกอบด้วย 2 วิธี คือวิธีที่เรียกว่าความเข้มข้น

เริ่มต้นคงที่ (CIC) และวิธีที่เรียกว่าอัตราการเติมของตะกั่ว-210 คงที่ (CRS) และยังใช้ วิธีการวัดซีเซียม-137 มาตรวจสอบความถูกต้องของวิธีการวัดตะกั่ว-210

Thesis Title	Applied radionuclides ^{7}Be, ^{210}Pb and ^{137}Cs to estimate soil erosion in the Khlong U-Tapao catchment and accumulated sedimentation rate in the Outer Songkhla Lagoon
Author	Mr. Santi Raksawong
Major Program	Physics
Academic Year	2016

ABSTRACT

Nowadays, the pollution problems in the Songkhla watershed and the Songkhla lagoon have continuously become worse as evidenced by several factors: high soil erosion affected from changing the land use, overall low water quality, contamination by toxic pollutants/nutrients, and rapid sedimentation in some areas. The study of soil erosion in the Songkhla watershed, sedimentation rates and its dynamic patterns in the Songkhla lagoon will provide understanding of these problems. Moreover, the obtained results will be used to manage sustainable land use area, and to protect the ecosystem of the Songkhla lagoon. In this research, we present the atmospheric concentration and deposition fluxes of ^{7}Be at three sites in the U-Tapao watershed, Songkhla province. The atmospheric depositional fluxes of ^{7}Be were positively related to the event rainfall, monthly rainfall, and event rainfall separated by NE, SW, and summer seasons. These relationships were used to understand the behavior of deposition of ^{7}Be in our study area where is in tropical monsoonal environment. Second, the reference inventory and relaxation mass depth of ^{7}Be in undisturbed and flat areas were reported and these parameters were used to calculate short-term erosion. Third, the vertical distribution and the maximum penetration depths of ^{7}Be in lagoon sediment were determined to estimate recent sedimentation patterns. Fourth**,** the sediment mixing rates to indicate the particle exchanged processes at the sediment-water interface derived by the $^{210}Pb_{ex}$ and ^{7}Be depth profiles and the spatial distribution of sediment mixing coefficients in the outer Songkhla lagoon were presented. Finally, we present the determination of sediment accumulation rate by using the vertical profiles of excess ^{210}Pb and ^{137}Cs in the outer Songkhla lagoon

located at southern Thailand. The Constant Initial Concentration (CIC) and the constant rate of ^{210}Pb supply (CRS) models were used to calculate sediment accumulation by the use of unsupported ^{210}Pb. Moreover, two-marker events technique based on ^{137}Cs activity was used to validate age of sediment layers obtained using $^{210}Pb_{ex}$ method.

ACKNOWLEDGMENTS

The work presented in this thesis was carried out at the Nuclear Research Laboratory and Geophysics Research Center, Department of Physics, Faculty of Science, Prince of Songkla University, Thailand. Thanks are due to the financial supports from the National Research Council of Thailand, the Physics Department, Geophysics Research Center, Faculty of Science and the graduate fellowship from the Graduate School, Prince of Songkla University. In addition, I would like to thank Prince of Songkla University for Graduate Studies Grant and the student exchange program between Prince of Songkla University and University of Novi Sad, the Republic of Serbia. The Thai Meteorological Department is acknowledged for providing the meteorological data at the Songkhla station.

It is a pleasure to complete this thesis work. I have received generous support from a lot of people since the beginning till the end of the present thesis work. On this occasion, I would like to express my gratitude to all of them.

Assoc. Prof. Dr. Tripob Bhongsuwan, my supervisor who was abundantly helpful and offered invaluable assistance, support and guidance. I could not have imagined having a better advisor and mentor for my Ph.D. study and research.

Prof. Dr. Miodrag Krmar, thank you so much for accepting me as a student in the laboratory and your kindness and continuous guidance.

I have furthermore to thanks all committees.

My senior and junior colleagues from our laboratory mates that support me in my research work and share the literature and invaluable assistance. I also want to thanks my beloved families for their understanding and endless love, through the duration of my study.

Thank you all so much!

Santi Raksawong

CONTENTS

CONTENTS (cont.)

CONTENTS (cont.)

LIST OF FIGURES

LIST OF FIGURES (cont.)

LIST OF FIGURES (cont.)

LIST OF FIGURES (cont.)

LIST OF PAPERS

I. **Santi Raksawong**, Miodrag Krmar, Tripob Bhongsuwan. Characteristics of Atmospheric ^{7}Be Deposition in the Songkhla Province, Thailand. **Manuscript for submission**

II. **Santi Raksawong**, Miodrag Krmar, Tripob Bhongsuwan.**2016**. ^{7}Be in soil profiles in the undisturbed area using for reference site to estimate the soil erosion. This paper was received and considered to publish in *Journal of Physics: Conference series* in International Nuclear Science and Technology Conference (INST 2016), Centara Grand at Central Plaza Ladprao Bangkok, Thailand.

III. **Santi Raksawong**, Miodrag Krmar, Tripob Bhongsuwan. **2016**. Measurement of ^{7}Be inventory in the Outer Songkhla Lagoon, Thailand**.** *Journal of Radioanalytical and Nuclear Chemistry*. 310, 33 – 44.

IV. **Santi Raksawong**, Miodrag Krmar, Tripob Bhongsuwan. Preliminary study of sediment mixing in the Outer Songkhla Lagoon, Southern Thailand demonstrated by the ^{7}Be and ^{210}Pb profiles. . **Manuscript for submission**

V. **Santi Raksawong**, Miodrag Krmar, Tripob Bhongsuwan. **2015.** Sedimentation rates in the U-Tapao estuary demonstrated by ^{210}Pb- and ^{137}Cs-dating methods. Proceeding the 4th Academic Conference on Natural Science for Young Scientists, Master & PhD Students from Asean Countries. 15-18 December, 2015 - Bangkok, Thailand, pp.74 – 79(Online).
Available URL: http://iop.vast.ac.vn/activities/conf_asean/2015/

SPRINGER LICENSE
TERMS AND CONDITIONS

May 31, 2017

This Agreement between Department of Physics, Faculty of Science, Prince of Songkla University -- Tripob Bhongsuwan ("You") and Springer ("Springer") consists of your license details and the terms and conditions provided by Springer and Copyright Clearance Center.

License Number	4119670213491
License date	May 31, 2017
Licensed Content Publisher	Springer
Licensed Content Publication	Journal of Radioanalytical and Nuclear Chemistry
Licensed Content Title	Measurement of 7Be inventory in the outer Songkhla lagoon, Thailand
Licensed Content Author	Santi Raksawong
Licensed Content Date	Jan 1, 2016
Licensed Content Volume	310
Licensed Content Issue	1
Type of Use	Thesis/Dissertation
Portion	Full text
Number of copies	7
Author of this Springer article	Yes and you are a contributor of the new work
Order reference number	
Title of your thesis / dissertation	Using Radionuclides 7Be, 210Pb and 137Cs to Estimate Soil Erosion in the Khlong U-Tapao Catchment and Accumulated Sedimentation Rate in the Outer Songkhla Lagoon
Expected completion date	Jun 2017
Estimated size(pages)	151
Requestor Location	Department of Physics, Faculty of Science, Prince of Songkla University 15 Kanchanawanitch road, Kho-Hong Hatyai, Songkhla 90110 Thailand Attn: Department of Physics, Faculty of Science, Prince of Songkla University
Billing Type	Invoice
Billing Address	Department of Physics, Faculty of Science, Prince of Songkla University 15 Kanchanawanitch road, Kho-Hong Hatyai, Thailand 90110 Attn: Department of Physics, Faculty of Science, Prince of Songkla University
Total	0.00 USD
Terms and Conditions	

Introduction
The publisher for this copyrighted material is Springer. By clicking "accept" in connection

with completing this licensing transaction, you agree that the following terms and conditions apply to this transaction (along with the Billing and Payment terms and conditions established by Copyright Clearance Center, Inc. ("CCC"), at the time that you opened your Rightslink account and that are available at any time at http://myaccount.copyright.com).

Limited License

With reference to your request to reuse material on which Springer controls the copyright, permission is granted for the use indicated in your enquiry under the following conditions:

- Licenses are for one-time use only with a maximum distribution equal to the number stated in your request.
- Springer material represents original material which does not carry references to other sources. If the material in question appears with a credit to another source, this permission is not valid and authorization has to be obtained from the original copyright holder.
- This permission
• is non-exclusive
• is only valid if no personal rights, trademarks, or competitive products are infringed.
• explicitly excludes the right for derivatives.
- Springer does not supply original artwork or content.
- According to the format which you have selected, the following conditions apply accordingly:
• **Print and Electronic:** This License include use in electronic form provided it is password protected, on intranet, or CD-Rom/DVD or E-book/E-journal. It may not be republished in electronic open access.
• **Print:** This License excludes use in electronic form.
• **Electronic:** This License only pertains to use in electronic form provided it is password protected, on intranet, or CD-Rom/DVD or E-book/E-journal. It may not be republished in electronic open access.

For any electronic use not mentioned, please contact Springer at permissions.springer@spi-global.com.

- Although Springer controls the copyright to the material and is entitled to negotiate on rights, this license is only valid subject to courtesy information to the author (address is given in the article/chapter).
- If you are an STM Signatory or your work will be published by an STM Signatory and you are requesting to reuse figures/tables/illustrations or single text extracts, permission is granted according to STM Permissions Guidelines: http://www.stm-assoc.org/permissions-guidelines/

For any electronic use not mentioned in the Guidelines, please contact Springer at permissions.springer@spi-global.com. If you request to reuse more content than stipulated in the STM Permissions Guidelines, you will be charged a permission fee for the excess content.

Permission is valid upon payment of the fee as indicated in the licensing process. If permission is granted free of charge on this occasion, that does not prejudice any rights we might have to charge for reproduction of our copyrighted material in the future.

-If your request is for reuse in a Thesis, permission is granted free of charge under the following conditions:

This license is valid for one-time use only for the purpose of defending your thesis and with a maximum of 100 extra copies in paper. If the thesis is going to be published, permission needs to be reobtained.

- includes use in an electronic form, provided it is an author-created version of the thesis on his/her own website and his/her university’s repository, including UMI (according to the definition on the Sherpa website: http://www.sherpa.ac.uk/romeo/);
- is subject to courtesy information to the co-author or corresponding author.

Geographic Rights: Scope

Licenses may be exercised anywhere in the world.

Altering/Modifying Material: Not Permitted

Figures, tables, and illustrations may be altered minimally to serve your work. You may not alter or modify text in any manner. Abbreviations, additions, deletions and/or any other alterations shall be made only with prior written authorization of the author(s).

Reservation of Rights
Springer reserves all rights not specifically granted in the combination of (i) the license details provided by you and accepted in the course of this licensing transaction and (ii) these terms and conditions and (iii) CCC's Billing and Payment terms and conditions.
License Contingent on Payment
While you may exercise the rights licensed immediately upon issuance of the license at the end of the licensing process for the transaction, provided that you have disclosed complete and accurate details of your proposed use, no license is finally effective unless and until full payment is received from you (either by Springer or by CCC) as provided in CCC's Billing and Payment terms and conditions. If full payment is not received by the date due, then any license preliminarily granted shall be deemed automatically revoked and shall be void as if never granted. Further, in the event that you breach any of these terms and conditions or any of CCC's Billing and Payment terms and conditions, the license is automatically revoked and shall be void as if never granted. Use of materials as described in a revoked license, as well as any use of the materials beyond the scope of an unrevoked license, may constitute copyright infringement and Springer reserves the right to take any and all action to protect its copyright in the materials.
Copyright Notice: Disclaimer
You must include the following copyright and permission notice in connection with any reproduction of the licensed material:
"Springer book/journal title, chapter/article title, volume, year of publication, page, name(s) of author(s), (original copyright notice as given in the publication in which the material was originally published) "With permission of Springer"
In case of use of a graph or illustration, the caption of the graph or illustration must be included, as it is indicated in the original publication.
Warranties: None
Springer makes no representations or warranties with respect to the licensed material and adopts on its own behalf the limitations and disclaimers established by CCC on its behalf in its Billing and Payment terms and conditions for this licensing transaction.
Indemnity
You hereby indemnify and agree to hold harmless Springer and CCC, and their respective officers, directors, employees and agents, from and against any and all claims arising out of your use of the licensed material other than as specifically authorized pursuant to this license.
No Transfer of License
This license is personal to you and may not be sublicensed, assigned, or transferred by you without Springer's written permission.
No Amendment Except in Writing
This license may not be amended except in a writing signed by both parties (or, in the case of Springer, by CCC on Springer's behalf).
Objection to Contrary Terms
Springer hereby objects to any terms contained in any purchase order, acknowledgment, check endorsement or other writing prepared by you, which terms are inconsistent with these terms and conditions or CCC's Billing and Payment terms and conditions. These terms and conditions, together with CCC's Billing and Payment terms and conditions (which are incorporated herein), comprise the entire agreement between you and Springer (and CCC) concerning this licensing transaction. In the event of any conflict between your obligations established by these terms and conditions and those established by CCC's Billing and Payment terms and conditions, these terms and conditions shall control.
Jurisdiction
All disputes that may arise in connection with this present License, or the breach thereof, shall be settled exclusively by arbitration, to be held in the Federal Republic of Germany, in accordance with German law.
Other conditions:
V 12AUG2015

Questions? customercare@copyright.com or +1-855-239-3415 (toll free in the US) or +1-978-646-2777.

CHAPTER 1

INTRODUCTION

1.1 Background

Recently, increasing population, developmental pressures, high demand of limited land resources, competition on water resources and lack of land use planning contribute to the degradation of environment. Several human activities such as deforestation, overgrazing, changing the land use, and non-sustainable agricultural practices are the causes of environmental problems such as high soil erosion and sedimentation, water pollutions, and sedimentation in lakes, reservior, and floodplains (Zapata, 2002). Moreover, the spreaded urban without land use management is also one of the causes of pollution problems. The pollution problems in the Songkhla lagoon, has been continuously increased due to several factors, the low quality of water, the contamination of toxic pollutants/nutrients and the rapid sedimentation in some areas (Bhongsuwan and Bhongsuwan, 2002; Chittrakarn et al., 1997; Gyawali et al., 2013; Ladachart et al., 2011; Pornpinatepong et al., 2010; Pradit et al., 2013; Sirinawin et al., 1998; Sirinawin and Sompongchaiyakul, 2005; Tanavud et al., 2001). The main sources of the pollutants for the outer part of the Songkhla lagoon include unsanitary drainage from the Songkhla and Hat Yai urban areas, waste from Songkhla harbor, near shore drainage, and the wastewater from large factories surrounding the lake and watershed (Angsupanich and Kuwabara, 1999; Chevakidagarn, 2006; Maneepong, 1996; Maneepong and Angsupanich, 1999; Pornpinatepong et al., 2010; Sirinawin et al., 1998; Sirinawin and Sompongchaiyakul, 2005). Moreover, the fine sediment eroded from the lake watershed is one of the water pollutions that can damage the ecosystems in the lake. This eroded sediment is usually caused by man-made activities (non-sustainable farming practice, overgrazing, deforestation, change in land use from farm to urban) and natural processes (runoff, flooding). From these increasing problems, there is an essential need to obtain reliable quantitative data to provide a more comprehensive assessment of the problems and to maintain the selection of effective sustainability, including assessment of their economic and environmental impacts.

The worldwide researchers have used environmental radionuclides (^{7}Be, ^{137}Cs and ^{210}Pb) to study the dynamic of sediment-deposition, erosion and distribution patterns. The first radionuclide, ^{7}Be is one of the most important environmental radionuclides as a tracer of environmental processes. It is naturally produced by the spallation reactions of the cosmic ray particles in stratosphere and troposphere. After production, cosmogenic ^{7}Be atoms become readily attached to airborne particulates and are removed to the earth's surface by precipitation and dry deposition (e.g. Papastefanou and Ioannidou, 1995). It has been used to determine the recent (short-term) soil erosion and sedimentation in the watershed that has been degraded by natural processes and/or human activities (e.g. Blake et al., 1999; Blake et al., 2002; Mabit et al., 2008; Schuller et al., 2006; Schuller et al., 2010; Sepulveda et al., 2008; Taylor et al.,2013; Walling, 2004; Zapata, 2002). Moreover, it may be used to estimate the recent sedimentation patterns in the lake, river and marine shore (e.g. Bai et al., 2002; Belmaker et al., 2014; Ciffroy et al., 2003; Feng et al., 1999; Matisoff et al., 2005; Palinkas et al., 2005; Schmidt et al., 2007b; Zhu and Olsen, 2009). The ^{137}Cs radionuclide has been used extensively as a tracer to reconstruct recent sedimentation rates. The radionuclide has a half-life 30.1 years and has been redistributed globally as fallout since the onset of atmospheric nuclear weapons testing in the 1950s. Within the sediment horizontal profiles two clear dating markers, 1963 and 1986 peaks that are corresponding to the high-yield atmospheric nuclear weapons testing and the fallout from the Chernobyl reactor accident on 26th April 1986, respectively, can be identified at most deposition sites (e.g. Ioannidou and Papastefanou. 2006; Kato et al., 2003; Mizugaki et al., 2006; Somayajulu et al., 1999; Yao et al., 2008). The ^{210}Pb is naturally occurring radionuclide of the ^{238}U series. Its closed parent is ^{222}Rn, a noble gas having short half-life, 3.8 day. This gas escapes into atmosphere from surface soil layers and provides ^{210}Pb with mobility in atmosphere. The ^{210}Pb is introduced into the estuarine environment through atmospheric precipitation, terrestrial runoff and in situ production from ^{226}Ra in the water column and soil or sediment. ^{210}Pb that falling directly into the lake is removed quickly to sediments by adsorption process and deposited on the bottom of the lake together with the sediment (e.g., Appleby, 2001; Kato et al., 2003; Somayajulu et al., 1999; Yao et al., 2008). Two sample models, which are known as the constant rate of

^{210}Pb supply (CRS) and the constant initial concentration (CIC) model are usually applied. The CIC model is suitable for constant sedimentation rates, based on the supply of ^{210}Pb to the sediments that will increase or decrease in response to changes in sediment flux (Yao et al., 2008). The CRS model is based on the assumption of the constant rate of supply unsupported ^{210}Pb to the sediment and insignificant mobility of ^{210}Pb in the sediment column (Appleby, 2001).

Nowadays, the pollution problems in the Songkhla watershed and the outer Songkhla lagoon have continuously become worse as evidenced by several factors: high soil erosion affected from changing the land use, overall low water quality, contamination by toxic pollutants/nutrients, and rapid sedimentation in some areas (Kitbamroong et al., 2009; Ladachart et al., 2011). The study of soil erosion in the Songkhla watershed, sedimentation rates and its dynamic patterns in the outer Songkhla lagoon will provide understanding of the problems in this area. This information will be used to manage sustainedly land use area, and to protect the ecosystem of the Songkhla lagoon.

1.2 Research objectives

The research objectives are (1) to study the characteristic of ^{7}Be deposition, the depositional running inventory of ^{7}Be calculated from event atmospheric depositional fluxes, and the reference sediment inventory and relaxation mass depth of the selected reference sites to evaluate the short-term erosion and deposition of sediment in the Songkhla watershed, (2) to apply the measurement of atmospheric ^{7}Be in lake-bottom sediment cores to estimate the short-term sedimentation pattern in the Outer Songkhla lagoon, (3) to calculate the sediment mixing rates in the Outer Songkhla lagoon by using the measurement of atmospheric ^{7}Be and ^{210}Pb in lake-bottom sediment cores, and (4) to evaluate the sedimentation rates in the Outer Songkhla lagoon by using the atmospheric radionuclides ^{137}Cs and ^{210}Pb.

1.3 Review of Literature

1.3.1 Nature of atmospheric radionuclides: ^{7}Be, ^{137}Cs and ^{210}Pb

The beryllium-7, ^{7}Be, is a cosmogenic radionuclide produced by the spallation reactions of the cosmic ray particles (protons and neutrons) with nuclei of light elements (carbon, oxygen and nitrogen) in stratosphere and troposphere. The reactions of these spallation processes are shown as (Papastefanou and Ioannidou, 1995):

$$^{12}_{6}C + {}^{1}_{1}p \rightarrow {}^{7}_{4}Be + {}^{6}_{3}Li + Q$$

$$^{12}_{6}C + {}^{1}_{0}n \rightarrow {}^{7}_{4}Be + {}^{6}_{2}He + Q$$

$$^{14}_{7}N + {}^{1}_{1}p \rightarrow {}^{7}_{4}Be + 2\,{}^{4}_{2}He + Q$$

$$^{14}_{7}N + {}^{1}_{0}n \rightarrow {}^{7}_{4}Be + {}^{8}_{3}Li + Q$$

$$^{16}_{8}O + {}^{1}_{1}p \rightarrow {}^{7}_{4}Be + {}^{10}_{5}Be + Q$$
$$\rightarrow {}^{7}_{4}Be + {}^{7}_{3}Li + {}^{3}_{2}He + Q$$

$$^{16}_{8}O + {}^{1}_{0}n \rightarrow {}^{7}_{4}Be + {}^{10}_{4}Be + Q$$
$$\rightarrow {}^{7}_{4}Be + {}^{6}_{2}He + {}^{4}_{2}He + Q$$

The ^{7}Be decays to lithium-7 (^{7}Li) via electron capture with half-life of 53.22 days as shown in **Figure 1.1** (Tilley et al., 2002).

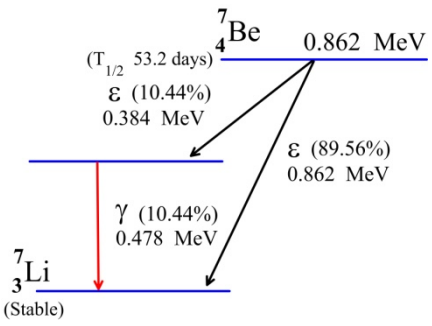

Figure 1.1 Thedecay scheme of ^{7}Be (Wikipedia, 2017a)

The gamma ray with energy of approximately 477.6 keV is emited from this decay. After production, cosmogenic ^{7}Be atoms become readily attached to airborne particulates and are removed to the earth's surface by precipitation and dry deposition (e.g. Papastefanou and Ioannidou, 1995). It has been used to determine the recent (short-term) soil erosion and sedimentation in the watershed that has been degraded by natural processes or human activities (e.g. Blake et al., 1999; Blake et al., 2002; Mabit et al., 2008; Schuller et al., 2006; Schuller et al., 2010; Sepulveda et al., 2008; Taylor et al.,2013; Walling, 2004; Zapata, 2002). Therefore, the ^{7}Be in the lake comprises of two components, first, it deposits directly from the atmosphere into the water column and the lake bottom, and second, it transports from the watershed through streams and overland flow (e.g. Appleby, 2001; Jweda et al., 2008; Matsunaga et al., 1995; Walling, 2004).

The caesium-137, ^{137}Cs, occurs from atmospheric nuclear-weapon tests in the 1950s and 1960s it has a half-life 30.1 years and emites the gamma-ray energy of 661.6 keV (e.g Yao et al., 2008). The decay scheme of ^{137}Cs can be seen in **Figure 1.2.**

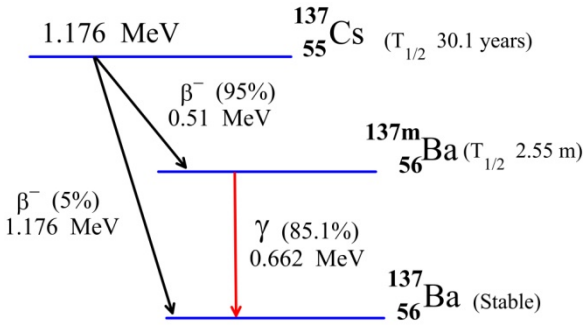

Figure 1.2 The decay scheme of ^{137}Cs (Wikipedia, 2017b)

Generally, The most common nuclear fuels are ^{235}U and ^{239}Pu in the nuclear reator or nuclear weapon. When the nuclear fissions in fissile fuels occured, two elements are produced with the most probable atomic masses around 95 and 137 as shown in **Figuer 1.3**. The ^{137}Cs fragment is produced from ^{235}U fission as shown

$$^{235}_{92}U + {}^{1}_{0}n \rightarrow {}^{236}_{92}U^{*} \rightarrow {}^{137}_{55}Cs + {}^{95}_{37}Rb + 4\,{}^{1}_{0}n + 191\ MeV$$

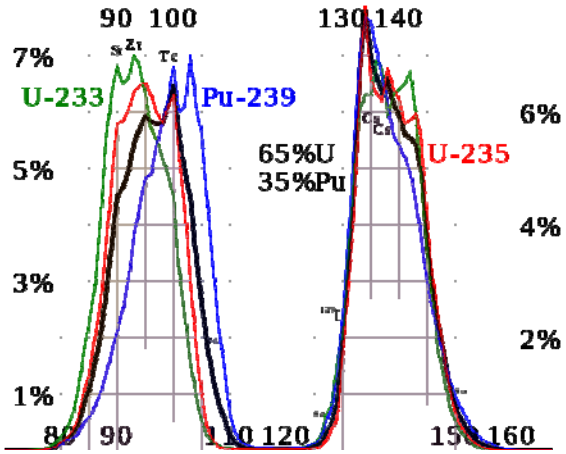

Figure 1.3 Fission product yields by mass for thermal neutronfission of ^{235}U, ^{239}Pu, a combination of the two typical of current nuclear power reactors, and ^{233}U used in the thorium cycle(Wikipedia, 2017c).

The ^{137}Cs radionuclide was injected into the stratosphere where mixed and circulated globally before being deposited on the Earth's suface since the onset of atmospheric nuclear weapons testing in the 1950s (e.g. Furuichi and Wasson. 2013; Zapata, 2002). The fallout peaked in 1963 to 1964 and has decreased since this maximum. There was another peak in 1986 from the Chernobyl reactor accident. Since, there are no natural sources of ^{137}Cs in the environment, it has been used extensively as a tracer to reconstruct recent sedimentation rates, soil erosion and sedimentation (e.g.Doering et al., 2006; Furuichi and Wasson. 2013; Zapata, 2002). After fallout onto the earth's surface, this radionuclide is strongly adsorbed especially on clays, fine sediment particles and colloids and accumulates in topsoils which make it a tracer of topsoil redistribution (e.g. Furuichi and Wasson. 2013;). Moreover, fine sediment and colloids carrying ^{137}Cs is transported downstream and deposited in the floodplains, wetlands, lakes and oceans (e.g. Mizugaki et al., 2006). Within the sediment horizontal profiles of ^{137}Cs concentrations two clear dating markers, 1963 and 1986 peaks that are corresponding to the high-yield atmospheric nuclear weapons testing and the fallout from the Chernobyl accident, respectively, can be identified at most deposition sites (e.g. Ahn et al., 2010; Ioannidou and Papastefanou. 2006; Kato et al., 2003; Mizugaki et al., 2006; Somayajulu et al., 1999; Yao et al., 2008).

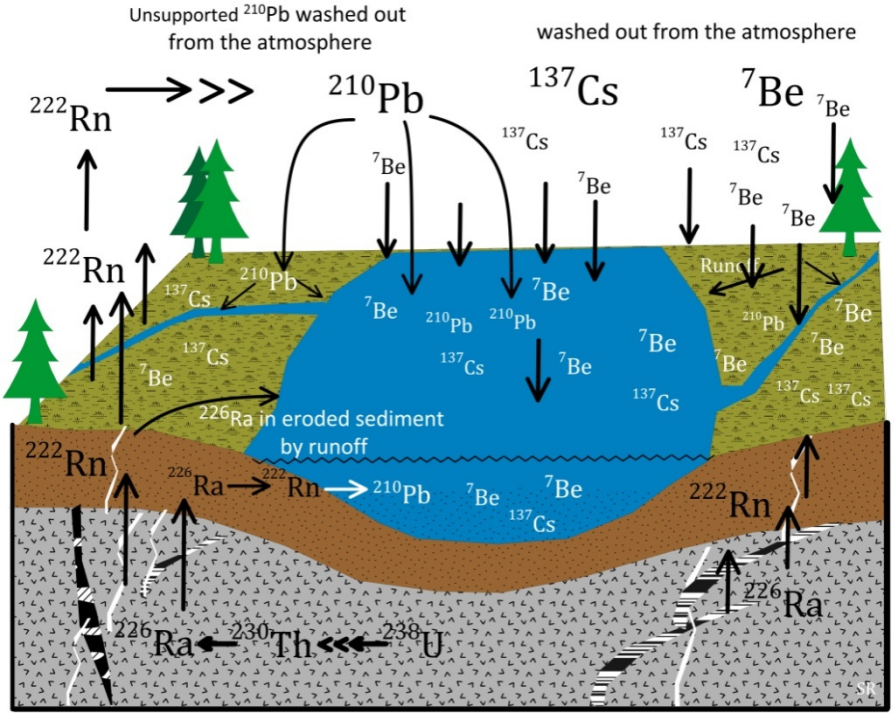

Figure 1.4 The pathways by which ^{7}Be, ^{137}Cs and ^{210}Pb reached the earth' s surface

The ^{210}Pb is naturally occurring radionuclide of the ^{238}U series. Its closed parent is ^{222}Rn, a noble gas having short half-life, 3.8 days. The ^{210}Pb decay to ^{206}Pb as shown in the decay chain scheme (Figure 1.4).

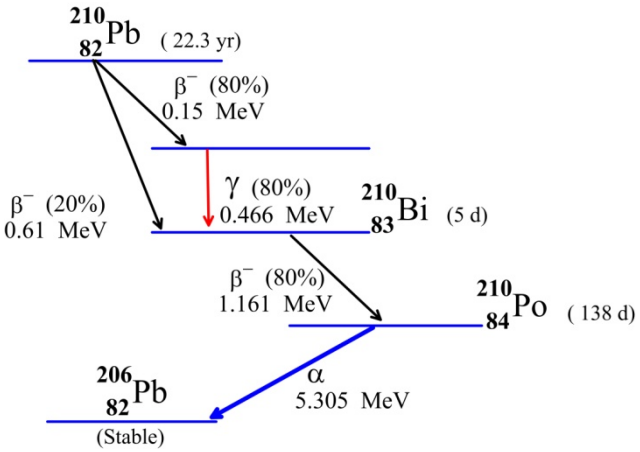

Figure 1.5 The decay scheme of ^{210}Pb (Anokhina et al., 2008)

This gas escapes into atmosphere from surface soil layers and decays to the ^{210}Pb with mobility in atmosphere. The ^{210}Pb produced by the in situ decay of ^{226}Ra in

soil and rocks is called "supported ^{210}Pb or excess ^{210}Pb" and it is in equilibrium with its parent (^{226}Ra). The atmospheric ^{210}Pb is produced from ^{222}Rn emanated from continental rocks and soils, and is called "unsupported ^{210}Pb" (e.g., Ahn et al., 2010; Alonso-Hernandez et al., 2006; Appleby, 2001). This radionuclide is attached to airborne particulates and removed from the atmosphere by both wet and dry deposition onto the catchments surface and into the lakes. The ^{210}Pb is introduced into the estuarine environment through atmospheric precipitation, terrestrial runoff and in situ production from ^{226}Ra in the water column and soil or sediment. ^{210}Pb that falling directly into the lake is removed quickly to sediments by adsorption process and deposited on the bottom of the lake together with the sediment (e.g., Appleby, 2001; Begy et al., 2009; Di Gregorio et al. 2007; Kirchner, 2011;).

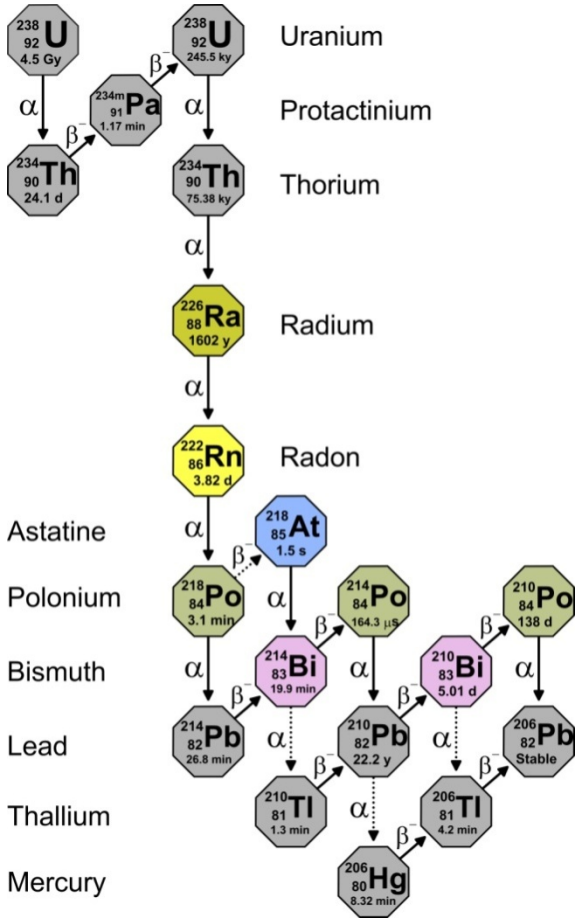

Figure 1.6 Decay chain of U-238 series (Wikipedia, 2016)

1.3.2 Applied atmospheric radionuclides

1.3.2.1 Principle of the estimation of sedimentation rates in the lake/lagoon

Aquatic sediment is one of natural archives recording the history of changing in environments such as sediment erosion in a catchments, water quality associated with eutrophication, atmospheric pollution (heavy metals, organic pollutants), and other contaminants (e.g., Appleby, 2001; Ladachart et al., 2011). Studies on the behavior of particle-associated tracers in aquatic sediment are of widespread interest (e.g., Abril, 2004). Measurements of sedimentation rates in the lakes and reservoirs are used in studies both of the integrated record of soil erosion in the catchment, and its impact on the status of the lake or reservoir. Over the past four decades in the sediment chronology, the ^{210}Pb and ^{137}Cs dating techniques have been widely used to reconstruct the sedimentation histories from a year up to 150 years. (e.g. Ahn et al., 2010; Baskaran et al., 2014; Rai et al., 2007; O' Reilly et al., 2011; Zapata, 2002).

^{137}Cs dating method

The ^{137}Cs measurement in sediment is widely used to estimate aquatic sedimentation rates, since ^{137}Cs fallout is rapidly and strongly fixed on the surface of clay and organic matter particles. When it deposited on the earth's surface, eroded sediments containing ^{137}Cs transported from the upstream catchments to the lake. Moreover, the ^{137}Cs falling directly into the water column of the lake is deposited on the bottom together with the sediment. The depth distribution of ^{137}Cs in the sediment profile will closely reflect the temporal pattern of the fallout input. The artificial ^{137}Cs in the atmosphere comes from weapon nuclear tests during the mid-twentieth century and the accident at the Chernobyl power plant in 1986. Atmospheric deposition of ^{137}Cs first began in 1954, with one peak in fallout occurring in 1963, and with another peak taking place in 1986. Therefore, the year of peak fallout will be marked by the peak ^{137}Cs activity in the sediment profile. The mean annual sedimentation rate *R*

(kg m^{-2} y^{-1}) has been assumed to be equal to that estimated for the ^{137}Cs profile from the adjacent undisturbed reference site using the following equation

$$R = \frac{m_p}{T} \tag{1.1}$$

where m_p is the cumulative dry mass depth between markers (kg m^{-2} y^{-1}) and T is the chronology time interval (y). (Ahn et al., 2010; Du and Walling, 2012; He and Walling, 1996; Appleby, 2001; Walling et al., 2003; Mizugaki et al.2006)

^{210}Pb dating method

A proportion of ^{210}Pb falling onto the catchments surface will be eroded and transported to the lake through the waterways, and ^{210}Pb falling directly into the lakes readily adsorbs to suspended matter in the water column, which may be deposited on the lake-bottom sediments (Appleby, 2001; Di Gregorio et al. 2007; Kirchner, 2011).

In consequence, in deeper layers that have been buried by more recent deposits, the total ^{210}Pb activity, $C_{tot}(t)$ decays with time in accordance with radioactive decay law:

$$C_{tot}(t) = C_{tot}(0)e^{-\lambda t} + C_{\sup}(0)\left(1 - e^{-\lambda t}\right) \tag{1.2}$$

where $C_{\sup}(0)$ is the supported ^{210}Pb activity, λ is the ^{210}Pb decay constant (0.03114 y^{-1}) and $C_{tot}(0)$ is the total ^{210}Pb activity of sediment at the time of burial. The unsupported or excess ^{210}Pb ($^{210}Pb_{ex}$) is determined by subtracting the supported ^{210}Pb activity that is in secular equilibrium with ^{226}Ra from the total ^{210}Pb activity for each sediment sample. Therefore, the unsupported or excess ^{210}Pb, $C_{uns}(t)$ can be obtained (Appleby, 2001) following

$$C_{uns}(t) = C_{uns}(0)e^{-\lambda t} \tag{1.3}$$

The study of $^{210}Pb_{ex}$ decay is the basis of ^{210}Pb-dating models. Thus, the radioactive decay law and profiles of $^{210}Pb_{ex}$ activity can be used to establish sediment

chronologies of the sediment cores. In general, there are commonly two ^{210}Pb dating models that are used to obtain an age of sedimentary layers and calculated sedimentation rates. Several models were developed and refined to accommodate different environmental and anthropogenic influences as well as geological and sedimentary processes (Bonotto and Garcia-Tenorio, 2014; Simsek and Cagatay, 2014).

The first model, the Constant Initial Concentration (CIC) model, also known as the constant specific activity model, is governed by a varying sediment accumulation rate that does not affect the $^{210}Pb_{ex}$ concentration. It means that an increased flux of sedimentary particles from the water column will remove proportionally increased amounts of ^{210}Pb from the water to the sediment. From equation (1.3) under this assumption, the age of a sediment layer of depth m can be calculated using the formula

$$t = \frac{1}{\lambda} \ln \frac{C(0)}{C(m)} \qquad (1.4)$$

Moreover, in case of the condition of a constant rate of sediment accumulation in lake, the $^{210}Pb_{ex}$ activity in sediment, $C(m)$ shows an exponentially decreasing function with depth m (cumulative dry mass depth, kg m^{-2}) in accordance with the formula

$$C(m) = C(0)e^{-\lambda m/R} \qquad (1.5)$$

where R is the dry mass sedimentation rate (kg m^{-2} y^{-1}). When plotted on a logarithmic scale the resulting $^{210}Pb_{ex}$ activity versus depth profile will appear linear. The mean sedimentation rate, R, can be determined from the slope of the graph using least-squares fit procedure (e.g., Abril, 2003; Appleby, 2001; Baskaran et al., 2014).

The second model, when rates of erosive sediment from the catchments that drains into the lake may be changed, the constant rate of ^{210}Pb supply, CRS model is applied. This model assumes the constant atmospheric flux of $^{210}Pb_{ex}$, efficient transfer from the water column to the surficial sediment, and non redistribution. In

this case, both the sedimentation rate and the initial $^{210}Pb_{ex}$ concentration in the sediment can vary through time. The shape of the $^{210}Pb_{ex}$ profile reflects the interaction of the sedimentation rate and radioactive decay law.

$^{210}Pb_{ex}$ inventory of sediment core are calculated from

$$I(m) = \int_{m}^{\infty} C(m)dm \quad \text{and} \quad I(0) = \int_{o}^{\infty} C(m)dm$$

where $I(m)$ is inventory of $^{210}Pb_{ex}$ at depth m ($Bq\ m^{-2}$) and $I(0)$ is inventory of $^{210}Pb_{ex}$ at the top of sediment cores. Therefore, the age t of the sediment at mass depth m can be estimated as:

$$t = \frac{1}{\lambda}\ln\left(\frac{I(0)}{I(m)}\right) \tag{1.6}$$

The mass sedimentation rate $R(m)$ (kg m^{-2} y^{-1}), is obtained directly as (Lu and Matsumoto, 2005):

$$R(m) = \lambda\frac{I(m)}{C(m)} \tag{1.7}$$

Sometime, the ^{210}Pb-dating models could probably provide erroneous or less reliable information on sediment accumulation rates, or researchers must provide a high level of confidence in the results of ^{210}Pb chronology. Thus, it must always be validated by at least one other independent method such as the ^{137}Cs profile for identifying the sharp peak corresponding to 1963 or 1986, or record of known contaminant inputs (e.g., Abril, 2003; Appleby, 2001; Baskaran et al., 2014).

1.3.2.2 Principle of the estimation of mixing rates in the lake

Naturally occurring radionulides, such as ^{210}Pb and ^{7}Be as good radionuclide tracers are widely used to determine the mixing rates in estuarine, marine and lake sediments with vertical diffusion model which is based on the analogy of eddy diffusion (e.g. Krishnaswami et al., 1980; Lecroart et al., 2007a and 2007b; Schmidt et al., 2007a; Palinkas et al., 2005). The mixing rates are simply estimated by steady-state vertical diffusion model with depth profiles of these radionuclides which are adsorbed with fine sediments.

The one-dimensional eddy diffusion is most generally widely used to calculate the vertical mixing rates at the water-sediment interface as expressed in Eq (1.8) (e.g. Aller and DeMaster, 1984; DeMaster et al., 1985; Krishnaswami et al., 1980; Lecroart et al., 2007a and 2007b; Lecroart et al., 2010; Meysman et al., 2003; Osaki et al., 1997; Pope et al., 1996; Reed et al., 2006; Schmidt et al., 2007a; Smith and Schafer, 1999; Wheatcroft, 2006).

$$\frac{\partial A}{\partial t} = D_b \frac{\partial^2 A}{\partial z^2} - S\frac{\partial A}{\partial z} - \lambda A \qquad (1.8)$$

where A refers to the activity of the selected radionuclide tracer at depth z in the sediment (Bq cm^{-3}) that corrects for sediment compaction. A is calculated from multiplying the in-situ wet density of the sediment (mass of dry solids per unit volume of wet sediment, ρ in kg cm^{-3}) and activity concentration of radionuclide tracer at depth z in the sediment (C, in Bq kg^{-1}). D_b is the particle mixing coefficient (cm^2 y^{-1}), S is the sediment accumulation rate (cm y^{-1}), and λ is the radioactive decay constant (y^{-1}).

Assumptions for easily estimating the derived-D_b from radionuclide tracer profiles by using the Eq. (1.8) include, i) the diffusion process is assumed to occur at constant intensity within a surface mixed layer under steady state ($\partial A/\partial t = 0$) and ii) the activity of radionuclide tracer is equal to $A(0)$ at the sediment-water interface and approaches 0 as depth approaches infinity (e.g. Aller and DeMaster, 1984; Appleby,

2001; DeMaster et al., 1985; Krishnaswami et al.,.1980; Lecroart et al., 2010; Pope et al., 1996; Schmidt et al., 2007a). Therefore, the steady-state solution is given by

$$A(z) = A(0)\exp\left(\frac{S - \sqrt{S^2 + 4\lambda D_b}}{2D_b} z\right) \qquad (1.9)$$

Moreover, in the simplest case, the depth profiles are fitted by least squares regressions to calculate mixing coefficient (D_b) when sedimentation rate is known.

Studying the particle exchanged processes at the sediment-water interface provides new insights into benthic processes. Therefore, the quantifications of the sediments mixing rates or diffusion coefficient (D_b) and a mixed depth (L) are required for understanding the sedimentation processes and ecological activities at the water-sediment interface in the lagoon. The D_b values representing the mixing intensity of sediment column are simply calculated by fitting the solution of the diffusion model to tracers-depth profiles (e.g. Krishnaswami et al., 1980; Lecroart et al., 2007a and 2007b; Lecroart et al., 2010; Schmidt et al., 2007a; Palinkas et al., 2005).

CHAPTER 2

RESEARCH METHODOLOGY

In this chapther, the research methodologies are explained including the study area focused in the outer Songkhla lagoon catchment, sampling and sample preparation methods of atmospheric ^{7}Be in wet and dry fallout samples, sampling and preparing methods of lake sediment and soil to measure the ^{7}Be, ^{210}Pb and ^{137}Cs activities, and gamma ray measurement by the gamma spectrometry.

2.1 Study areas

For this research study, the outer Songkhla lagoon and the U-Tapao subcatchment were especially focused. Two these areas are in the outer Songkhla lagoon catchment for studying the atmospheric ^{7}Be in fallout sample to understand the factors of variation, the soil erosion and sedimentation by estimating from ^{7}Be depth profiles, and the patterns and rates of sedimentation in the outer Songkhla lagoon by estimating from ^{7}Be, ^{137}Cs and ^{210}Pb depth profiles. The outer Songkhla lagoon catchment, the southern part of the Songkhla lagoon catchment, is located in southern Thailand between latitudes 6°30′N and 7°50′ N and longitudes 99°15′ E and 100°40′ E. The Songkhla lagoon catchment is a part of the east coast of Malay peninsula and it has three main parts including the samall part called the Thale Noi catchment where is located north of the Songkhla lagoon in Phattalung province, the inner Songkhla lagoon catchment that is located between the Phattalung and Songkhla provinces and it has local name “Thale Luang” and the third part called the outer Songkhla lagoon catchment where is located in the Songkhla province and it has local name “Thale Sap Songkhla” as shown in **Figure 2.1**. The outer Songkhla lagoon catchment has area 3,369 km^2 and has four subcatchment including the U-Tapao subcatchment, the Rattapum subcatchment and two easthern coast subcatchments.

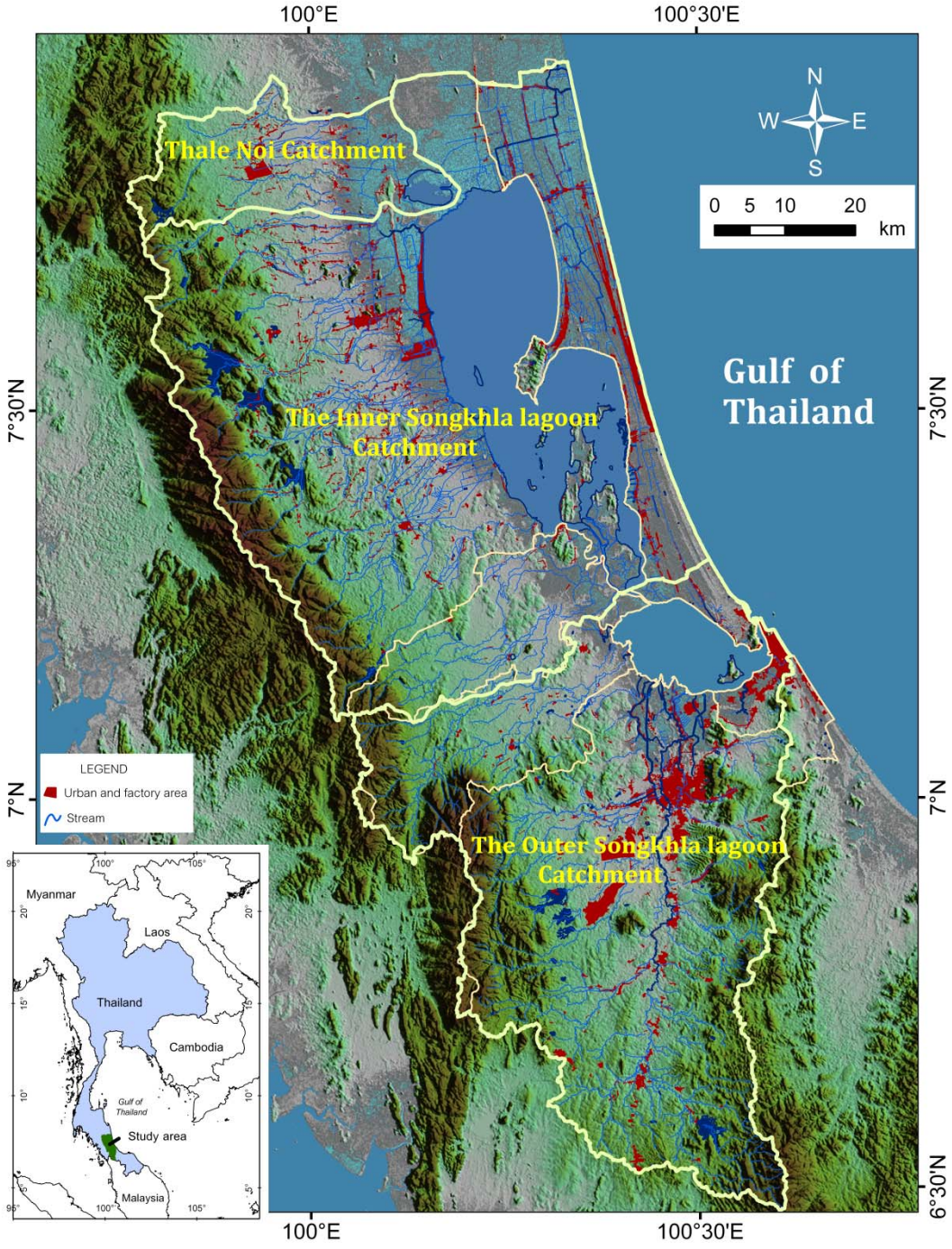

Figure 2.1. The Songkhla lagoon catchment, there are three subcatchments including the outer Songkhla lagoon subcatchment, the inner Songkhla lagoon subcatchment and the Thale Noi subcatchment.

2.1.1 The selected reference sites

The reference site is used to establish the reference ^{7}Be inventory that is compared with the ^{7}Be inventory in the areas where the soil erosion and sedimentation are studied. Generally, the reference site has experienced neither soil loss nor sediment deposition, and has been under perennial grass or continuous vegetation cover. Moreover, it should be located as close as possible to the disturbed areas or study ares (Zapata, 2002).

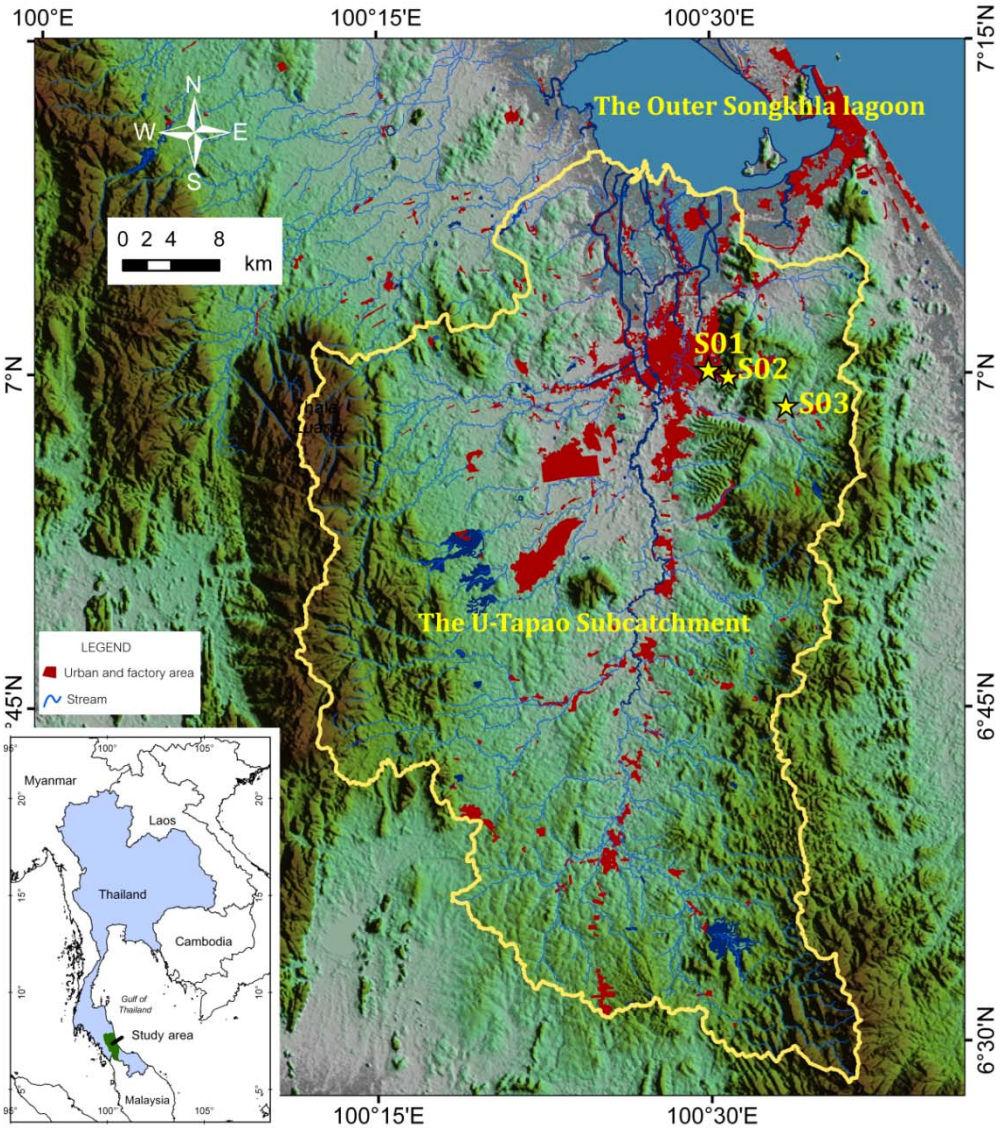

Figure 2.2. The U-Tapao subcatchment, there are three selected stations S01, S02 and S03 for collecting the throughfall, fallout, and soil cores.

The site S01 was selected, located the top roof of Physics department (7°00′24.6″N, 100°29′57.8″E), Faculty of Science, Prince of Songkla University where was the control site to estimate the running inventory of ^{7}Be and to study the factors controlling the atmospheric deposition of ^{7}Be. Two reference sites were selected, the undisturbed soil area that is a park area in Prince of Songkla University (7°00′30.9″N, 100°30′22.0″E), and the undisturbed soil area (non-tilled argricultural area) in the Na Mom district (6°59′32.1″N, 100°33′04.8′E), called S02 and S03, respectively. All three stations S01, S02 and S03 were located in the U-Tapao subcatchment as shown in **Figure 2.2.**

2.1.2 Study area for collecting the sediment cores

The sediment cores were collected in the Outer Songkhla lagoon to measure the ^{7}Be, ^{210}Pb and ^{137}Cs activities in sediment layer. The selected sampling locations of sediment cores are shown in **Figure 2.3.**

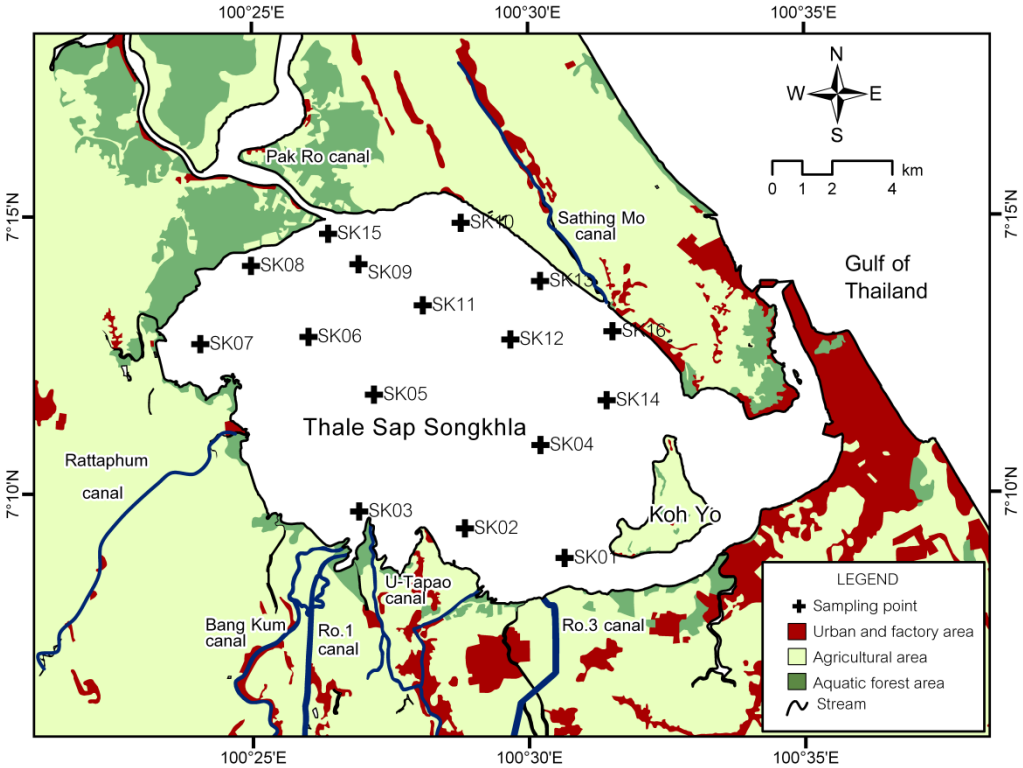

Figure 2.3 The selected sampling locations of sediment cores (black cross) are in the Outer Songkhla lagoon

The Outer Songkhla Lagoon is located in southern Thailand between latitudes 7^{o} 05' N and 7^{o} 50' N and longitudes 100^{o} 05' E and 100^{o} 37' E, a part of the east coast of Malay peninsula. Generally, this lagoon is a shallow coastal lagoon and has an average depth around 2.0 m in rainy season and 1.5 m in summer season. At the lower east side near the Songkhla harbor and the Songkhla town, it has a deep channel (5 – 12 m depth) connecting the lagoon with the sea of the Gulf of Thailand and allowing the tides to propagate into the lagoon as shown in **Figure 2.3**. Therefore the aquatic environment in this lagoon is a combination of seawater and freshwater, and the hydrodynamic complexity of this system is mainly controlled by tide, runoff, wind and wave.

2.2 Sampling and sample preparation methods

In this section, the sampling and preparing methods are described in subsections as following below. The sampling and preparing the atmospheric deposition of ^{7}Be, soil cores, and lake sediment cores before measuring the radionuclides activity by gamma spectrometry are explained in **subsection 2.2.1, 2.2.2.** and **2.23**, respectively.

2.2.1 Sampling and preparing the atmospheric deposition of ^{7}Be samples

To study the factors controlling the atmospheric deposition of ^{7}Be, the wet and dry deposited samples were collected by using three polyethelene buckets that were exposed to atmosphere continuously at three stations S01, S02 and S03 located in the U-Tapao subcatchment between December, 2012, and January, 2014. The collection procedure for wet deposition, firstly, the large rainwater samples were collected into the tanks after rainfall events. Secondly, the inside of the buckets was rinsed with 1.5 L acidified distilled water by 30 mL 6 N nitric acid, and the rinsing water was combined with the rainwater sample. Finally, 20 L rainwater sample was justified to pH ~7 by 2 N NaCl and filtered through MnO_2-fiber (5 g) in a 15 cm long and 1.8 cm inner diameter cylinder. During periods without rainfall event, the

acidified distilled water was added in the buckets to prevent any loss of atmospheric deposited material. The distilled water was processed like rainwater sample.

a) **b)**

c) **d)**

Figure 2.4 **a)** the buckets for receiving the throughfall and direct fallout samples, **b)** rainwater sample was filtered through MnO_2-fiber in a 15 cm long and 1.8 cm inner diameter cylinder, **c)** the filtering MnO_2-fiber, and **d)** the filtered rainwater sample by MnO_2-fiber put into the polyethylene containers

2.2.2 Sampling and preparing soil and grass samples

For study the soil erosion and sedimentation by ^{7}Be technique, the ^{7}Be inventory activity is related to the erosion and sedimentation rates as comparing with the reference inventory of ^{7}Be on undisturbed sites. The high ^{7}Be inventory corresponds to the high sedimentation rates well as the depth distribution processes. Low ^{7}Be inventories correspond to the low sedimentation rate or increased effects of erosion and redistribution. Consequently, the soil and cover grass samples were collected from two selected reference sites S02 and S03 in the U-Tapao

subcatchment, Songkhla province, Southern Thailand, to determine the reference inventory of ^{7}Be. In each site, the cover grasses were cut and put into the plastic bag as shown in **Figure 2.6a**. The grass samples were washed by distilled water and dried at 105 °C for 24 hours by electric oven, then cut to <5 mm fraction by nail scissors, weighed and put into a polyethelene bottle. Using a hand-operated corer equipped with the PVC core tubes of 8.5 cm internal diameter, and 20 cm length as shown in **Figure 2.6b**, eight soil cores were collected from two selected reference sites S02 and S03 on January 10, 2014. All the soil cores were kept vertically and returned to the laboratory, and then sliced at 0.5 cm intervals through its depth using the hand-held extruder as shown in **Figure 2.6c**. All the cut samples were dried at 105 °C for 24 hours by electric oven, grinded by ceramic mortar, sieved to < 2 mm fraction, homogenized, weighed and put into a polyethelene bottle as shown in **Figure 2.6d**.

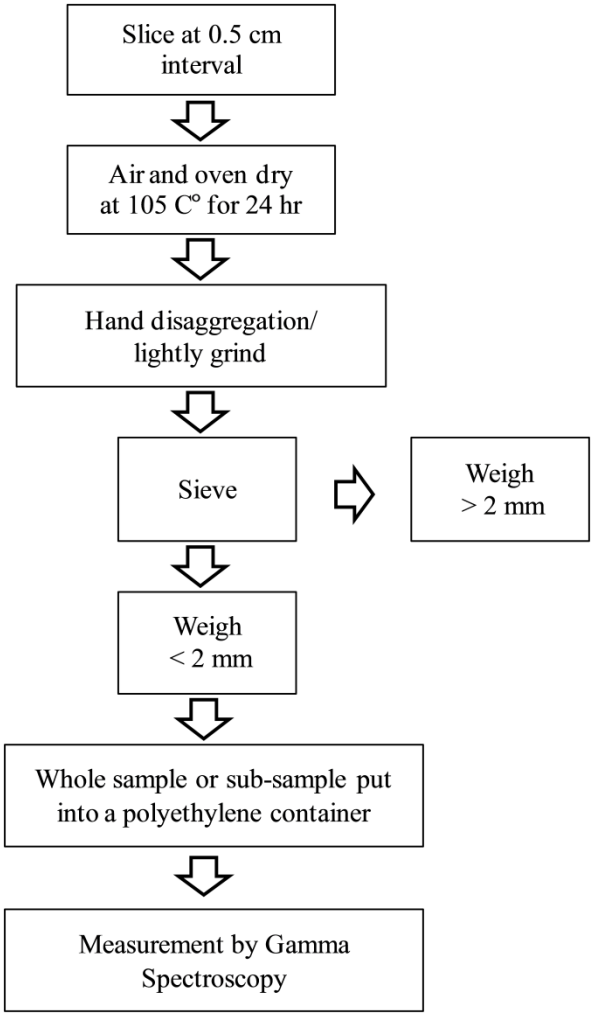

Figure 2.5 Simplified flow chart of lagoon sediment sample processing for radionuclide measurement

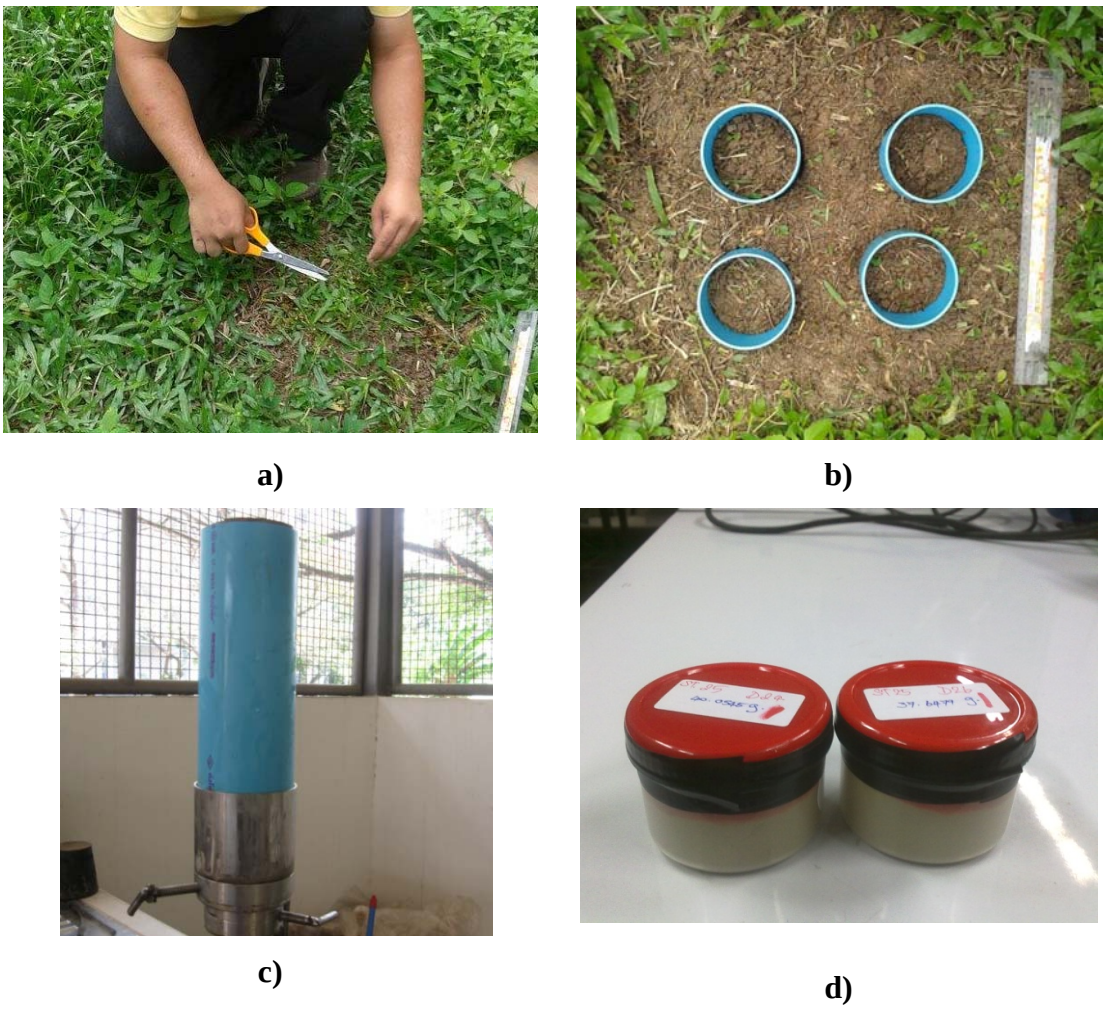

a) **b)**

c) **d)**

Figure 2.6 **a)** cutting the cover grasses, **b)** coring the soil samples, **c)** slicing the soil core sample by using the hand-held extruder, and **d)** the soil sample put into container for measuring radionuclide activity

a)

b)

c)

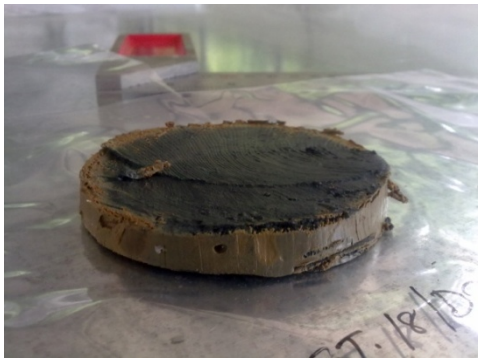

d)

e)

f)

Figure 2.7 **a)** a hand-operated corer equipped with the PVC core tubes, **b)** coring the lake sediment in the outer Songkhla lagoon, **c)** slicing the sediment at 0.5 cm intervals through its depth using the hand-held extruder, **d)** spacimen after slicing, **e)** the electric oven for drying the spacimens, **f)** the lake sediment sample put into container for measuring radionuclide activity

2.2.3 Sampling and preparing the lake sediment

The sediment cores were collected using a hand-operated corer equipped with the PVC core tubes as shown in **Figure 2.7a** (8.5 cm internal diameter, 150 cm length) from the outer Songkhla Lagoon on May, 2011. All the sediment cores were returned to the laboratory, and were horizontally sliced at 0.5 cm intervals through its depth using the hand-held extruder as shown in **Figure 2.7c.** All the specimens were dried at 105 °C for 24 hours by electric oven, and grinded by ceramic mortar, and sieved to < 2 mm fraction, homogenized, weighed and put into a polyethylene container of a similar geometry with the certified standard calibration source.

2.3 Measurement method of the radionuclides

2.3.1 Equipment

In this research, three Gamma-spectrometry systems were used. They include (1) the gamma spectrometric system including the HPGe detector in the aluminum window, model GC7020 (Canberra Industries, USA) in a low-background cylindrical shield (Model 747, Canberra Industries, USA) and coupled to a multichannel analyzer (DSA1000, Canberra, USA) onwed by Department of Physics, Faculty of Science, Prince of Songkla University, Thailand, (2) the Gamma spectrometry system that the HPGe detector in the carbon window onwed by Department of Physics, Faculty of Science, University of Novi Sad, Serbia were used for measuring the gamma rays emitted from ^{210}Pb and ^{137}Cs radionuclides in some lake sediment samples, and (3) the Gamma spectrometry system equipped with the HPGe detector in the beryllium window onwed by Department of Applied Radiation and Isotopes, Faculty of Science, Kasetsart University, Thailand was used for measuring the gamma rays emitted from ^{210}Pb radionuclide in some lake sediment samples.

a) **b)**

Figure 2.8 The gamma spectrometry systems **a)** at Physics Department, Faculty of Science, Prince of Songkla University, Thailand, **b)** at Physics Department, Faculty of Science, University of Novid Sad, Serbia

2.3.2 Measuring the ^{7}Be radionuclide in the rainwater samples

After rainwater samples were filtered, a gamma spectrometry system with the HPGe detector in a low-background cylindrical shield and coupled to a multichannel analyzer at Physics Department, Faculty of Science, Prince of Songkla University was used to measuring the ^{7}Be activity in the rainwater filtered by MnO_2-fibers. The Figure 2.5a shows the measuring gamma-ray spectrum from the rainwater sample that was collected on December 31, 2013. The efficiency calibration of the detection system (**Figure 2.8b**) was made using a certified Europium-152 solution (Gamma data Instrument AB, Sweden), at 477.7 keV gamma energy. The counting-time was set to 21600 s for each sample, to provide a reasonably low analytical error (less than 25% or 1σ).

From the measurement of certified Europium-152 solution, the experimental efficiencies are calculated. The absolute efficiency (ε_i) at energy line (E_i) for a given set of measuring conditions can be calculated by

$$\varepsilon_i = \frac{N_i}{TA_i I_i} \qquad (2.1)$$

where N_i is net count area under the full-energy photopeak corresponding to E_i energy emitted by a radionuclide with a known activity, T is the counting-time, A_i is the activity of radionuclide emitting photons energy line E_i, and I_i *is* the emission probability of emitting photons energy from radionuclide.

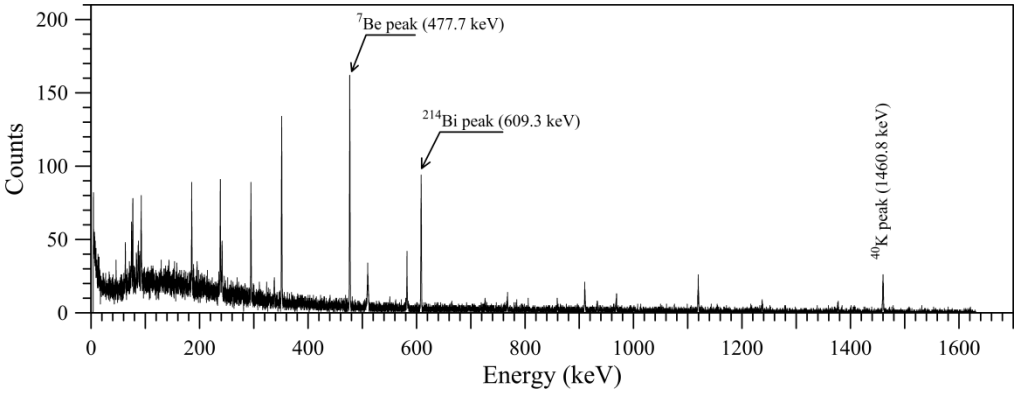

a)

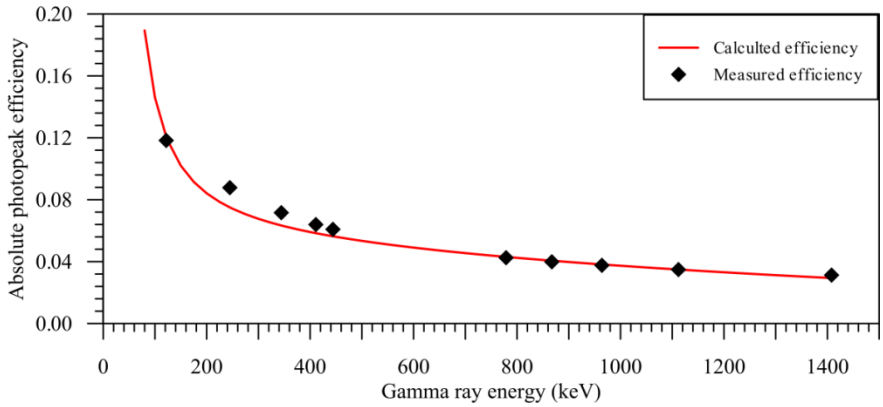

b)

Figure 2.9 **a)** the spectrum of a rainwater filtered by MnO_2-fibers, sampling date December 31, 2013, **b)** the efficiency calibration curve of the detection system from activity of a certified Europium-152 solution

2.3.2 Measuring the ^{7}Be radionuclide in the soil samples

The gamma spectrometry system at Physics Department, Faculty of Science, Prince of Songkla University was used for measuring the ^{7}Be activity in soil samples. **Figure 2.6a** shows gamma-ray spectrum from the first layer (0 - 0.5 cm) of soil sample of site S02 that was collected on January 10, 2014. The efficiency calibration of the detection system (**Figure 2.6b**) was made with the IAEA TEL 2011-03 WWOPT soil-04 sample, at 477.7 keV gamma energy. The counting-time was set to 50000 s for each sample, to provide a reasonably low analytical error (less than 25% or 1σ).

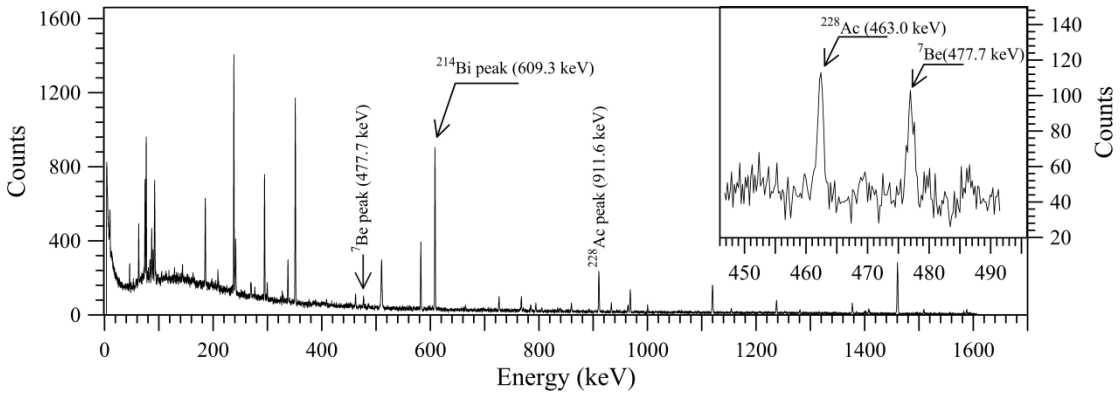

a)

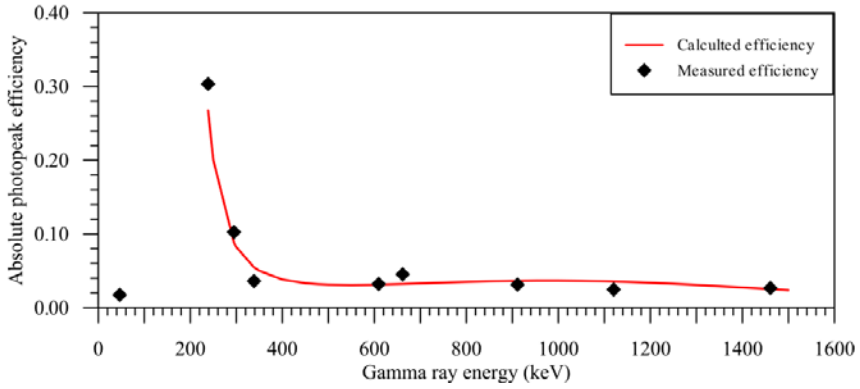

b)

Figure 2.10 **a)** the spectrum of a soil layer (0- 0.5 cm), sampling date January 10, 2014, **b)** the efficiency calibration curve of the detection system from activity of the IAEA TEL 2011-03 WWOPT soil-04 sample

2.3.3 Measuring the ^{7}Be radionuclide in the sediment samples

Totally 16 bottom sediment cores were collected from the outer Songkhla lagoon on December 25, 2013. The ^{7}Be activity in the sediment samples was measured using gamma spectrometry at the Department of Physics, Faculty of Science, Prince of Songkla University (as described in section 2.3.1). The counting-time period for each sample was about 40,000 – 100,000s to provide the lowest reasonable analytical error (less than 25% or 1σ). Gamma ray energy at 477.7 keV was monitored for ^{7}Be determination. The IAEA TEL 2011-03 WWOPT soil-04 sample with certified radionuclide activities was used to calculate the relative efficiency of ^{7}Be at 477.7 keV similar to those used for soil samples. The ^{7}Be activities were corrected for decay to the sampling time on December 25, 2013.

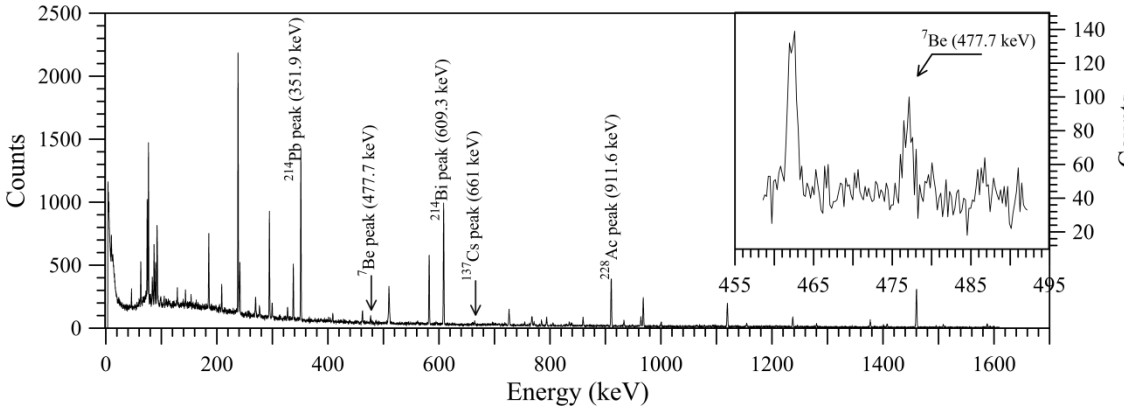

Figure 2.11 the spectrum of a lake sediment layer (0- 0.5 cm), sampling date on December 25, 2013 which shows the ^{7}Be peak

2.3.4 Measuring the ^{210}Pb and ^{137}Cs radionuclides in the sediment samples

The sub-sediment samples were put into a polyethylene container of a similar geometry with the calibration source. The selected sediment samples were sent to laboratory at the Department of Applied Radiation and Isotopes, Faculty of Science, Kasetsart University, Thailand, and some were sent to the Faculty of Sciences, University of Novi Sad, Republic of Serbia, to measure the ^{210}Pb activity by

gamma spectrometry systems having good efficiency at gamma energy 46.6 keV. Other samples were measured in our laboratory by using gamma spectrometry in a low-background cylindrical shield, high-purity germanium detector coupled to a DSA 1000 multichannel analyzer. The ^{137}Cs activity (gamma ray energy 661.6 keV) of each sediment sample was measured by counting time of minimum 40,000s to maximun 100,000s to provide the lowest reasonable analytical error. The IAEA TEL 2011-03 WWOPT soil-04 sample with known radionuclide activities was used to directly calculate the absolute efficiency of ^{137}Cs at gamma energy line 661.6 keV.

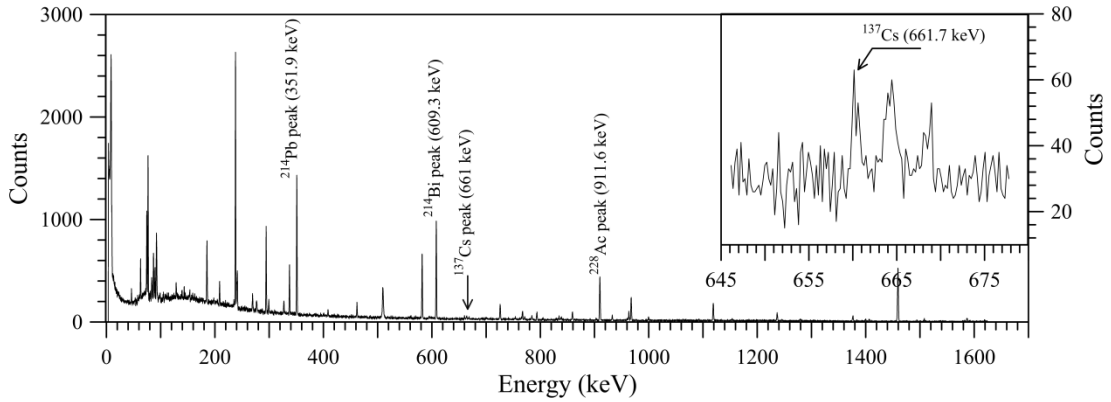

Figure 2.12 the spectrum of a lake sediment layer (0- 0.5 cm), sampling date on December 25, 2013 which shows the ^{137}Cs peak

CHAPTER 3

SUMMARIZED RESULTS AND DISCUSSIONS

This chapter presents the summarized results and discussions which are divided into four parts. First part presents the relationships between atmospheric depositional fluxes of ^{7}Be in the Songkhla province and event rainfall, monthly rainfall, and event rainfall separated by NE, SW, and summer seasons (**see in the paper I**). Furthermorer, we reported the annual depositional flux of ^{7}Be to record in the databases. These relationships were used to understand the behavior of deposition of ^{7}Be in our study area. Moreover, the depositional running inventory of ^{7}Be was calculated from event atmospheric depositional fluxes. It was used as reference value for the soil erosion and sedimentation model, and for evaluation of erosion and/or deposition patterns of sediment in the Outer Songkhla lagoon. The second part presents the reference sediment inventory and relaxation mass depth of the selected reference sites to document short-term erosion (**see in the paper II**). These reference sediment inventories collected from two study sites were compared with the running atmospheric depositional fluxes and activity of ^{7}Be in cover grasses. The third part presents two applications of using ^{7}Be technique: (1) using the measurement of atmospheric beryllium-7 in lake-bottom sediment cores to estimate the short-term sedimentation pattern in the Outer Songkhla Lagoon, Thailand (**see in the paper III**) and (2) using the measurement of atmospheric ^{7}Be and ^{210}Pb in lake-bottom sediment cores to calculate the sediment mixing rates (**see in the paper IV**). The final part presents the application of atmospheric radionuclides (^{137}Cs and ^{210}Pb) to evaluate the sedimentation rates in the Outer Songkhla lagoon (**see in the paper V**).

3.1 Atmospheric deposition fluxes of ^{7}Be in Songkhla Province (paper I)

This section shows the characteristics of deposition of the natural radionuclide ^{7}Be widely used as tracers of aerosols for the study of pollution and atmospheric transport processes, and to estimate soil erosion and sedimentation, river or lake sediment dynamic, sediment transport distance, etc. We reported ^{7}Be concentrations and deposition fluxes of ^{7}Be observed from three sites in the Songkhla

province on the U-Tapao watershed during December 2012 – January 2014, and discussed the factors controlling the deposition of this radionuclide. The atmospheric depositional fluxes of ^{7}Be have been decay-corrected to the collecting time of rainfall sample due to the differences of the rainfall period and frequency. The deposited fluxes of each individual event, expressed in Bq m^{-2}, varied widely from 0.6 ± 0.1 to 34 ± 2 Bq m^{-2}, 2.0 ± 0.5 to 69 ± 12 Bq m^{-2} and 3 ± 2 to 103 ± 15 Bq m^{-2}, for sites S01, S02 and S03, respectively, as shown in paper I. Their mean values were 11.6, 18.5 and 27.1 Bq m^{-2}, respectively. In order to calculate the atmospheric deposition running inventory of ^{7}Be following Zhu and Olsen (2009), all preceding atmospheric deposition fluxes were decay-corrected to the time of the current event and adding with the current value as present in Figure 3.1. The calculated running inventory values range between 29 ± 1 and 156 ± 14 Bq m^{-2} for site S01, 17 ± 2 and 169 ± 7 Bq m^{-2} for site S02, and 28 ± 5 and 215 ± 17 Bq m^{-2} for site S03.

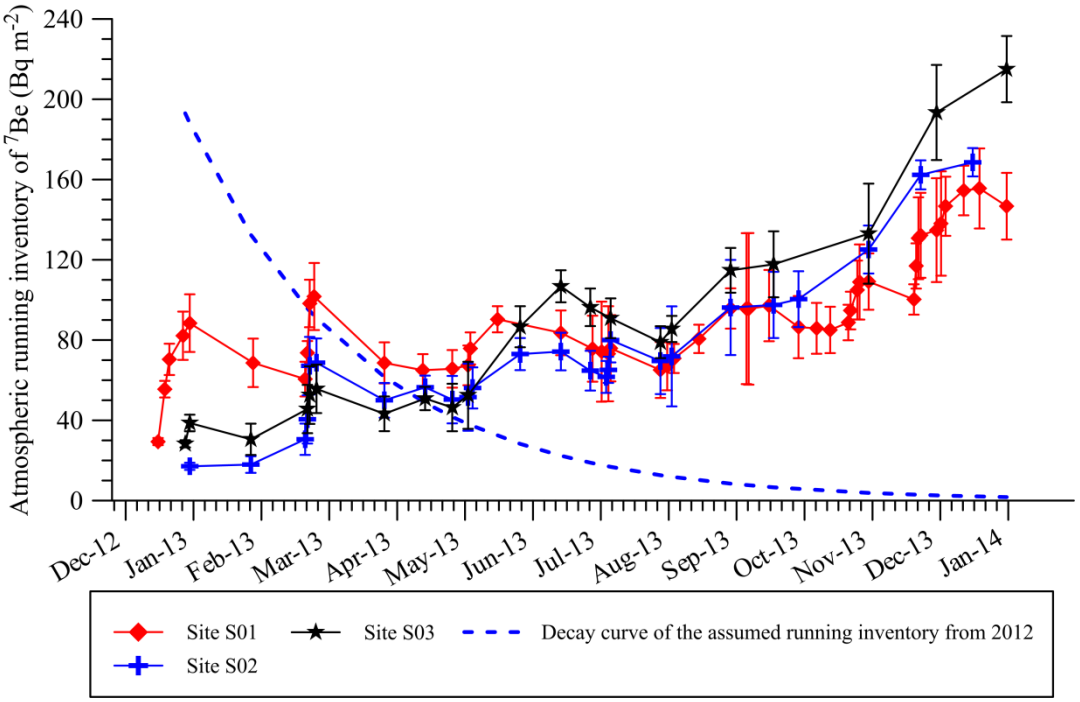

Figure 3.1 Atmospheric deposition flux and running inventory of ^{7}Be from study sites; S01(red diamond), S02 (blue cross) and S03 (black star)

The mean values of specific concentrations of ^{7}Be in rain water were 0.24 ± 0.17, 0.23 ± 0.13 and 0.18 ± 0.06 Bq l^{-1} for sites S01, S02 and S03, respectively.

The mean values of depositional fluxes of ^{7}Be were 11.6, 18.5 and 27.1 Bq m^{-2} for sites S01, S02 and S03, respectively. The average annual depositional flux of ^{7}Be was 480.8 Bq m^{-2} that was lower than those previously reported in other locations in the world. The monthly depositional flux of ^{7}Be did not remain constant but varied between 0.6 and 103 Bq m^{-2} depending on the amount of monthly rainfall.

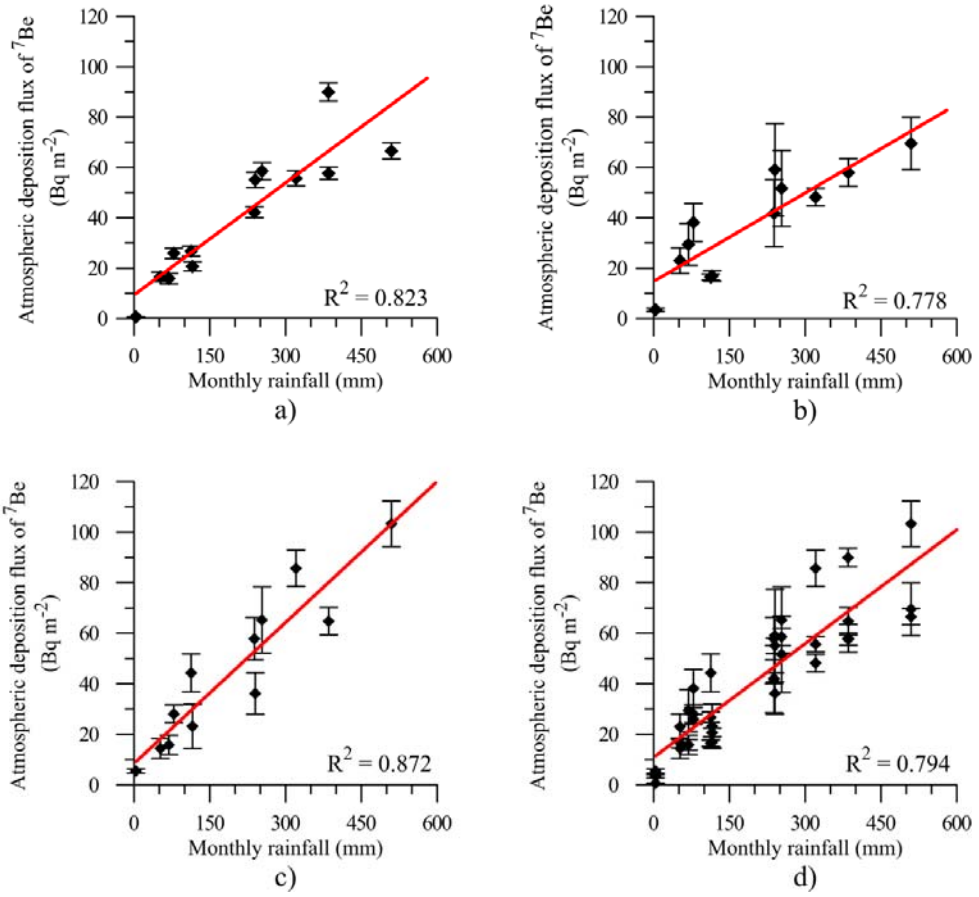

Figure 3.2 Correlation between monthly precipitation and deposition flux of ^{7}Be for sites S01, S02, S03 and total all sites as shown in a), b), c) and d) respectively.

The monthly depositional fluxes of ^{7}Be plotted against monthly rainfall (Figure 3.2) show a strong positive correlations at all sampling sites, suggesting that the atmospheric ^{7}Be is removed from atmosphere by washout and rainout processes (Narazaki et al, 2003; Yi et al, 2007). Moreover, the relationships between atmospheric depositional fluxes of ^{7}Be in the Songkhla province and event rainfall, and event rainfall separated by NE, SW, and summer seasons were present **in the**

paper I. Figure 3.3 shows the event depositional fluxes of ^{7}Be plotted against rainfall separated by NE, SW, and summer seasons. The linear relationships obtained by the regression test between the event depositional flux of ^{7}Be and amount rainfall are significant positively related at all duration of monsoon.

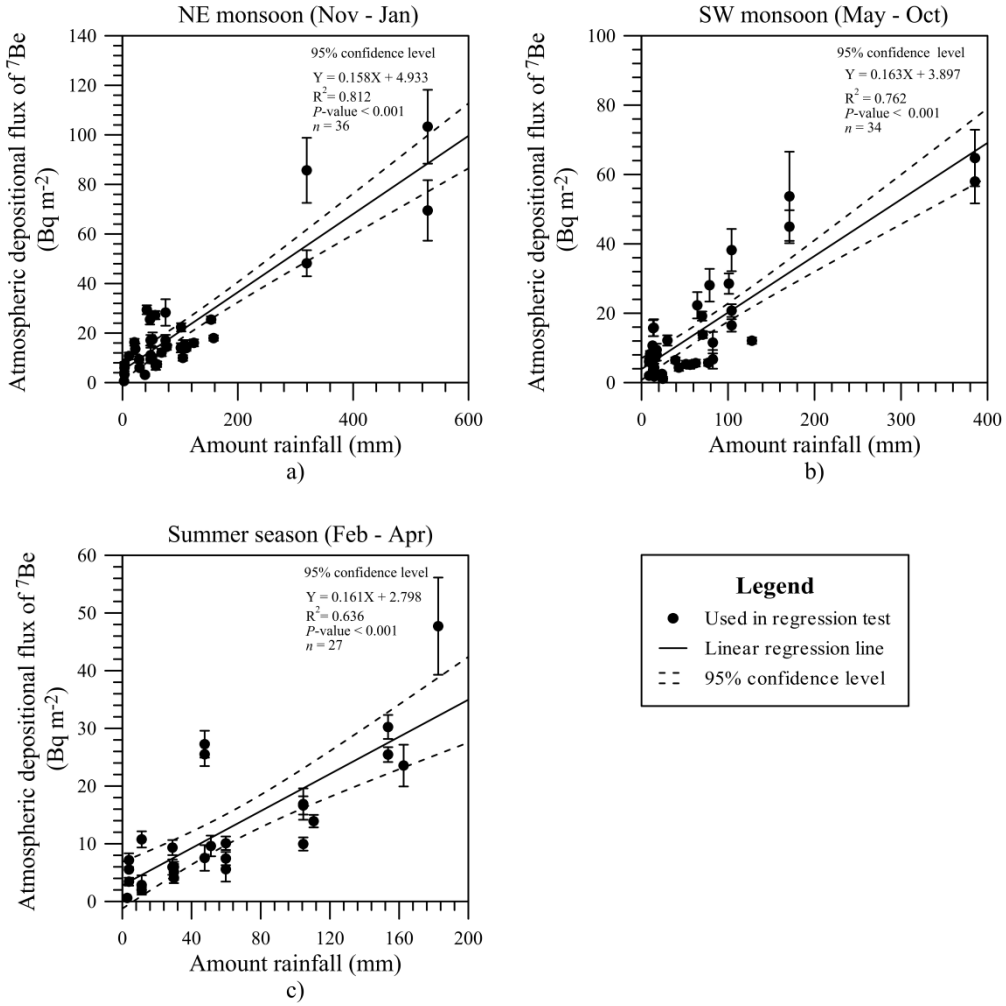

Figure 3.3 Relationships between the event depositional fluxes of ^{7}Be and amount rainfall classified by duration of monsoon: a) November to January (NE monsoon), b) May to October (SW monsoon) and c) February to April (summer season)

The slopes of linear relationship between these are 0.158, 0.163 and 0.161 for the NE monsoon seasons (R^2 = 0.812, p < 0.001), the SW monsoon seasons (R^2 = 0.429, p < 0.001), and the summer season (R^2 = 0.864, p < 0.001) respectively. It can be considered that the removing of ^{7}Be-bearing aerosols to the ground surface

was dominantly regulated by precipitation. In the Figure 3.3, atmospheric depositional fluxes of ^{7}Be vary with seasonal monsoons. High values show in the North-East monsoon and summer season months, and low values show in South-West monsoon months. The significant linear correlations between the daily deposition fluxes of ^{7}Be and precipitation suggested that the atmospheric deposition of ^{7}Be was related to rainfall. Consequently, the precipitation was the dominant removal pathway of ^{7}Be out of the atmosphere in Songkhla. This observation was similar to that reported from other regions (e.g. Kim et al., 2000; McNeary and Baskaran, 2003; Su et al., 2003; Zhang et al. 2016). The depositional flux of ^{7}Be in northeast monsoon months was higher than that in the southwest monsoon months indicating more atmospheric ^{7}Be carried by the same amount of rainwater from the middle latitude.

The amount of ^{7}Be that reaches the Earth's surface is dependent on its production rate, stratosphere-troposphere air exchange, and troposphere circulation (e.g Baskaran, 1995; Conaway et al., 2013; Ishikawa et al., 1995). The geographic latitude was plotted with the annual atmospheric depositions of ^{7}Be reported in the several locations in the world and our result as shown in Figure 3.4a. The high fluxes of ^{7}Be appear at the middle latitude (30 – 40°) where are influenced from the folding effect by stratosphere-troposphere air exchange and horizontal transport of air mass. Generally, the geomagnetic field deflects incoming galactic cosmic rays (GCRs) toward the magnetic poles. The ^{7}Be production rate depends on the geomagnetic field (Conaway et al., 2013). For example, its production rate is much higher at high geomagnetic latitudes than at low geomagnetic latitude (Feely et al, 1989). In this report, the vertical, horizontal, and total intensities of geomagnetic field, absolute geomagnetic latitude, and geographic latitude were plotted with the annual atmospheric depositions of ^{7}Be reported in the several locations in the world and our result as shown in Figure 3.4. There are correlations between the annual depositional flux of ^{7}Be including our data and the previously reported data in publications and horizontal, total geomagnetic field intensities, and the geomagnetic latitude.

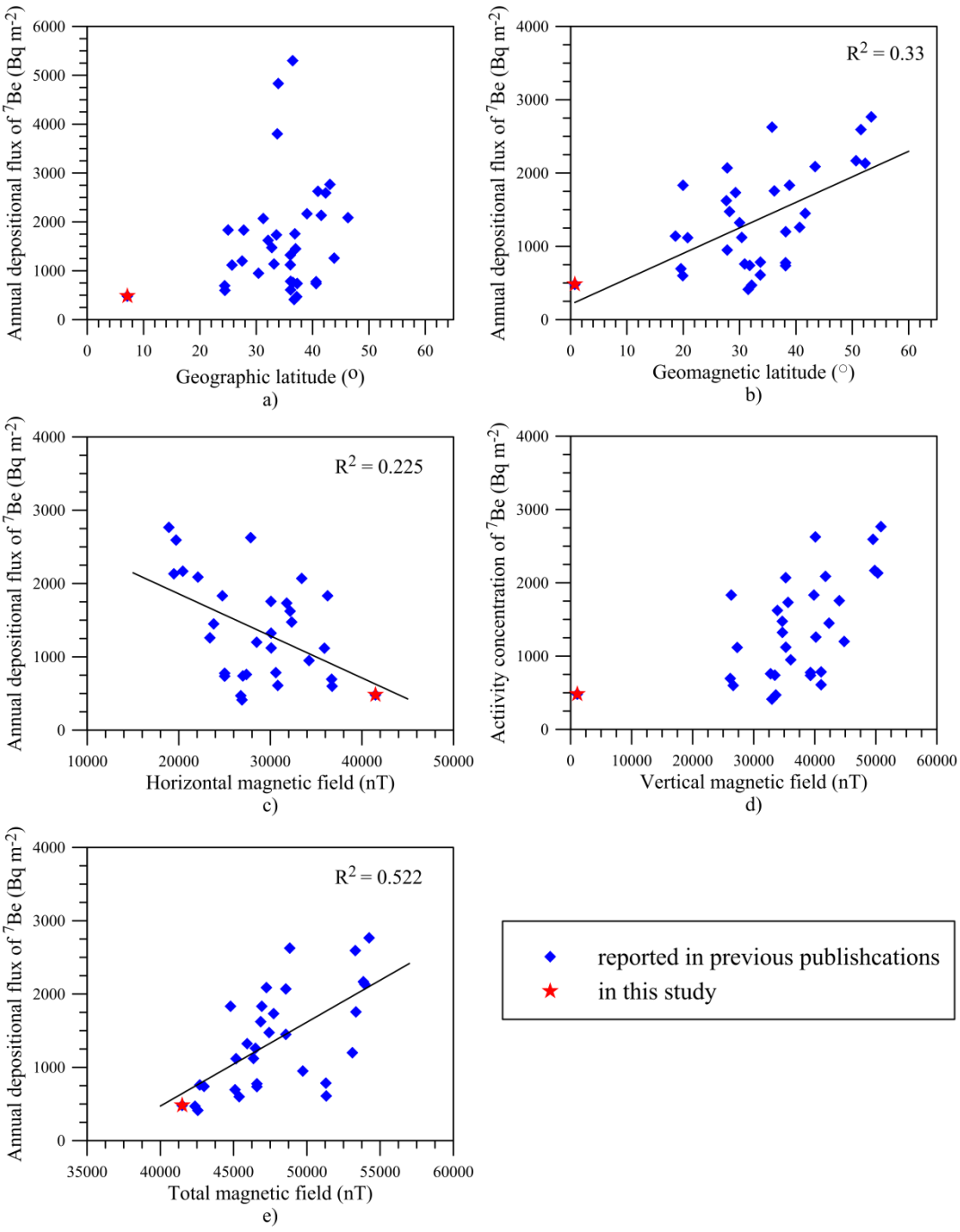

Figure 3.4 The effect of ^{7}Be depositional fluxes from a) absolute geographic latitude, b) geomagnetic latitude, c) horizontal, d) vertical and e) total geomagnetic field intensities.

For discussion of geomagnetic field, we cut out three points of high annual atmospheric depositions of ^{7}Be. Figure 3.4b shows that geomagnetic latitude have affected with the ^{7}Be depositional fluxes, and the ^{7}Be depositional fluxes are

depended on the magnetic field intensities such as horizontal, vertical and total intensities as shown in Figure 3.4c, d and e, respectively. Figure 3.4c shows the negative correlation between the horizontal magnetic field intensity and the ^{7}Be depositional fluxes. Although, it is poor correlation which may be influenced from other factors such as horizontal movement of atmospheric aerosols carried the ^{7}Be, and folding effect of exchange of aerosols between stratosphere and troposphere. The related correlation of these is negative, because the charged GCRs are turned out by high magnetic force from the horizontal magnetic field intensity. The ^{7}Be depositional fluxes as shown in Figure 3.4d seem that it depends on the vertical magnetic field intensity, but the vertical magnetic field intensity do not in fact affect to the movement of the GCRs. Therefore, the GCRs can move through the Earth's atmosphere for interaction of the light particle producing ^{7}Be. The effect of total magnetic field intensity to the ^{7}Be depositional fluxes are shown in Figure 3.4e. It seems that the magnetic field intensity influence the ^{7}Be depositional fluxes because of the total magnetic field intensity including the factors such as geomagnetic latitude, horizontal and vertical magnetic field intensities.

3.2 The ^{7}Be activity in soil profiles for selected reference sites (paper II)

In this section, we show the results of the ^{7}Be in soil profiles from the selected two undisturbed and flat areas to calculate the reference inventory and relaxation mass depth for using ^{7}Be technique to document short-term erosion.

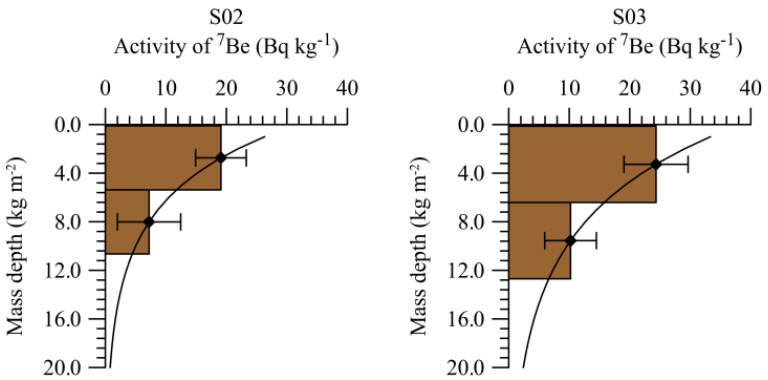

Figure 3.5 The depth distribution of ^{7}Be in the soil profiles within the selected reference site.

Our results show that the depth distribution of ^{7}Be in undisturbed soil profiles is 1.0 cm in sites S02 and S03; the initial activities are 31.6 and 38.8 Bq kg^{-1} for the first and the second, respectively. The ^{7}Be activities for both locations declined exponentially with mass depth as shown in Figure 3.5. The relaxation mass depths obtained are 5.4 and 7.2 kg m^{-2} and the measured reference ^{7}Be inventories in the sediment are 71 and 110 Bq m^{-2} for sites S02 and S03, respectively. The estimated ^{7}Be running inventories at the time of sediment sampling are 156 ± 20 Bq m^{-2}, 169 ± 7 Bq m^{-2} and 215 ± 17 Bq m^{-2} for S01, S02 and S03, respectively. Atmospheric running inventories for the selected reference sites S02 and S03 are shown in the Figure 3.6.

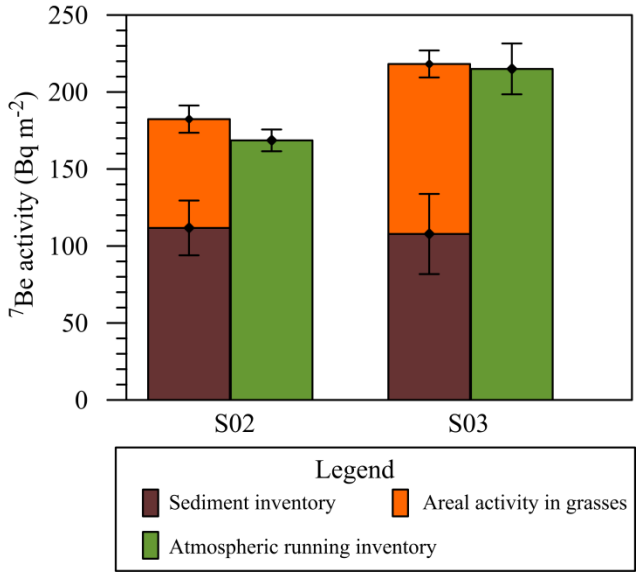

Figure 3.6 The bar charts comparing the atmospheric running inventory and the stacked columns between measured sediment inventory and areal activity in grasses.

The measured ^{7}Be inventories in soil cores of 71 ± 18 and 110 ± 26 Bq m^{-2} were stacked with the areal activities in cover grasses of 112 ± 9 and 108 ± 9 Bq m^{-2} for the selected reference sites S02 and S03, respectively. The atmospheric running inventories are similar to the stacked activities between the areal activities in cover grasses and the measured ^{7}Be inventories in soil cores for both sites S02 and S03. Event though, the calculated reference inventories, 170 and 279 Bq m^{-2}, are

larger than the measured inventories. The measured inventories in soil cores, 71 ± 18 and 110 ± 26 Bq m^{-2} for both sites S02 and S03, may be used as the reference inventories, A_{ref}, in the model to calculate the soil erosion and deposition rates in study area. This is in fact the calculated reference inventories are not possible to be larger than the atmospheric running inventory. This problem may occur due to the thicker section of soil cores. In the future work, the thin sliced section of soil cores will be made, because there will be more than two points in the ^{7}Be profiles with mass depth to estimate the calculated reference inventory and relaxation mass depth.

3.3 Application of ^{7}Be activity in the lagoon sediment (paper III and IV)

3.3.1 The short-term sedimentation pattern in the outer Songkhla lagoon, Thailand, revealed by the measurement of atmospheric beryllium- 7 in sediment cores (paper III)

This section shows the application of the cosmogenic ^{7}Be in the lake bottom sediment cores to demonstrate the quantifying short-term changes of sediment dynamic and to estimate the recent sedimentation pattern in the outer part of Songkhla Lake (Thale Sap Songkhla), southern Thailand. The sediment depocenters, the extent of the sediment accumulation and the distribution zonations can be excellently demonstrated by the inventories of ^{7}Be in the sediment cores.

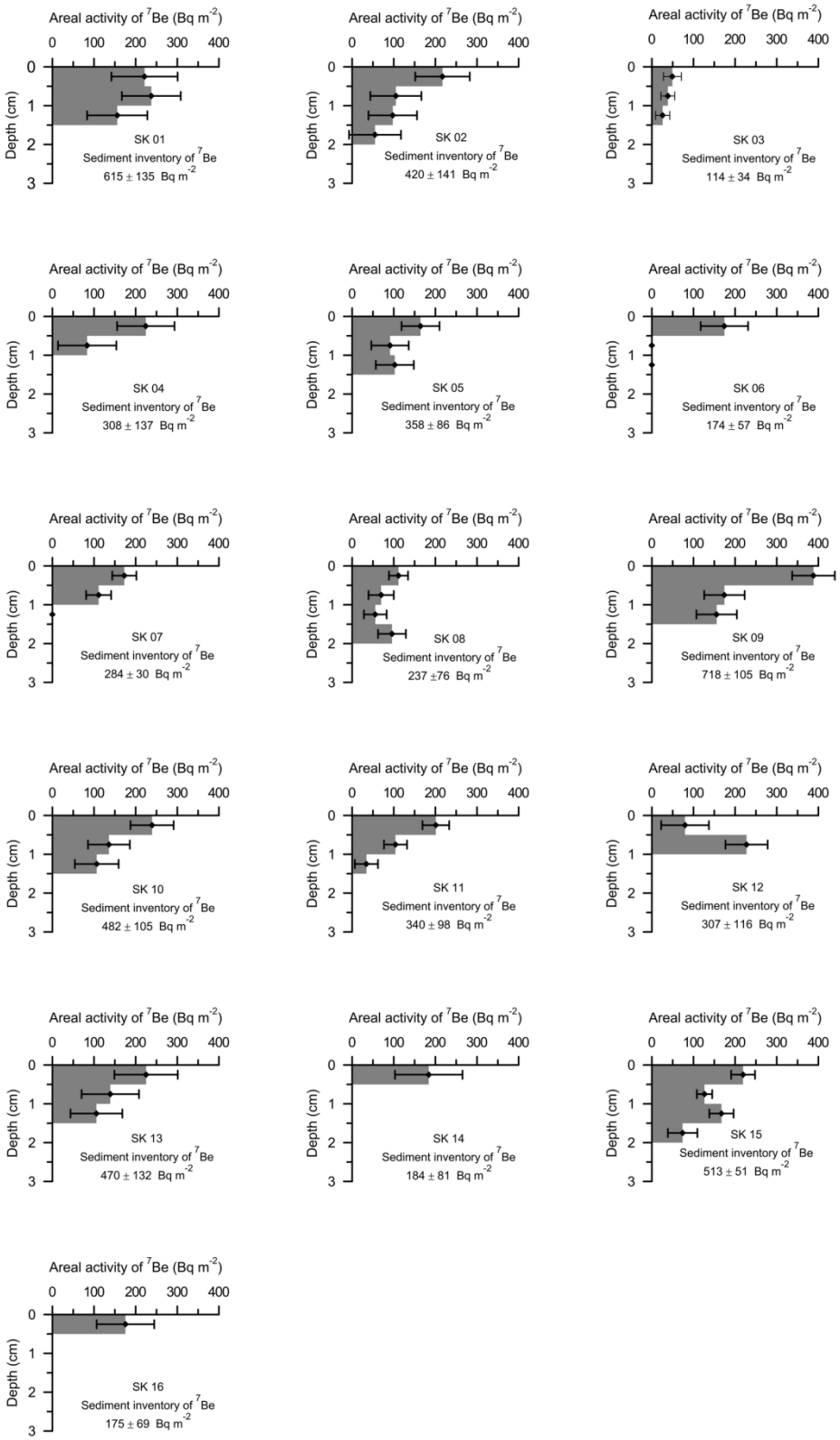

Figure 3.7 The vertical profiles of areal activity of ^{7}Be in lake sediment versus sediment depth, the measured sediment inventory of ^{7}Be in these sampling cores in the outer part of the Songkhla Lagoon

For the topmost sediment layer at 0 - 0.5 cm depth, the minimum and maximum areal activities of ^{7}Be are 49 ± 22 and 338 ± 51 Bq m^{-2}, found at site SK03 and SK09, respectively. The maximum depths at which the ^{7}Be is still measurable in the cores ranged from 0.5 cm at sites SK06, SK14 and SK16 to 2.0 cm at sites SK02 and SK15. The vertical depth profiles of areal activities of ^{7}Be at some locations: SK01, SK02, SK05, SK08, SK09, SK12 and SK15 show the nonuniformly decreased curve with depths. This pattern probably reflects nonuniform deposition of sediment on the lake bottom due to resuspension of early deposited sediment, excess sediment deposited on the opposite sense, the horizontal dynamic movements and the bioturbation. The sediment inventories of ^{7}Be and the penetration depths are high in sites SK01, SK02, SK05, SK09, SK13 and SK15 (Figure 3.7) likely indicating a high sediment accumulation rate or high vertical and spatial heterogeneity in these sites.

However, the maximum depths of ^{7}Be penetration of about 1.5 – 2.0 cm may not relate to the rate of sedimentation because the bed sediments can be probably redistributed by wind that occur strongly during 10.00 a.m. – 19.00 p.m. every day. It can generate strong wind waves, simultaneously even when the tidal stages (flood and ebb) change. Therefore, influences by the wind waves and diurnal variation of tide naturally affect the sediment redistribution in the Thale Sap Songkhla.

In this study, we used the assumption that the direct deposition of ^{7}Be is constant, because the production of ^{7}Be is relatively constant in the atmosphere over a region. Although, its value can vary spatially by up to an order of magnitude, depending on factors such as rainfall and geographical location (e.g. Schuller et al., 2006; Schuller et al., 2010; Sepulveda et al., 2008; Steinmann et al., 1999; Walling, 2004; Zhu and Olsen, 2009). The principle method applied in this study is as follows; ^{7}Be reaches the soil surface and attaches strongly to fine particles (e.g. Schmidt et al., 2007a and 2007b; Schuller et al., 2006; Schuller et al., 2010; Sepulveda et al., 2008). The ^{7}Be attached soil is then eroded from the watershed and transported to the lake, and the ^{7}Be inventory activity is therefore applied to estimate the deposition. The highest ^{7}Be inventory activity corresponds to the greatest sedimentation rate, and depth distribution processes. Moreover, it can be used to describe the short-term sedimentation patterns and the distribution of ^{7}Be inventory activity can be used to define the sediment depocenters in the lake. The ^{7}Be sediment inventories in the outer

Songkhla lagoon ranged between 114 ± 34 Bq m^{-2} at site SK03 and 718 ± 105 Bq m^{-2} at site SK09. They are presented together with the difference values between the ^{7}Be sediment inventory and the expected running inventory (156 Bq m^{-2}). The ^{7}Be sediment inventory is plotted on the colored contour map as shown in Figure 3.8b. This Figure shows the two highest ^{7}Be inventory area where can be interpreted as the rapid sedimentation zones, at the northern part of the lagoon (Pak Ro delta; Zone A) and the south of the lagoon (U-Tapao, Ro-1, Ro-3 deltas; Zone B), and the two lowest ^{7}Be inventory zones where a slow sedimentation occurred, including the southwest of the lagoon (Ratthaphum delta; zone C) and the northern tip of the Ko Yo island (zone D).

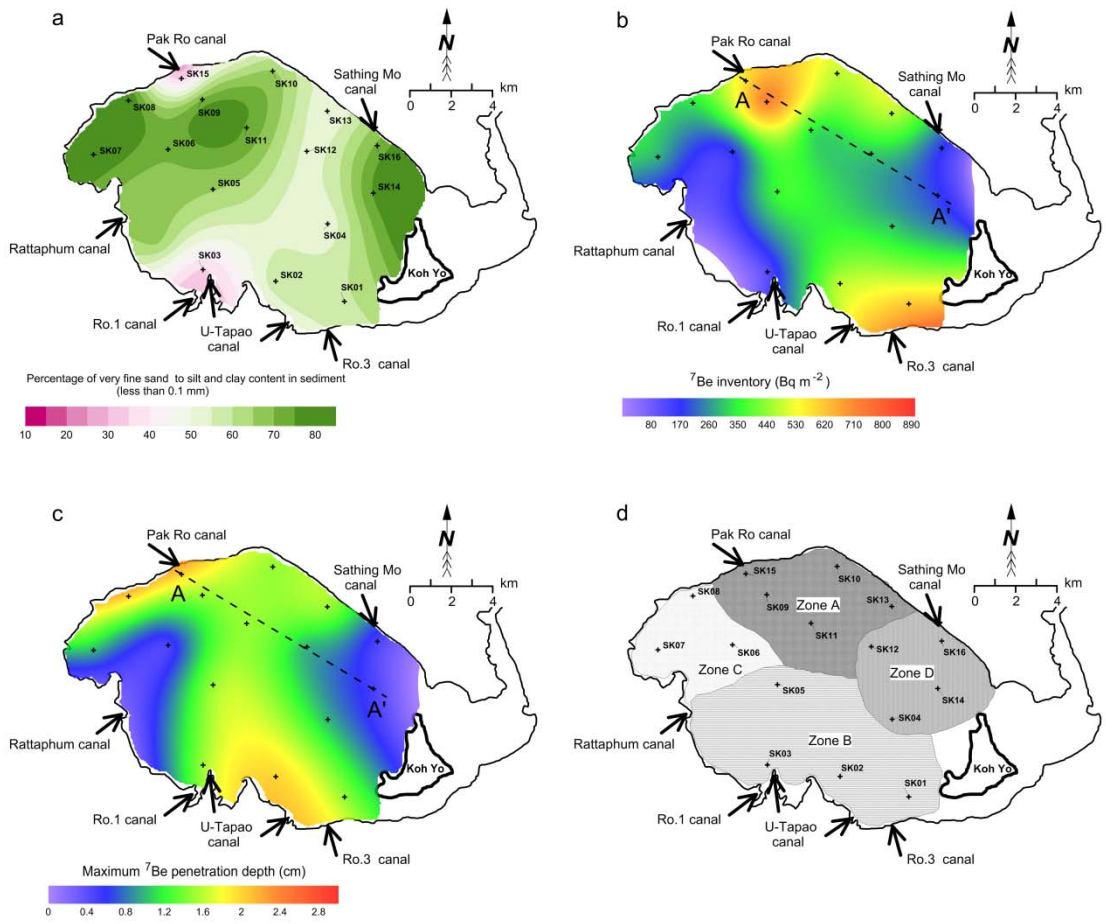

Figure 3.8 Shaded color map of **a)** percentage of very fine sand to silt and clay content in sediment **b)** ^{7}Be inventory, **c)** maximum penetration depth of ^{7}Be, and **d)** separated zones of sedimentation/erosion pattern

It is true that the velocity of the water current will be slower when the runoff and flood carrying eroded sediments from their subcatchment flow into the lake, and therefore the sediment mainly deposits near to the mouth of the river or canal depending on grain sizes and distance from the mouth. At the Pak Ro delta area (zone A in Figure 3.8d), the ^{7}Be sediment inventory is high ranging between 340 Bq m^{-2} and 718 Bq m^{-2}. These results reveal that large amount of sediments are transported from the Middle Songkhla Lagoon and nearby subcatchment and deposited near the mount of the Pak Ro canal. The large portion of eroded sediments probably occurs in the modern rubber and palm plantations and cultivated rice fields in the subcatchment. So, the measured ^{7}Be in the top layer of lake sediment can be applied to estimating the recent sedimentation patterns in the lake.

Zone B or U-Tapao delta has the rapid sedimentation and deeper vertical distribution process, because the extreme water inflow and the eroded sediment from U-Tapao subbasin were immediately transported to this area by Ro-1 and Ro-3 canals that were constructed to bypass the overflow and to protect flooding in Hat-Yai city in the rainy season. The inventory of ^{7}Be in Zone C is low indicating a quiet sedimentation that is probably due to a small size of the Khlong Ratthapum subcatchment (625 km^{2}) with soil erosion less than that of a much bigger U-Tapao subcatchment (2357 km^{2}). In zone D, the sediment inventories of ^{7}Be for sites SK04, SK12, SK14 and SK16 are less than those of Zone A and B, and are comparable to the atmospheric running inventory. This reveals therefore that this area experiences both sedimentation and erosion because this zone is strongly influenced by the tidal current and wind wave coming from the Gulf of Thailand.

3.3.2 Sediment mixing in the outer Songkhla lagoon demonstrated by the ^{7}Be and ^{210}Pb profiles (paper IV)

In this section, we present the sediment mixing rates derived by the $^{210}Pb_{ex}$ and ^{7}Be in lagoon sediment. The long-term sediment mixing rates evaluated by $^{210}Pb_{ex}$ profiles rage from 8.7 to 41.9 cm^{2} y^{-1}. Moreover, these $^{210}Pb_{ex}$ profiles demonstrated the sedimentation rates between 0.37 and 0.81 cm y^{-1} as shown in Figure 3.9.

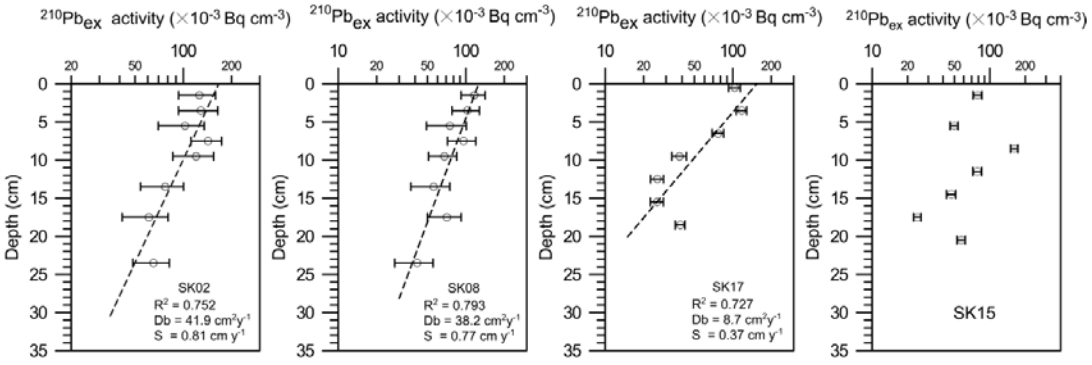

Figure 3.9 the $^{210}Pb_{ex}$ activity profiles from the outer Songkhla lagoon.

The ^{7}Be activity profiles show the maximum penetration depths or the thickness of particle mixed layer ranged from 0.5 cm to 2.0 cm as shown in Figure 3.10. The sediment mixing rates derived by the ^{7}Be range from 0.04 to 37.69 cm^{2} y^{-1} at the central of lagoon and discharge area, respectively.

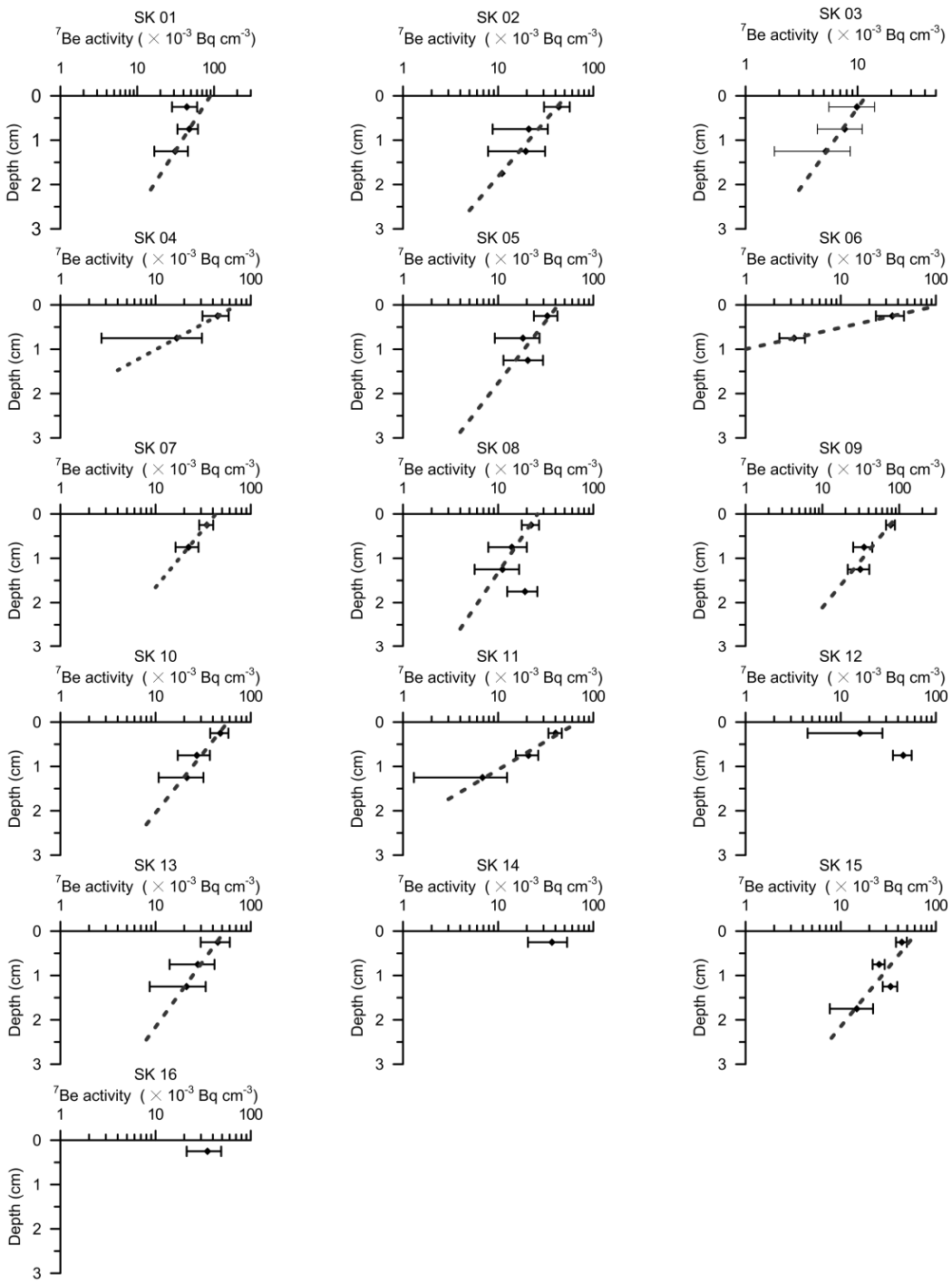

Figure 3.10 ^{7}Be activity profiles from the outer Songkhla lagoon. The curves correspond to those used with Equation to estimate mixing rates.

The mixing depths obtainted from the penetration depths of ^{7}Be activity are high in sites SK01, SK02, SK05, SK09, SK13 and SK15 (**Figure 3.10**).The classified sediment mixing coefficients are plotted on the shaded color maps of the clay-normalized ^{7}Be activities (**Figure 3.11a**) which remove any effects related to particle size changes in vertical activity and of the sediment inventory of ^{7}Be (**Figure 3.11b**). The contour maps of the clay-normalized ^{7}Be activities (**Figure 3.11a**) and the sediment inventory of ^{7}Be (**Figure 3.11b**) illustrate identically two high activity zones located adjacent to the Pak Ro and Ro.3 canal mouths. These two zones can probably imply that both high recent sediment deposition and bioturbation or bioturbation plus sediment accumulation were occurred, because the clay-normalized ^{7}Be activities were indicated in two pathways: 1) rapid transport and deposition during floods resulting in low activities, and 2) slow transport and deposition such that bioturbation rates exceeded burial rates resulting in high activities (e.g. Addington et al., 2007; Kniskern et al., 2010; Sommerfield et al., 1999). By the same way, the ^{7}Be inventories in the sediment control both the sediment deposition/erosion (e.g. Aller and DeMaster, 1984; Crusius et al., 2004; Fitzgerald et al., 2001; Krishnaswami et al., 1980; Neubauer et al., 2002; Palinkas et al., 2005; Sommerfield et al., 1999) and the bioturbation (Osaki et al., 1997; Aller and DeMaster, 1984). Moreover, there is high distribution of particle-reactive radionuclide in the sediment column also indicating that high sedimentation and bioturbation are occurred at these zones (Palinkas et al., 2005; Schmidt et al., 2007a). The high sediment mixing coefficients (8.5 – 37.7 cm^2 y^{-1}) observed at sites SK01, SK02, SK08, SK09, SK10 and SK15 using the sedimentation rates calculated from ^{210}Pb profile confirm high bioturbation occurring at the Pak Ro and Ro.3 canal mouths.

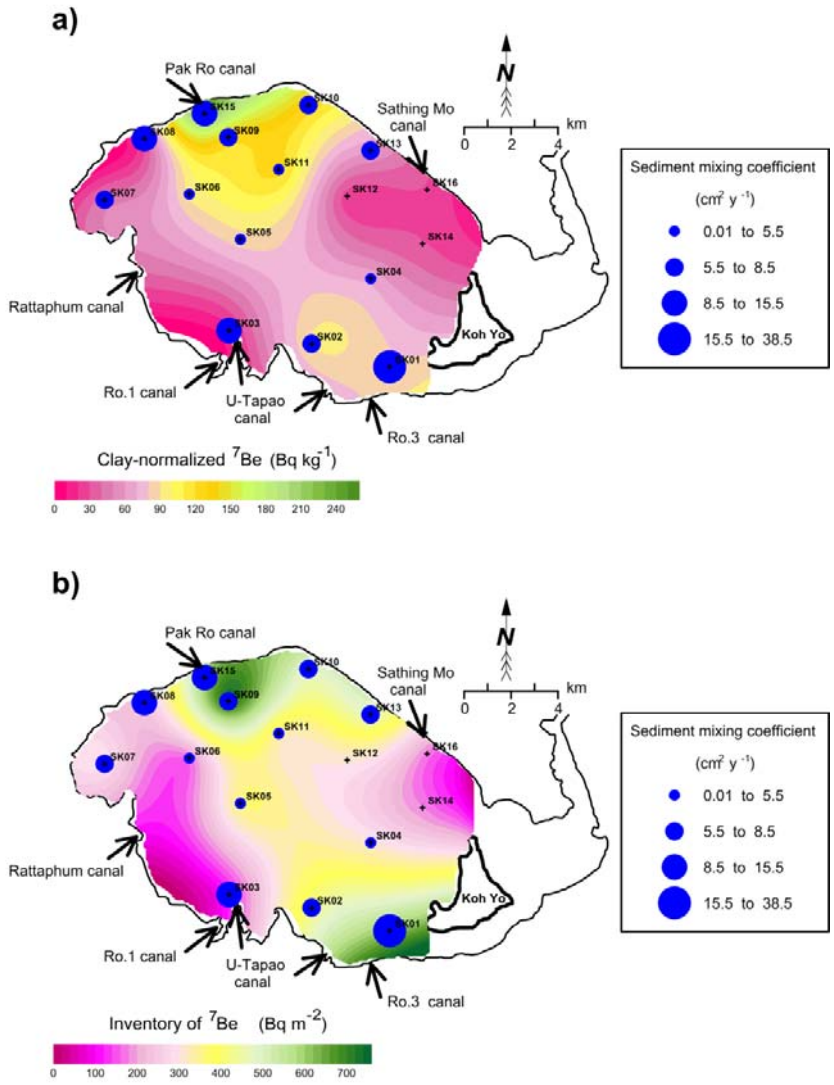

Figure 3.11 Shaded color map of **a**) clay-normalized ^{7}Be activity, and **b**) the inventory of ^{7}Be activity with the classified plot of sediment mixing coefficients on the Outer Songkhla lagoon map.

The result shows that the high sediment mixing coefficients (8.5 – 37.6 $cm^2\ y^{-1}$) are observed to occur near the shore line of the lagoon and mouth of canal as demonstrated at sites SK01, SK03, SK08 and SK15, whereas low mixing coefficients (0.04 – 5.5 $cm^2\ y^{-1}$) are present at the central lagoon area (sites SK04, SK05, SK06, and SK11). It indicates that the biological activities or bioturbation processes occur near the shore line of the lagoon and mouth of canal more than the central lagoon area.

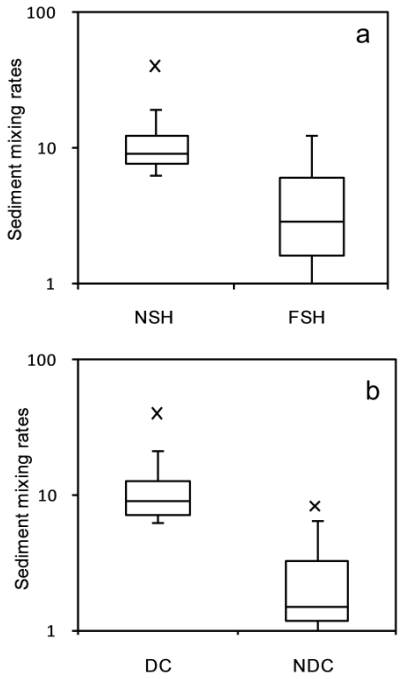

Figure 3.12 Box plots of ^{7}Be activity are classified by a) near shrimp farming (NSH) and far shrimp farming (FSH) groups and b) discharge (DC) and non-discharge (NDC) area groups

To test the effect of bioturbation, we classify the sampling sediment cores to the near shrimp farming (NSH) group being within 2.5 km from shrimp farms and the far shrimp farming (FSH) group and discharge (DC) and non-discharge (NDC) area groups. The average sediment mixing rates of each group are compared by using the statistical test, the *Wilcoxon signed-rank test* which is a non-parametric statistical hypothesis test for non-normal distribution data. The comparison between the sediment cores in NSH and FSH areas shows the average sediment mixing coefficients of 13.6 cm y^{-1} and 4.4 cm y^{-1}, respectively, (**Figure 3.12**) that are significantly different at $p < 0.05$. The group of the sediment mixing rates, near shrimp farming areas, shows that it is significantly higher than other groups, far shrimp farming areas. Moreover, the averages of mixing rates in the discharge and non discharge areas show significantly different as shown in **Figure 3.12**. Considering in preliminary, the shrimp farms and discharge areas are influenced the redistribution of sediment at the water-sediment interface.

3.4 Dating method by radionuclides (^{137}Cs and ^{210}Pb) in the sediment (paper V)

In this section, we present the preliminary analyses and results of sedimentation rates. One site from U-Tapao estuary located in the outer Songkhla lagoon, southern Thailand was selected and the vertical profiles of excess ^{210}Pb and ^{137}Cs were used for analyses as shown in Figure 3.13.

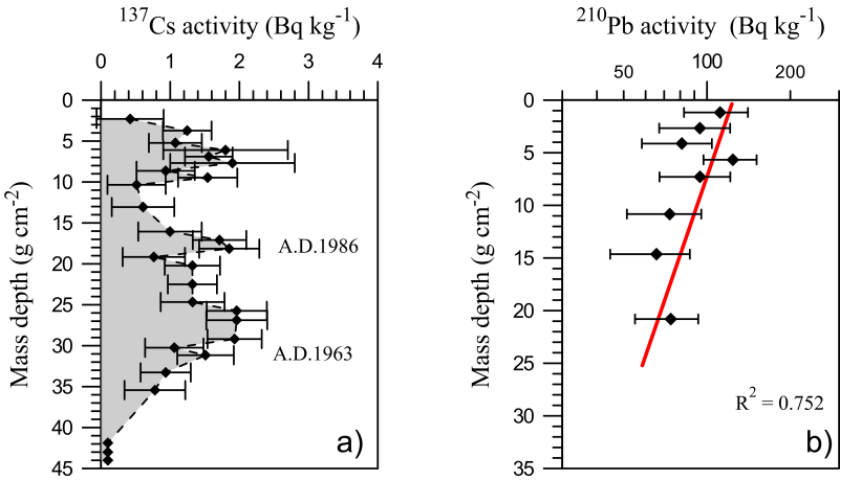

Figure 3.13 a) ^{137}Cs depth profile, **b)** ^{210}Pb activity profiles from the outer Songkhla lagoon. The curve corresponds to those used by the CIC model to estimate sedimentation rate.

The results of sediment samples from a single core coded SK02 selected for interpretation of two different sedimentation processes. It can be seen that the ^{137}Cs time-markers correspond to the fallout from the Chernobyl nuclear accident in 1986 and the highest atmospheric thermonuclear weapon testing in 1963. Both chronologic markers can be identified as shown in **Figure 3.13**. The average accumulation rates determined by ^{137}Cs method are 5.7 (linear sedimentation rate 0.52 cm y^{-1}), and 6.5 kg m^{-2} year^{-1} (linear sedimentation rate 0.78 cm y^{-1}) from 1963 to 1986 and 1986 to sampling time, respectively. For previous study in the Outer Songkhla Lagoon, Chittrakarn et al (1997) was reported the sedimentation rate of 0.57 cm y^{-1} near the Pak Ro channel by this method also. Moreover, the total sediment discharged into the outer Songkhla lagoon system in 2002 was estimated by the

Universal Soil Loss Equation (USLE) model in GIS environment to be 6.89×10^9 kg, an average of 8.14×10^5 kg km^{-2} of the basin. The sedimentation rate of 0.44 cm y^{-1} was approximately estimated (Tanavud et al., 2006), which is lower than our rates at SK02 and SK08 but little higher than our rate at SK17.

The $^{210}Pb_{ex}$ dating method can be used to estimate the sedimentation rates in this site. The depth distribution of $^{210}Pb_{ex}$ activity shows some regular decreasing trend. It was supposed that the simplest CIC model can be applied in the estimation of sediment mass accumulation at this location. The mean sedimentation rate is 9.62 kg m^{-2} y^{-1}, calculated from the slope of the graph between the logarithmic scale of the $^{210}Pb_{ex}$ activity and mass depth. Moreover, the mass accumulation rates obtained by the CRS model are between 8.3 and 3.3 kg m^{-2} y^{-1}. The CRS model provides the best result that the marker-peak values of ^{137}Cs are validated as shown in **Figure 3.14**.

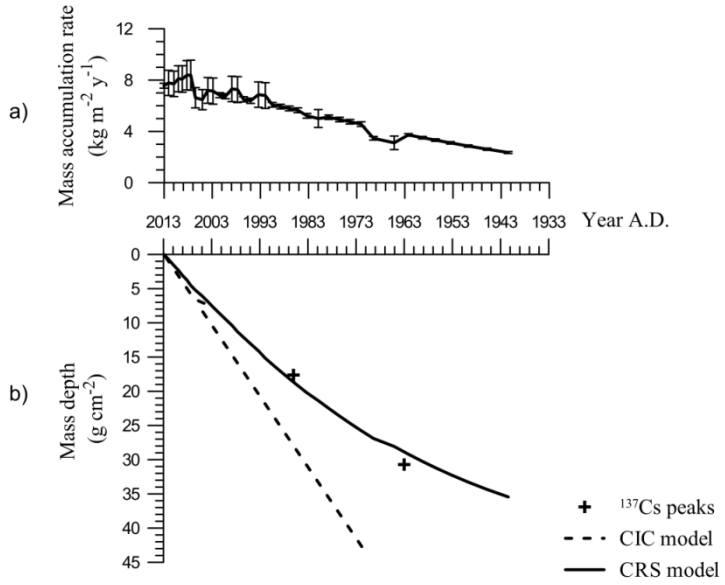

Figure 3.14 a) results obtained by estimating from CIC and CRS models and validated by ^{137}Cs markers, **b)** comparison between mass accumulation rates obtained from CRS model and ^{137}Cs method

CHAPTER 4

CONCLUDING REMARKS

This study uses the atmospheric radionuclides (^{7}Be, ^{137}Cs and ^{210}Pb) to understand aerosols deposition processes at the Songkhla province, Southern Thailand where is low latitude and the tropical zone, to classify the sediment deposition and erosion zones in the Songkhla lagoon, and to apply for calculation of sedimentation rates on the Songkhla lagoon. First part, the atmospheric concentration and deposition fluxes of ^{7}Be were measured at three sites in the U-Tapao watershed, Songkhla province during December 2012 – January 2014. Based on this study, mean values of specific concentrations of ^{7}Be are influenced by seasonal variations and washout and rainout effects. The average annual depositional flux of ^{7}Be of 480.8 Bq m^{-2} is lower than those reported in other locations in the world. The monthly depositional flux of ^{7}Be did not remain constant which varied between 0.6 and 103 Bq m^{-2}. The correlation between atmospheric depositional fluxes of ^{7}Be and event rainfall, monthly rainfall, and event rainfall separated by NE, SW, and summer seasons are strong significantly. These relationships were used to understand the behavior of deposition of ^{7}Be in our study area. In addition, the depositional running inventory of ^{7}Be was calculated from event atmospheric depositional fluxes. It was used as reference value for the soil erosion and sedimentation model, and for evaluation of erosion and/or deposition patterns of sediment in the Outer Songkhla lagoon. In the future, the fluxes of atmospheric ^{7}Be should be measured continuously in long term for baseline data to apply in other studies.

The second part is the preliminary study being successful to detect ^{7}Be in the soil and atmospheric deposition in the South of Thailand located near equatorial zone where is known to very low ^{7}Be activity. The ^{7}Be activity in soil profiles of the selected reference sites can be used to estimate the relaxation mass depth and reference inventory for approached model of the soil erosion and deposition. This reference sediment inventories collected from two study sites were compared with the running atmospheric depositional fluxes and activity of ^{7}Be in cover grasses. We know that the cover grasses can absorb the ^{7}Be, therefore future study and reference

sites should be carefully collected less than ^{7}Be absorption effect. Further works, we will investigate the magnitudes of both soil erosion and deposition obtained from the ^{7}Be measurement technique in this study area.

The applications of using the atmospheric radionuclides (^{7}Be, ^{137}Cs and ^{210}Pb) are shown in the third and forth parts. For concluding our study in the third part, the measurement of atmospheric beryllium-7 in lagoon-bottom sediment cores can evaluate the short-term sedimentation pattern in the Outer Songkhla Lagoon. The sediment inventories as well as depth distributions of ^{7}Be in sediment samples taken in Songkhla Lagoon indicate sediment accumulation zones at the Pak Ro zone and the U-Tapao zone, while the northern tip of Koh Yo island is probably an erosion zone. These results suggest that ^{7}Be can serve as a useful tool for quantifying short-term changes in sediment dynamics. We found that the vertical profile of ^{7}Be in the sediment cores indicating continuous sediment deposition without mixing (exponential uniformly decreasing) was observed at just a few locations, but other sampling sites the vertical distributions of ^{7}Be inventories were not uniform indicating high dynamic and changes in sedimentation process, probably caused by hydrodynamic properties of lagoon water system. Obtained results are very encouraging and complete understanding of sedimentation can be gained after repeated measurements and comparison of measured short-term changes in the ^{7}Be sediment inventories and depth profiles with respect to characteristic seasonal and hydrological conditions in this area.

Moreover, the measurement of atmospheric ^{7}Be and ^{210}Pb in lagoon-bottom sediment cores from the Outer Songkhla lagoon to calculate the sediment mixing rates indicating the particle exchanged processes at the sediment-water interface. We present the sediment mixing rates derived by the long- and short- term sediment mixing rates evaluated by $^{210}Pb_{ex}$ profiles and ^{7}Be profiles, respectively. The sediment mixing rates derived $^{210}Pb_{ex}$ profiles are 41.9, 38.2 and 8.7 $cm^2\ y^{-1}$ for selected three sites SK02, SK08 and SK17, respectively. The sediment mixing rates derived by the ^{7}Be range from 0.04 to 37.69 $cm^2\ y^{-1}$ at the central of lagoon and discharge area, respectively. The spatial distribution of sediment mixing coefficients derived from ^{7}Be activity in the Outer Songkhla lagoon can be considered. The group of the

sediment mixing rates, near shrimp farmimg areas, shows that it is significantly higher than other groups, far shrimp farmimg areas. Moreover, the averages of mixing rates in the discharge and non discharge areas show significantly different. Considering in preliminary, the shrimp farms and discharge areas influence the redistribution of sediment at the water-sediment interface.

The final part, the sedimentation rates in the Outer Songkhla lagoon were evaluated by using the atmospheric radionuclides (^{137}Cs and ^{210}Pb) profiles in the sediment cores. The vertical profiles of excess ^{210}Pb and ^{137}Cs from selected site from U-Tapao estuary located in the Outer Songkhla lagoon, southern Thailand was selected to calculate the sedimentation rates. The results of sediment profile can be seen that the ^{137}Cs time-markers correspond to the fallout from the Chernobyl nuclear accident in 1986 and the highest atmospheric thermonuclear weapon testing in 1963. The average accumulation rates determined by ^{137}Cs method are 5.7 and 6.5 kg m^{-2} year^{-1} from 1963 to 1986 and 1986 to sampling time, respectively. The sediment accumulation rates obtained by ^{210}Pb dating models (CIC and CRS) range from 3.3 to 8.8 kg m^{-2} year^{-1} during sampling time to 1954. Moreover, using two-marker events based on ^{137}Cs activity to validate age of sediment layers obtained by ^{210}Pb method shows good result.

Our study shows that the atmospheric radionuclides (^{7}Be, ^{137}Cs and ^{210}Pb) can measure and apply in the Songkhla province, southern Thailand located near equatorial zone at low latitude ,where the atmospheric radionuclide activities are low. Therefore, the application of these radionuclides would be benefit for future study. It will provide an understanding of the dynamics of pollutants, and aid in developing sustainable effective management.

REFERENCES

Abril, J. M., 2004. Constraints on the use of ^{137}Cs as a time-marker to support CRS and SIT chronologies. Environ. Pollut. 129, 31–37.

Addington, L. D., Kuehl, S. A., McNinch, J. E., 2007. Contrasting modes of shelf sediment dispersal off a high-yield river: Waiapu River, New Zealand. Mar. Geol. 243, 18–30.

Ahn, Y. S., Nakamura, F., Chun, K. W., 2010. Recent history of sediment dynamics in Lake Toro and applicability of ^{210}Pb dating in a highly disturbed catchment in northern Japan. Geomorphology 114, 284–293.

Aller, R. C., DeMaster, D. J., 1984. Estimates of particle flux and reworking at the deep-sea floor using $^{234}Th/^{238}U$ disequilibrium. Earth Planet. Sci. Lett. 67, 308–318.

Alonso-Hernandez, C. M., Diaz-Asencio, M., Munoz-Caravaca, a., Delfanti, R., Papucci, C., Ferretti, O., Crovato, C., 2006. Recent changes in sedimentation regime in Cienfuegos Bay, Cuba, as inferred from ^{210}Pb and ^{137}Cs vertical profiles. Cont. Shelf Res. 26, 153–167.

Angsupanich, S., Kuwabara, R., 1999. Distribution of macrobenthic fauna in Phawong and U-Taphao canals flowing into a lagoonal lake, Songkhla, Thailand. Lakes Reserv. Res. Manag. 4, 1–13.

Anokhina, A., et al., 2008. Study of the effects induced by lead on the emulsion films of the OPERA experiment. J. Instrum. 3, 1–17.

Appleby, P. G., 2001. Chronostratigraphic techniques inrecent sediments, in: Last, W.M., J. P. Smol (Eds.), Tracking Environmental Change Using Lake Sediments. Vollume 1: Basin Analysis, Coring, and Chronological Techniques. Kluwer Academic Publishers, Dordrecht, the Netherlands, pp. 171–203.

Bai, Z. G., Wan, G. J., Huang, R. G., Liu, T. S., 2002. A comparison on the accumulation characteristics of ^{7}Be and ^{137}Cs in lake sediments and surface soils in western Yunnan and central Guizhou , China. Catena 49, 253–270.

Baskaran, M., 1995. A search for the seasonal variability on the depositional fluxes of Be-7 and Pb-210. J. Geophys. Res. 100, 2833–2840.

Baskaran, M., Nix, J., Kuyper, C., Karunakara, N., 2014. Problems with the dating of sediment core using excess ^{210}Pb in a freshwater system impacted by large scale watershed changes. J. Environ. Radioact. 138, 355–363.

Begy, R., Cosma, C., Timar, A., 2009. Recent changes in Red Lake (Romania) sedimentation rate determined from depth profiles of ^{210}Pb and ^{137}Cs radioisotopes. J. Environ. Radioact. 100, 644–648.

Belmaker, R., Stein, M., Beer, J., Christl, M., Fink, D., Lazar, B., 2014. Beryllium isotopes as tracers of Lake Lisan (last Glacial Dead Sea) hydrology and the Laschamp geomagnetic excursion. Earth Planet. Sci. Lett. 400, 233–242.

Bhongsuwan, T., Bhongsuwan, D., 2002. Concentration of heavy metals Mn, Fe, Ni, Pb, Cr and Cd in bottom sediments of the Outer Songkhla Lake deposited between the year B.E. 2520-2538. Songklanakarin J. Sci. Technol. 24, 89–106.

Blake, W. H., Walling, D. E., He, Q., 2002. Using cosmogenic beryllium-7 as a tracer in sediment budget investigations. Geogr. Ann. 84 A, 89–102.

Blake, W. H., Walling, D. E., He, Q., 1999. Fallout beryllium-7 as a tracer in soil erosion investigations. Appl. Radiat. Isot. 51, 599–605.

Bonotto, D. M., García-Tenorio, R., 2014. A comparative evaluation of the CF:CS and CRS models in ^{210}Pb chronological studies applied to hydrographic basins in Brazil. Appl. Radiat. Isot. 92, 58–72.

Chevakidagarn, P., 2006. Operational problems of wastewater treatment plants in Thailand and case study: wastewater pollution problems in Songkhla Lake Basin. Songklanakarin J. Sci. Technol. 28, 633–639.

Chittrakarn, T., Bhongsuwan, T., Nunnin, P., Thong-jerm, T., 1997. The determination of sedimentation rate in Songkhla Lake using isotopic technique. Songkhla.

Ciffroy, P., Reyss, J. -L., Siclet, F., 2003. Determination of the residence time of suspended particles in the turbidity maximum of the Loire estuary by ^{7}Be analysis. Estuar. Coast. Shelf Sci. 57, 553–568

Conaway, C. H., Storlazzi, C. D., Draut, A. E., Swarzenski, P. W., 2013. Short-term variability of ^{7}Be atmospheric deposition and watershed response in a Pacific coastal stream, Monterey Bay, California, USA. J. Environ. Radioact. 120, 94–103.

Crusius, J., Bothner, M. H., Sommerfield, C. K., 2004. Bioturbation depths, rates and processes in Massachusetts Bay sediments inferred from modeling of ^{210}Pb and $^{239+240}$Pu profiles. Estuar. Coast. Shelf Sci. 61, 643–655.

DeMaster, D. J., McKee, B. A., Nittrouer, C. A., Brewster, D. C., Biscaye, P. E., 1985. Rates of sediment reworking at the HEBBLE site Based on measurements of Th-234 , Cs-137 and Pb-210. Mar. Geol. 66, 133 – 148.

Di Gregorio, D. E., Fernández Niello, J. O., Huck, H., Somacal, H., Curutchet, G., 2007. Pb dating of sediments in a heavily contaminated drainage channel to the La Plata estuary in Buenos Aires , Argentina. Appl. Radiat. Isot. 65, 126–130.

Doering, C., Akber, R., Heijnis, H., 2006. Vertical distributions of ^{210}Pb excess, ^{7}Be and ^{137}Cs in selected grass covered soils in Southeast Queensland, Australia. J. Environ. Radioact. 87, 135–47.

Du, P., Walling, D. E., 2012. Pb measurements to estimate sedimentation rates on river floodplains. J. Environ. Radioact. 103, 59–75.

Feely, H. W., Larsen, R. J., Sanderson, C.G., 1989. Factors that cause seasonal variations in Beryllium-7 concentrations in surface air. J. Environ. Radioact. 9, 223–249.

Feng, H., Cochran, J. K., Hirschberg, D. J., 1999. ^{234}Th and ^{7}Be as tracers for the transport and dynamics of suspended particles in a partially mixed estuary. Geochim. Cosmochim. Acta 63, 2487–2505.

Fitzgerald, S. A., Klump, J. V., Swarzenski, P. W., Mackenzie, R. A., Richards, K. D., 2001. Beryllium-7 as a tracer of short-term sediment deposition and resuspension in the Fox River Wisconsin. Environ. Sci. Technol. 35, 300–305.

Furuichi, T., Wasson, R. J., 2013. Caesium-137 in Southeast Asia: Is there enough left for soil erosion and sediment redistribution studies? J. Asian Earth Sci. 77, 108–116.

Gyawali, S., Techato, K., Monprapussorn, S., Yuangyai, C., 2013. Integrating Land Use and Water Quality for Environmental based Land Use Planning for U-Tapao River Basin, Thailand. Procedia - Soc. Behav. Sci. 91, 556–563.

He, Q., Walling, D. E., 1996. Interpreting particle size effects in the adsorption of ^{137}Cs and unsupported ^{210}Pb by mineral soils and sediments. J. Environ. Radioact. 30, 117–137.

Ioannidou, A, Papastefanou, C., 2006. Precipitation scavenging of ^{7}Be and ^{137}Cs radionuclides in air. J. Environ. Radioact. 85, 121–36.

Ishikawa, Y., Murakami, H., Sekine, T., Yoshihara, K., 1995. Precipitation scavenging studies of radionuclides in air using cosmogenic ^{7}Be. J. Environ. Radioact. 26, 19–36.

Jweda, J., Baskaran, M., van Hees, E., Schweitzer, L., 2008. Short-lived radionuclides (^{7}Be and ^{210}Pb) as tracers of particle dynamics in a river system in southeast Michigan. Limnol. Ocean. 53, 1934–1944.

Kato, Y., Kitazato, H., Shimanaga, M., Nakatsuka, T., Shirayama, Y., Masuzawa, T., 2003. ^{210}Pb and ^{137}Cs in sediments from Sagami Bay, Japan: Sedimentation rates and inventories. Prog. Oceanogr. 57, 77–95.

Kim, G., Hussain, N., Scudlark, J.R., Church, T.M., 2000. Factors influencing the atmospheric depositional fluxes of stable Pb , ^{210}Pb , and ^{7}Be into Chesapeake Bay. J. Atmos. Chem. 36, 65–79.

Kirchner, G., 2011. ^{210}Pb as a tool for establishing sediment chronologies: examples of potentials and limitations of conventional dating models. J. Environ. Radioact. 102, 490–494.

Kitbamroong, K., Sompongchaiyaku, P., Padmanabhan, G., 2009. Improving non-point source pollution model input parameters using substance flux analysis. J. Appl. Sci. 9, 2519–2531.

Kniskern, T. A., Kuehl, S. A., Harris, C. K., Carter, L., 2010. Sediment accumulation patterns and fine-scale strata formation on the Waiapu River shelf, New Zealand. Mar. Geol. 270, 188–201.

Krishnaswami, S., Benninger, L. K., Aller, R. C., Von Damn, K. L., 1980. Atmospherically-derived radionuclides as tracers of sediment mixing and accumulation in near-shore marine and lake sediment: evidence from ^{7}Be, ^{210}Pb, and $^{239, 240}$Pu. Earth Planet. Sci. Lett. 47, 307–318.

Ladachart, R., Suthirat, C., Hisada, K., Charusiri, P., 2011. Distribution of heavy metals in core sediments from the Middle part of Songkhla lake, Southern Thailand. J. Appl. Sci. 11, 3117–3129.

Lecroart, P., Maire, O., Schmidt, S., Grémare, A., Anschutz, P., Meysman, F. J. R., 2010. Bioturbation, short-lived radioisotopes, and the tracer-dependence of biodiffusion coefficients. Geochim. Cosmochim. Acta 74, 6049–6063.

Lecroart, P., Schmidt, S., Anschutz, P., Jouanneau, J. -M., 2007a. Modeling sensitivity of biodiffusion coefficient to seasonal bioturbation. J. Mar. Res. 65, 417–440.

Lecroart, P., Schmidt, S., Jouanneau, J. M., 2007b. Numerical estimation of the error of the biodiffusion coefficient in coastal sediments. Estuar. Coast. Shelf Sci. 72, 543–552.

Lu, X., Matsumoto, E., 2005. Recent sedimentation rates derived from ^{210}Pb and methods in Ise Bay , Japan. Estuar. Coast. Shelf Sci. 65, 83–93.

Mabit, L., Benmansour, M., Walling, D. E., 2008. Comparative advantages and limitations of the fallout radionuclides ^{137}Cs, $^{210}Pb_{ex}$ and ^{7}Be for assessing soil erosion and sedimentation. J. Environ. Radioact. 99, 1799–807.

Maneepong, S., 1996. Distribution of heavy metals in sediments from outer part of Songkhla Lagoon, southern Thailand. Songklanakarin J. Sci. Technol. 18, 87 – 97.

Maneepong, S., Angsupanich, S., 1999. Concentrations of arsenic and heavy metals in sediments and aquatic fauna from the outer part of Songkhla Lagoon, Phawong and U-Taphao canals. Songklanakarin J. Sci. Technol. 21, 111 – 121.

Matisoff, G., Wilson, C. G., Whiting, P. J., 2005. The$^{7}Be/^{210}Pb_{xs}$ ratio as an indicator of suspended sediment age or fraction new sediment in suspension. Earth Surf. Process. Landforms 30, 1191–1201.

Matsunaga, T., Amano, H., Ueno, T., Yanase, N., Kobayashi, Y., 1995. The role of suspended particles in the discharge of ^{210}Pb and ^{7}Be within the Kuji River watershed , Japan. J. Environ. Radioact. 26, 3–17.

McNeary, D., Baskaran, M., 2003. Depositional characteristics of ^{7}Be and ^{210}Pb in southeastern Michigan. J. Geophys. Res. 108, 4210.

Meysman, F. J. R., Boudreau, B. P., Middelburg, J. J., 2003. Relations between local, nonlocal, discrete and continuous models of bioturbation. J. Mar. Res. 61, 391–410.

Mizugaki, S., Nakamura, F., Araya, T., 2006. Using dendrogeomorphology and ^{137}Cs and ^{210}Pb radiochronology to estimate recent changes in sedimentation rates in Kushiro Mire , Northern Japan , resulting from land use change and river channelization. Catena 68, 25–40.

Narazaki, Y., Fujitaka, K., Igarashi, S., Ishikawa, Y., Fujinami, N., 2003. Seasonal variation of ^{7}Be deposition in Japan. J. Radioanal. andNuclear Chem. 256, 489–496.

Neubauer, S. C., Anderson, I. C., Constantine, J. A., Kuehl, S. A., 2002. Sediment deposition and accretion in a Mid-Atlantic (U.S.A.) tidal freshwater marsh. Estuar. Coast. Shelf Sci. 54, 713–727.

O' Reilly, J., Vintró, L. L., Mitchell, P. I., Donohue, I., Leira, M., Hobbs, W., Irvine, K., 2011. Pb-dating of a lake sediment core from Lough Carra (Co. Mayo, western Ireland): use of paleolimnological data for chronology validation below the Pb dating horizon. J. Environ. Radioact. 102, 495–499.

Osaki, S., Sugihara, S., Momoshima, N., Maeda, Y., 1997. Biodiffusion of ^{7}Be and ^{210}Pb in intertidal estuarine sediment. J. Environ. Radioact. 37, 55–71.

Palinkas, C. M., Nittrouer, C. A., Wheatcroft, R. A., Langone, L., 2005. The use of ^{7}Be to identify event and seasonal sedimentation near the Po River delta, Adriatic Sea. Mar. Geol. 222-223, 95–112.

Papastefanou, C., Ioannidou, A., 1995. Aerodynamic size association of ^{7}Be in ambient aerosols. J. Environ. Radioact. 26, 273–282.

Pope, R. H., Demaster, D. J., Smith, C. R., Seltmann, H., 1996. Rapid bioturbation in equatorial pacific sediments: Evidence from excess ^{234}Th measurements. Deep. Res. Part II Top. Stud. Oceanogr. 43, 1339–1364.

Pornpinatepong, K., Kiripat, S., Treewanchai, S., Chongwilaikasaem, S., Pornsawang, C., Chantarasap, P., Chandee, C., Jantrakul, P., 2010. Pollution conrol and sustainable Fisheries management in Songkhla Lake, Thailand. Songkhla.

Pradit, S., Pattarathomrong, M. S., Panutrakul, S., 2013. Arsenic Cadmium and Lead concentrations in sediment and biota from Songkhla Lake: A review. Procedia - Soc. Behav. Sci. 91, 573–580.

Rai, S. P., Kumar, V., Kumar, B., 2007. Sedimentation rate and pattern of a Himalayan foothill lake using ^{137}Cs and ^{210}Pb. Hydrol. Sci. J. 52, 181–191.

Reed, D. C., Huang, K., Boudreau, B. P., Meysman, F. J. R., 2006. Steady-state tracer dynamics in a lattice-automaton model of bioturbation. Geochim. Cosmochim. Acta 70, 5855–5867.

Schmidt, S., Gonzalez, J. -L., Lecroart, P., Tronczyński, J., Billy, I., Jouanneau, J. -M., 2007a. Bioturbation at the water-sediment interface of the Thau Lagoon: impact of shellfish farming. Aquat. Living Resour. 20, 163–169.

Schmidt, S., Jouanneau, J. -M., Weber, O., Lecroart, P., Radakovitch, O., Gilbert, F., Jézéquel, D., 2007b. Sedimentary processes in the Thau Lagoon (France): From seasonal to century time scales. Estuar. Coast. Shelf Sci. 72, 534–542.

Schuller, P., Iroumé, A., Walling, D. E., Mancilla, H. B., Castillo, A., Trumper, R. E., 2006. Use of beryllium-7 to document soil redistribution following forest harvest operations. J. Environ. Qual. 35, 1756–1763.

Schuller, P., Walling, D. E., Iroumé, A., Castillo, A., 2010. Use of beryllium-7 to study the effectiveness of woody trash barriers in reducing sediment delivery to streams after forest clearcutting. Soil Tillage Res. 110, 143–153.

Sepulveda, A, Schuller, P., Walling, D. E., Castillo, A, 2008. Use of ^{7}Be to document soil erosion associated with a short period of extreme rainfall. J. Environ. Radioact. 99, 35–49.

Simsek, F. B., Cagatay, M. N., 2014. Geochronology of lake sediments using ^{210}Pb with double energetic window method by LSC: an application to Lake Van. Appl. Radiat. Isot. 93, 126–33.

Sirinawin, W., Sompongchaiyakul, P., 2005. Nondetrital and total metal distribution in core sediments from the U-Tapao canal, Songkhla, Thailand. Mar. Chem. 94, 5–16.

Sirinawin, W., Turner, D. R., Westerlund, S., Kanatharana, P., 1998. Trace metals study in the Outer Songkla Lake, Thale Sap Songkhla, a southern Thai estuary. Mar. Chem. 62, 175–183.

Smith, J. N., Schafer, C. T., 1999. Sedimentation, bioturbation, and Hg uptake in the sediments of the estuary and Gulf of St. Lawrence. Limnol. Oceanogr. 44, 207–219.

Somayajulu, B. L. K., Bhushan, R., Sarkar, A., Burr, G. S., Jull, A. J. T., 1999. Sediment deposition rates on the continental margins of the eastern Arabian Sea using ^{210}Pb, ^{137}Cs and ^{14}C. Sci. Total Environ. 237-238, 429–439.

Sommerfield, C. K., Nittrouer, C. A., Alexander, C. R., 1999. ^{7}Be as a tracer of flood sedimentation on the northern California continental margin. Cont. Shelf Res. 19, 335–361.

Steinmann, P., Billen, T., Loizeau, J. -L., Dominik, J., 1999. Beryllium-7 as a tracer to study mechanisms and rates of metal scavenging from lake surface waters. Geochim. Cosmochim. Acta 63, 1621–1633.

Su, C. -C., 2003. Factors controlling atmospheric fluxes of ^{7}Be and ^{210}Pb in northern Taiwan. Geophys. Res. Lett. 30, 2018.

Tanavud, C., Yongchalermchai, C., Bennui, A., Densrisereekul, O., 2001. The expansion of inland shrimp farming and its environmental impacts in Songkla Lake Basin. Kasetsart J. (Natural Sci). 35, 326 – 343.

Taylor, A., Blake, W. H., Smith, H. G., Mabit, L., Keith-Roach, M. J., 2013. Assumptions and challenges in the use of fallout beryllium-7 as a soil and sediment tracer in river basins. Earth-Science Rev. 126, 85–95.

Walling, D. E., 2004. Using environmental radionuclides to trace sediment mobilisation and delivery in river basins as an aid to catchment management. Proc. Ninth Int. Symp. River Sediment. October 18, 121–135.

Walling, D. E., Collins, A. L., Sichingabula, H. M., 2003. Using unsupported Lead-210 measurements to investigate soil erosion and sediment delivery in a small Zambian catchment. Geomorphology 52, 193–213.

Wheatcroft, R. A., 2006. Time-series measurements of macrobenthos abundance and sediment bioturbation intensity on a flood-dominated shelf. Prog. Oceanogr. 71, 88–122.

Wikimedia, last modified 2016. Decay chain. Free Encycl. (Available https://en. wikipedia.org/wiki/Decay_chain)

Wikimedia, 2017a. Isotopes of beryllium. Free Encycl. (Available https://en. Wikipedia.org/wiki/Isotopes_of_beryllium)

Wikimedia, 2017b. Caesium-137. Free Encycl. (Available https://en.wikipedia.org/ wiki/Caesium-137)

Wikimedia, 2017c. Fission product yield. Free Encycl. (Available https://en. wikipedia.org/ wiki/ Fission_product_yield)

Yao, S. C., Li, S. J., Zhang, H. C., 2008. ^{210}Pb and ^{137}Cs dating of sediments from Zigetang Lake , Tibetan Plateau. J. Radioanal. Nucl. Chem. 278, 55–58.

Yi, Y., Zhou, P., Liu, G., 2007. Atmospheric deposition fluxes of ^{7}Be , ^{210}Pb and ^{210}Po at Xiamen , China. J. Radioanal. Nucl. Chem. 273, 157–162.

Zapata, F., 2002. Handbook for the assessment of soil erosion and sedimentation using environmental radionuclides. At. Energy.

Zhang, L., Yang, W., Chen, M., Wang, Z., Lin, P., Fang, Z., Qiu, Y., Zheng, M., 2016. Atmospheric Deposition of ^{7}Be in the Southeast of China: A Case Study in Xiamen. Areosol Air Qual. Res. 16, 105–113.

Zhu, J., Olsen, C.R., 2009. Beryllium-7 atmospheric deposition and sediment inventories in the Neponset River estuary, Massachusetts, USA. J. Environ. Radioact. 100, 192–197.

APPENDIX

This appendix shows the articles published in the international journal and in proceeding of international conferences, and the manuscripts for submission.

Paper I

Characteristics of Atmospheric ^{7}Be Deposition in the Songkhla Province, Thailand

Santi Raksawong[1], Miodrag Krmar[2], Tripob Bhongsuwan[1*]

[1] Nuclear Physics Research Laboratory and Geophysics Research Center, Department of Physics, Faculty of Science, Prince of Songkla University, Thailand

[2] Department of Physics, Faculty of Science, University of Novi Sad, Trg D. Obradovica 4, Novi Sad, 21000, Serbia

* Corresponding author. Tel: +66-0-7428-8761; fax: +66-0-7455-8849.

E-mail address: tripop.b@psu.ac.th (T. Bhongsuwan).

Manuscript for submission

Abstract

The natural radionuclide ^{7}Be has been widely used as tracers of aerosols for the study of pollution and atmospheric transport processes, and applied as a tracer to estimate soil erosion and sedimentation, river or lake sediment dynamic, sediment transport distance, etc. However, there are a few data of applications of ^{7}Be in the South East Asia. In this paper, we reported ^{7}Be concentrations and deposition fluxes of ^{7}Be observed from three sites in the Songkhla province on the U-Tapao watershed during December 2012 – January 2014, and discussed the factors controlling the deposition of this radionuclide. The mean values of specific concentrations of ^{7}Be in rain water were 0.24 ± 0.17, 0.23 ± 0.13 and 0.18 ± 0.06 Bq l^{-1} for sites S01, S02 and S03, respectively. The mean values of depositional fluxes of ^{7}Be were 11.6, 18.5 and 27.1 Bq m^{-2} for sites S01, S02 and S03, respectively. The average annual depositional flux of ^{7}Be of 480.8 Bq m^{-2} was lower than those previously reported in other locations in the world. The monthly depositional flux of ^{7}Be did not remain constant but varied between 0.6 and 103 Bq m^{-2} depending on the amount of monthly rainfall. Moreover, the depositional flux of ^{7}Be in northeast monsoon months was higher than that in the southwest monsoon months indicating more atmospheric ^{7}Be carried by the same amount of rainwater from the middle latitude. There are correlations between the annual depositional flux of ^{7}Be from our data and the previously reported in publications and horizontal, total geomagnetic field intensity.

Key words: ^{7}Be, wet deposition, 7Be rainwater content, geomagnetic field**,** Songkhla

Highlights

- ^{7}Be in precipitation was measured at the Songkhla province on the U-Tapao watershed during December 2012 – January 2014.
- Wet depositional flux of ^{7}Be was linearly correlated with precipitation, geomagnetic latitude, and horizontal and total geomagnetic field intensities.
- This relationship may be applied as a tool for assessing environmental processes.

1. Introduction

The natural radionuclide ^{7}Be has been widely used as tracers of aerosols for the study of pollution and atmospheric transport processes (e.g. Ayub et al., 2009; Blake et al., 1999; Kaste et al., 2002; Kim et al., 200; Krmar et al., 2009; Zhang et al., 2016). The knowledge of the vertical distribution in the atmosphere is a key parameter for modeling studies of dry and wet depositions, which are important processes to be taken into account in the case of a nuclear accident. Furthermore, this fallout radionuclide has been applied as a tracer to estimate soil erosion and sedimentation, river or lake sediment dynamic, sediment transport distance, etc (e.g. Balke et al., 1999; Jweda et al., 2008; Schuller et al., 2006; Sepulveda et al., 2008; Taylor et al., 2013; Zhu and Olsen. 2009;). Therefore, studying the deposition and removal processes of ^{7}Be-bearing aerosols is also helpful in understanding various atmospheric processes and influences of environmental variations.

^{7}Be (haft-life of 53.3 days) is continuously produced by interaction between the secondary particles (protons and neutrons) produced by galactic cosmic rays and light atmospheric nuclei such as carbon, nitrogen and oxygen (e.g. Conaway et al.,2013; Doering and Akber, 2008; González-Gómez et al., 2006; Ioannidou and Papastefanou, 2006; Krmar et al., 2007; Schuller et al., 2006; Yamamoto et al., 2006;). Its production rate depends on the flux of galactic cosmic rays (GCR), but the GCR are modulated by the solar activity and geomagnetic field (e.g. Akata et al., 2008; Krmar et al., 2013; Leppänen et al., 2010; Sakurai et al., 2005). The production of ^{7}Be occurs mainly in the upper stratosphere, and it decrease from the upper stratosphere to the lower troposphere (e.g. Caillet et al., 2001; Doering and Akber, 2008; Feely et al., 1989; González-Gómez et al., 2006; Renfro et al., 2013). Approximately, about 70 % of the production of ^{7}Be in the atmosphere, they are produced in the stratosphere, while the remaining part about 30% is produced in the upper troposphere (Piñero et al., 2012; Tositit et al., 2014; Usoskin and Kovaltsov., 2008). The deposition of ^{7}Be in the atmosphere depends not only on the influence of different air exchange rates between the stratosphere and troposphere but also on the rate of circulation and advection within the troposphere (Lecroart et al., 2005; Caillet et al., 2001; Renfro et al., 2013; Ali et al., 2011; Feely et al., 1989; Hirose et al.,

2004). Moreover, the concentrations of ^{7}Be in the atmosphere near the ground level are controlled by the latitude and the local meteorological conditions (Sakurai et al., 2004; Ali et al., 2011).

Although, there are the large databases of deposition fluxes of ^{7}Be reported by expert researchers from various regions in the world, a few data from Asia, especially from South East Asia are available compared with other regions. For Thailand, the ^{7}Be activity concentrations in mosses are reported by Krmar et al. (2013). They compared the ^{7}Be activity concentrations in mosses samples collected at the south of Thailand and in Serbia, the mean values of ^{7}Be activity concentration in the south of Thailand was almost 40% lower than activity of those collected in the Serbia. In this paper, we report ^{7}Be concentrations and deposition fluxes of ^{7}Be observed from three sites in the Songkhla province on the U-Tapao watershed, and discus the factors controlling the deposition of this radionuclide. The obtained atmospheric fluxes of ^{7}Be are expected to the application of understanding the sedimentary dynamics in the U-Tapao watershed and comparing with sediment inventory of ^{7}Be in the Songkhla lagoon.

2. Methodology

Three stations (S01, S02, and S03) are located in the U-Tapao subcatchment to collect the dry and wet depositions of ^{7}Be. The collectors were continuously deployed since December 2012 through January 2014 for periods from 1 to 31 days depending on the frequency of rain. The precipitations samples were collected after rainfall event. The precipitation sample was filtered through the MnO_2-fiber (5 g) in the cylinder of 15 cm long and 1.8 cm inner diameter. After filtering, the MnO_2-fiber was measured by a gamma spectrometer installed with a HPGe detector (GC7020, Canberra Industries, USA) in a low-background cylindrical shield (Model 747, Canberra, USA) and coupled on a multichannel analyzer (DSA1000, Canberra, USA). The energy resolution is 0.88 keV (FWHM) at 122 keV(^{57}Co) and 1.77 keV (FWHM) at 1332 keV(^{60}Co). The efficiency calibration of detection system was made using of a certified Europium-152 solution (Gammadata Instument AB, Sweden) to calculate the efficiency at gamma energy of 477.7 keV. The counting-time was set to

21600 s for each sample to provide the lowest reasonable analytical error (less than 25% or 1σ). The prominent points of using MnO_2-fiber to absorb the ^{7}Be in rain water are (1) spending less time for preparing the samples and (2) also less counting-time measured by gamma spectrometry than other methods.

The exposure time as period of sample collection (day), the amount of rainfall (mm), ^{7}Be specific activity in bulk deposition samples (Bq l^{-1}), ^{7}Be atmospheric deposition flux (Bq m^{-2}), the calculated running inventory of ^{7}Be atmospheric deposition (Bq m^{-2}) and its corresponding uncertainty are shown in Table 1, 2 and 3 for sites S01, S02 and S02, respectively. The activities of ^{7}Be integrated over the sampling interval, and it have been decay-corrected to the collecting time. For this study, we report a record of event ^{7}Be atmospheric deposition fluxes to the Songkhla province and discuss the atmospheric process associated with its several variations.

3. Results and discussions

3.1 The ^{7}Be concentration in the rainfall sample

The activity concentration values of ^{7}Be (Bq l^{-1}) in rain samples are shown in Table 1, 2 and 3 for S01, S02 and S03, respectively. The ^{7}Be concentrations which were integrated over the exposure time ranged from 0.06 ± 0.01 to 0.9 ± 0.1 Bq l^{-1}, 0.08 ± 0.02 to 0.56 ± 0.04 Bq l^{-1} and 0.09 ± 0.01 to 0.29 ± 0.02 Bq l^{-1} for S01, S02 and S03, respectively. Their mean values (mean ± S.D.) were 0.24 ± 0.17, 0.23 ± 0.13 and 0.18 ± 0.06 Bq l^{-1} for sites S01, S02 and S03, respectively. The ranges of our values are within that generally have been reported in other locations around the world for ^{7}Be in rainwater, which is about 0.01 – 10 Bql^{-1} (Ayub et al., 2009). Our concentration values are similar to those found in the Houay Xon, Luang Prabang, Lao PDR (about 17°N, 102°E) by Gourdin et al. (2014) reporting that ^{7}Be activity concentrations ranged from 0.174 to 0.640 ± 0.008 Bq l^{-1}, but they are lower than those found in Murree city, Pakistan (33°54'N, 73°22'E) where the ^{7}Be activity concentration varied from 0.08 to 1.68 Bq l^{-1} and mean value of 0.570± 0.201 Bq l^{-1} (Ali et al., 2011).

As data from site S01, there are high concentrations corresponding to low rainfall. For example, the highest value (0.9 ± 0.1 Bq l^{-1}) corresponded to low rainfall (26.9 mm) and exposure period of 8 days (1-7 days do not have rain). Besides, there is the lower one (0.092 ± 0.006 Bq l^{-1}) corresponding to high rainfall (158 mm) and exposure period of one day. These results indicate that ^{7}Be grows continuously in the atmosphere, and is quickly removed by washout from rainfall, and when there heavy rainfall the ^{7}Be is diluted by more rain water sample as low concentration in this event.

When a linear regression analysis was applied, negative and weak Pearson's correlation coefficient (r = – 0.253, P-value < 0.05) and non-linear relationship (R^2 < 0.094, P-value < 0.05) was found between the ^{7}Be content in rainwater and rainfall as shown in Figure 1. There are high concentrations of ^{7}Be in rainwater corresponding to the low rainfall events. Moreover, the concentrations quickly decreased to ~0.2 Bq l^{-1} with increasing rainfalls. It shows a similar response to those reported by Caillet et al. (2001) who studied the ^{7}Be concentration in rainfall during individual rainfall events. This result indicated that the dry ^{7}Be-bearing aerosols in the below the cloud at lower atmosphere are quickly washed by rainfall, called washout, in the early rain event. There are two components in the rainwater which the washout part is more than the rainout part, Therefore, the high concentrations of ^{7}Be in rainwater show at the low rainfall events (Ayub et al., 2012; Caillet et al., 2001; Conaway et al., 2013; Ishikawa et al., 1995). When the rain event is long duration and high precipitation (>40 mm per event), the ^{7}Be concentrations in the rainwater are pretty constant which indicates that the ^{7}Be-bearing aerosols in the cloud or rain drops are constants because the rainout part is more than the washout part in the rainwater samples.

Table 1 Exposure time, event of total rainfall, ^{7}Be atmospheric deposition flux, and the calculated running inventory of ^{7}Be atmospheric deposition during December 21, 2012 to December 31, 2013 at the top roof of Physics Building, Prince of Songkla University (site S01)

Time interval (day/month/year)	Exposure time (day)	Precipitation (mm)	^{7}Be concentration (Bq l^{-1})	Deposited flux of ^{7}Be (Bq m^{-2})	Running inventory of ^{7}Be flux (Bq m^{-2})
20/12/12 - 21/12/12	1	42.2	0.51 ± 0.03	34 ± 2	29 ± 2
21/12/12 - 24/12/12	3	56.8	0.45 ± 0.03	30 ± 2	56 ± 3
24/12/12 - 26/12/12	2	20.8	0.71 ± 0.06	18 ± 2	70 ± 6
26/12/12 - 01/01/13	4	74.7	0.17 ± 0.02	17 ± 2	82 ± 9
01/01/13 - 04/01/13	3	48.8	0.22 ± 0.04	14 ± 2	88 ± 10
04/01/13 - 01/02/13	27	3.8	dry	7 ± 1	69 ± 9
01/02/13 - 24/02/13	23	51.2	0.30 ± 0.05	10 ± 2	61 ± 6
24/02/13 - 25/02/13	1	110.6	0.14 ± 0.01	15 ± 1	74 ± 4
25/02/13 - 26/02/13	1	47.6	0.43 ± 0.03	27 ± 2	98 ± 8
26/02/13 - 28/02/13	3	29.8	0.19 ± 0.03	6.1 ± 0.9	102 ± 12
28/02/13 - 31/03/13	31	2.8	dry	0.6 ± 0.1	69 ± 7
31/03/13 - 17/04/13	17	104.6	0.14 ± 0.02	12.0 ± 1.4	65 ± 6
17/04/13 - 30/04/13	13	11.2	0.39 ± 0.05	10.9 ± 1.4	66 ± 7
30/04/13 - 07/05/13	7	59.8	0.22 ± 0.03	10.3 ± 1.6	67 ± 7
07/05/13 - 08/05/13	1	29	0.16 ± 0.02	12.8 ± 1.8	76 ± 6
08/05/13 - 20/05/13	22	153.6	0.33 ± 0.02	29.8 ± 1.5	90 ± 5
01/06/13 - 17/06/13	17	104.1	0.26 ± 0.02	25.0 ± 2.2	84 ± 8
17/06/13 - 01/07/13	13	8.8	dry	6.1 ± 1.1	76 ± 12
01/07/13 - 05/07/13	4	23.6	0.15 ± 0.04	3.4 ± 0.9	74 ± 18
05/07/13 - 08/07/13	1	14.6	0.21 ± 0.08	2 ± 1	73 ± 17
08/07/13 - 09/07/13	1	13.4	0.17 ± 0.04	5 ± 1	76 ± 12
09/07/13 - 01/08/13	24	17.4	dry	8 ± 2	65 ± 10
01/08/13 - 03/08/13	2	43.2	0.13 ± 0.03	6 ± 1	67 ± 8
03/08/13 - 06/08/13	2	39.2	0.25 ± 0.03	9 ± 1	71 ± 5
06/08/13 - 17/08/13	11	70	0.24 ± 0.02	20 ± 1	81 ± 5
17/08/13 - 01/09/13	13	101	0.30 ± 0.03	29 ± 3	96 ± 7
01/09/13 - 07/09/13	6	10	0.33 ± 0.04	11 ± 1	96 ± 27
07/09/13 - 08/09/13	1	24.6	0.11 ± 0.06	1.5 ± 0.8	96 ± 27
08/09/13 - 17/09/13	11	29.9	0.9 ± 0.1	15 ± 2	97 ± 13
17/09/13 - 30/09/13	13	14.2	0.37 ± 0.08	4 ± 1	86 ± 11
30/09/13 - 08/10/13	8	12	0.25 ± 0.03	11 ± 1	86 ± 9
08/10/13 - 14/10/13	6	62.6	0.11 ± 0.02	7 ± 1	85 ± 8
14/10/13 - 22/10/13	8	127.6	0.17 ± 0.01	14 ± 1	89 ± 6
22/10/13 - 23/10/13	1	15.8	0.40 ± 0.05	8 ± 1	95 ± 7
23/10/13 - 26/10/13	3	70.8	0.16 ± 0.01	15 ± 1	105 ± 10
26/10/13 - 27/10/13	1	51.4	0.11 ± 0.02	6 ± 1	109 ± 13
27/10/13 - 31/10/13	4	77.2	0.10 ± 0.02	5.8 ± 0.9	109 ± 10
31/10/13 - 20/11/13	20	123.6	0.15 ± 0.01	19 ± 2	100 ± 5
20/11/13 - 21/11/13	1	158	0.092 ± 0.006	21 ± 1	117 ± 8
21/11/13 - 22/11/13	1	107.4	0.11 ± 0.01	17 ± 2	131 ± 14
22/11/13 - 23/11/13	1	39	0.06 ± 0.01	3.5 ± 0.6	132 ± 15
23/11/13 - 30/11/13	7	101.3	0.14 ± 0.02	14 ± 2	135 ± 18
30/11/13 - 02/12/13	2	57.8	0.06 ± 0.01	10 ± 2	138 ± 18
02/12/13 - 04/12/13	2	67.7	0.09 ± 0.01	18 ± 2	147 ± 10
04/12/13 - 12/12/13	8	101.8	0.19 ± 0.01	29 ± 2	155 ± 9
12/12/13 - 19/12/13	5	76.6	0.24 ± 0.02	17 ± 2	156 ± 14
19/12/13 - 31/12/13	11	22.2	0.17 ± 0.03	14 ± 2	147 ± 12

Table 2 Exposure time, event of total rainfall, ^{7}Be atmospheric deposition flux, and the calculated running inventory of ^{7}Be atmospheric deposition during January 1, 2013 to December 16, 2013 in the open lawn at the site S02

Time interval	**Exposure time**	**Precipitation**	**^{7}Be concentration**	**Deposited flux of ^{7}Be**	**Running inventory of 7Be flux**
(day/month/year)	(day)	(mm)	(Bq l^{-1})	(Bq m^{-2})	(Bq m^{-2})
1/01/13 - 4/01/13	3	48.8	0.37 ± 0.03	17 ± 2	17 ± 2
4/01/13 - 31/01/13	27	3.4	dry	6 ± 1	18 ± 4
31/01/13 - 24/02/13	23	52.2	0.24 ± 0.03	17 ± 3	31 ± 8
24/02/13 - 25/02/13	1	110.4	0.11 ± 0.02	10 ± 2	40 ± 12
25/02/13 - 26/02/13	1	47.6	0.56 ± 0.04	27 ± 2	67 ± 14
26/02/13 - 1/03/13	3	29.8	0.32 ± 0.07	4.1 ± 0.9	69 ± 12
1/03/13 - 31/03/13	30	3.8	dry	3.4 ± 0.7	50 ± 9
31/03/13 - 18/04/13	18	104.6	0.11 ± 0.01	17 ± 3	56 ± 6
18/04/13 - 30/04/13	12	11.2	dry	2.0 ± 0.5	50 ± 12
30/04/13 - 7/05/13	7	59.8	0.16 ± 0.04	6 ± 2	52 ± 17
7/05/13 - 9/05/13	2	29	0.15 ± 0.02	6 ± 1	56 ± 10
9/05/13 - 30/05/13	21	153.6	0.24 ± 0.01	30 ± 2	73 ± 8
30/05/13 - 17/06/13	17	104.1	0.16 ± 0.01	16 ± 2	74 ± 9
17/06/13 - 30/06/13	13	8.8	dry	2.0 ± 0.5	65 ± 10
30/06/13 - 7/07/13	7	23.6	dry	2.5 ± 0.5	62 ± 8
7/07/13 - 8/07/13	1	14.6	0.21 ± 0.04	4 ± 1	65 ± 7
8/07/13 - 9/07/13	1	13.4	0.30 ± 0.03	16 ± 2	80 ± 11
9/07/13 - 31/07/13	22	17.4	dry	9 ± 2	70 ± 16
31/07/13 - 5/08/13	5	82.4	0.08 ± 0.02	7 ± 3	72 ± 25
5/08/13 - 31/08/13	26	171	0.29 ± 0.03	45 ± 5	96 ± 24
31/08/13 - 19/09/13	19	64.5	0.16 ± 0.02	22 ± 4	98 ± 17
19/09/13 - 30/09/13	11	14.2	0.50 ± 0.07	16 ± 2	100 ± 14
30/09/13 - 31/10/13	31	385.4	0.12 ± 0.01	58 ± 6	125 ± 12
31/10/13 - 23/11/13	23	529.3	0.12 ± 0.02	69 ± 12	162 ± 7
23/11/13 - 16/12/13	23	319.5	0.14 ± 0.01	48 ± 5	169 ± 7

Table 3 Exposure time, event of total rainfall, ^{7}Be atmospheric deposition flux, and the calculated running inventory of ^{7}Be atmospheric deposition during December 26, 2012 to December 31, 2013 in the open lawn at the site S03

Time interval (day/month/year)	Exposure time (day)	Precipitation (mm)	^{7}Be concentration (Bq l^{-1})	Deposited flux of ^{7}Be (Bq m^{-2})	Running inventory of 7Be flux (Bq m^{-2})
26/12/2012 - 2/01/2013	6	74.6	0.27 ± 0.02	28 ± 5	28 ± 5
2/01/2013 - 4/01/2013	3	48.8	0.16 ± 0.03	11 ± 3	39 ± 4
4/01/2013 - 1/02/2013	27	3.4	dry	3.3 ± 0.5	31 ± 8
1/02/2013 - 25/02/2013	24	162.6	0.13 ± 0.02	24 ± 4	46 ± 12
25/02/2013 - 26/02/2013	1	47.6	0.23 ± 0.03	8 ± 2	53 ± 14
26/02/2013 - 1/03/2013	3	29.8	0.19 ± 0.03	5 ± 1	56 ± 12
1/03/2013 - 1/04/2013	31	3.8	dry	5.5 ± 0.5	43 ± 9
1/04/2013 - 17/04/2013	16	104.6	0.09 ± 0.01	17 ± 2	51 ± 6
17/04/2013 - 1/05/2013	15	11.2	0.16 ± 0.06	3 ± 2	46 ± 12
1/05/2013 - 7/05/2013	7	59.8	0.09 ± 0.01	10 ± 1	52 ± 17
7/05/2013 - 1/06/2013	23	182.6	0.24 ± 0.02	48 ± 8	87 ± 10
1/06/2013 - 17/06/2013	17	104.1	0.29 ± 0.2	38 ± 6	107 ± 8
17/06/2013 - 1/07/2013	13	8.8	dry	6 ± 0.5	96 ± 9
1/07/2013 - 9/07/2013	8	56.2	0.15 ± 0.02	5 ± 1	91 ± 10
9/07/2013 - 1/08/2013	23	12.8	dry	10.7 ± 0.7	79 ± 8
1/08/2013 - 5/08/2013	4	82.4	0.16 ± 0.03	12 ± 3	86 ± 7
5/08/2013 - 1/09/2013	26	171	0.23 ± 0.02	54 ± 13	115 ± 11
1/09/2013 - 19/09/2013	18	78.7	0.13 ± 0.02	28 ± 5	118 ± 16
1/10/2013 - 1/11/2013	31	385.4	0.15 ± 0.01	65 ± 8	133 ± 25
1/11/2013 - 1/12/2013	30	529.3	0.16 ± 0.01	103 ± 15	193 ± 24
1/12/2013 - 31/12/2013	31	319.5	0.18 ± 0.02	86 ± 13	215 ± 17

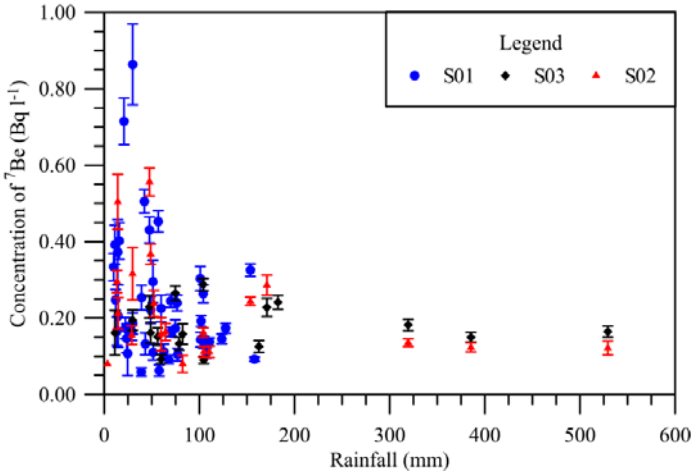

Figure 1 ^{7}Be concentrations are plotted against the precipitation amount in period of sampling time

3.2 ^{7}Be deposition flux

The deposited fluxes of each individual event, expressed in Bq m^{-2}, varied widely from 0.6 ± 0.1 to 34 ± 2 Bq m^{-2}, 2.0 ± 0.5 to 69 ± 12 Bq m^{-2} and 3 ± 2 to 103 ± 15 Bq m^{-2}, as shown in Table 1, 2 and 3, respectively. Their mean values were 11.6, 18.5 and 27.1 Bq m^{-2} for sites S01, S02 and S03, respectively. The atmospheric deposition activities of ^{7}Be and the event precipitation amount during the sampling period were shown in Figure 2. The temporal pattern in ^{7}Be deposition closely matches the temporal pattern in rainfall.

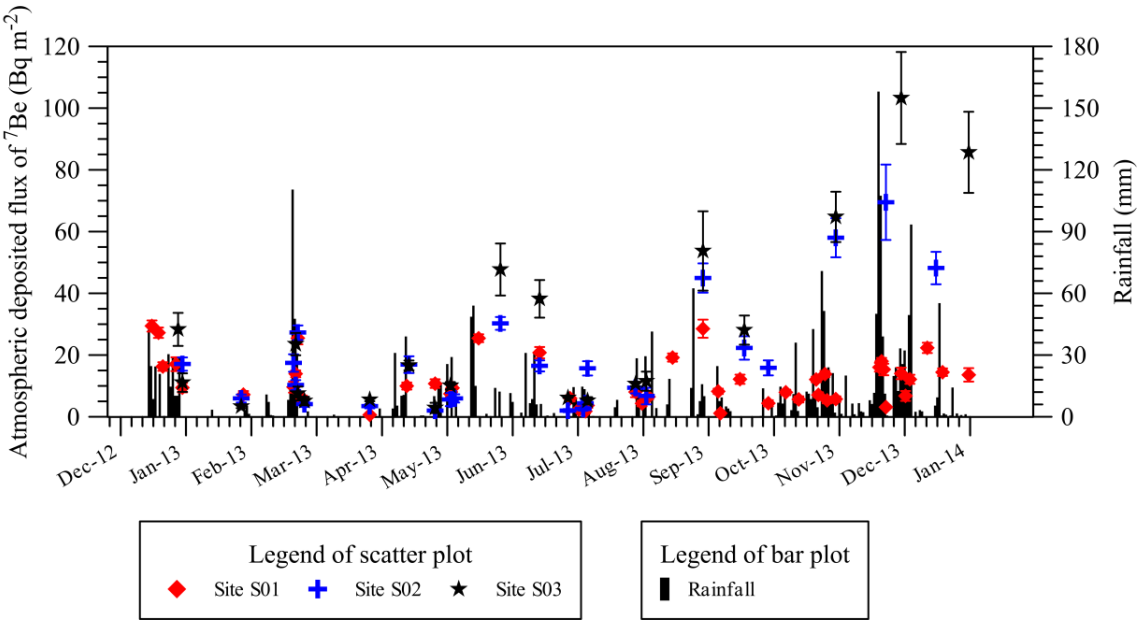

Figure 2 Time series plots of the activity fluxes of atmospheric ^{7}Be and rainfall amount during each sampling period

The relationships between atmospheric deposited activity of ^{7}Be and the amount of rainfall for sites S01, S02, and S03 are shown in the Figure 3, and the Pearson's correlation and the linear regression test were used. The Pearson's correlation coefficients are 0.658 (p-value = 0.000), 0.921 (p-value = 0.000), and 0.944 (p-value = 0.000) for sites S01, S02, and S03 respectively. The linear regression results are shown in the Figure 3 that they were significant at more than 95% confidence level. It may be explained by the mechanism that the washout by rainfall

is the most important process for ^{7}Be removal from the atmosphere (Ioannidou and Papastefanou, 2006; Pham et al., 2013; Shi et al., 2011).

The linear relationship between ^{7}Be depositional fluxes and rainfall amount are reported as strong positive correlation (Dueñas et al., 2002), and our study showed a similar trend. Caillet et al. (2001) reported $R^2 = 0.66$ ($p<0.001$) for a site in Switzerland; and Ayub et al. (2012) reported $R^2 = 0.82$ ($p<0.0001$) for a site in Argentina. These results of the strong positive correlation indicated that the ^{7}Be – bearing aerosols contained in the atmosphere at this location are constant.

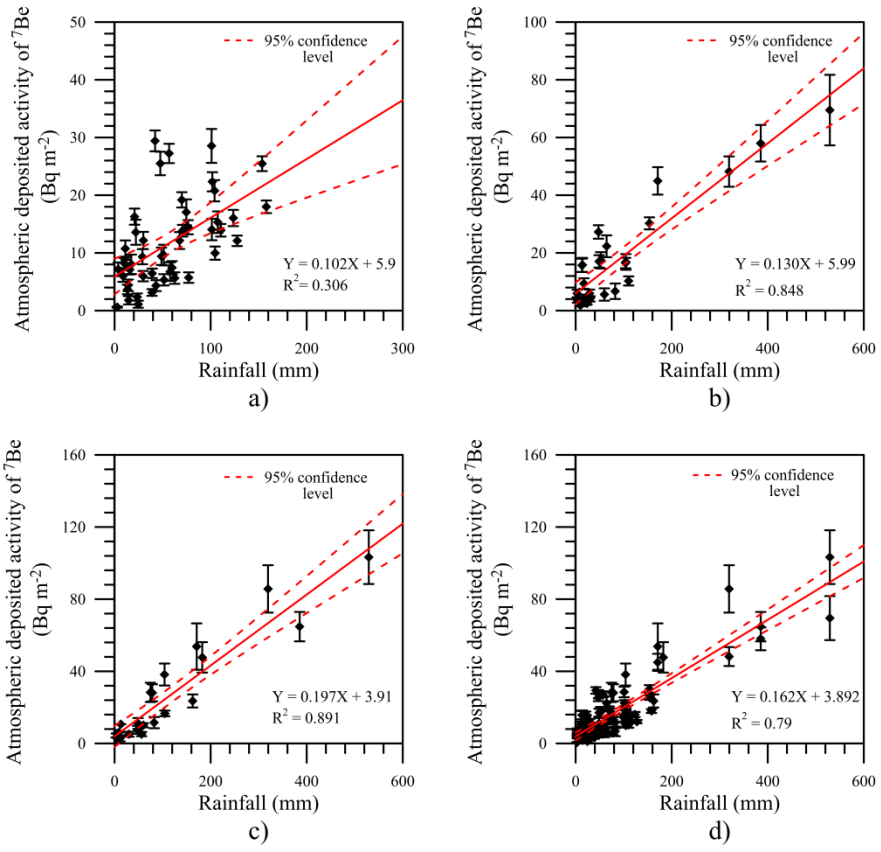

Figure 3 Relationships between the ^{7}Be depositional flux and the amount of precipitation during each sampling period for sites S01, S02 and S03 as shown in a), b) and c) respectively

3.3 Effect from season in ^{7}Be removing process by precipitation

The climate of the Songkhla province, south of Thailand is controlled by tropical monsoons that consist of the southwest (May – October) and northeast (October – Febuary) monsoons. There are generally two seasons – the rainy season and dry season. The rainy season is influenced by the southwest monsoon (May – September) that brought the moist and warm air from the Indian Ocean whereas the northeast monsoon (October – January), brought the moist air from the Gulf of Thailand. During the periods A.D. 2003 – 2013, the mean annual rainfall is 2,451 mm and frequently occurs in October to December. Meteorological data were provided by the Thai Meteorological Department at the Songkhla Meteorological station (WMO Index: 568501/48568, located 7°12’14” N 100°36’11” E). The monsoon system has affected the wind speed and direction in the Songkhla lagoon. In A.D. 2013, the monthly mean wind speeds at the Songkhla Especially, the wind speeds are strong during the period of April to October. The wind direction is predominantly from ENE, WSW and ENE directions during the inter-monsoon (Febuary – April), SW monsoon (April – October) and NE monsoon (October – January), respectively (Figure.4).

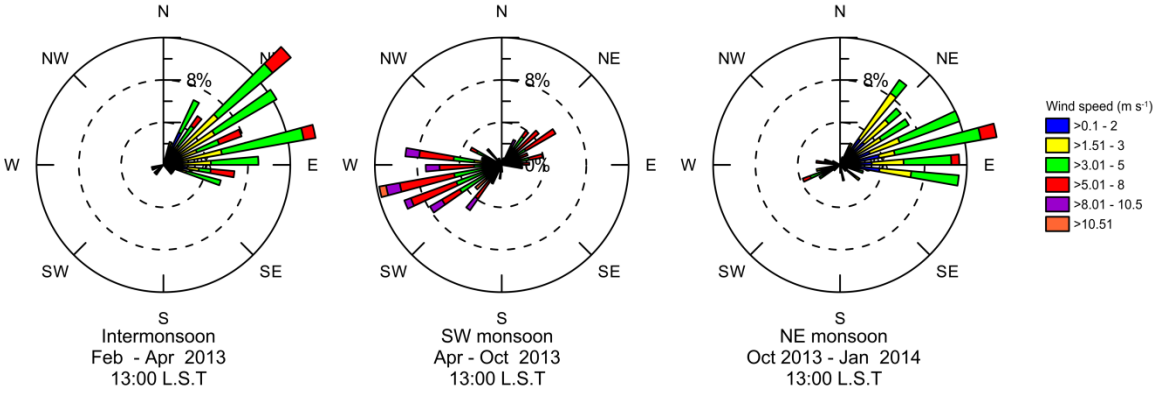

Figure. 4 Wind diagram showing percentage of wind direction at the Songkhla meteorological station (WMO Index: 568501/48568, located 7°12’14” N 100°36’11” E) during January 2013 – January 2014. (data from Thai Meteorological Department)

The depositional fluxes of ^{7}Be and precipitations selected from all sites (S01, S02, and S03) were classified into three groups: Northeast monsoon (Nov – Jan), Southwest monsoon (May – Oct), and summer season (Feb – Apr). The

Pearson's correlation test was used to measure the strength of the relationship between the event depositional fluxes of ^{7}Be and amount rainfall. These correlation coefficients were 0.902 (p-value = 0.000), 0.873 (p-value = 0.007) and 0.798 (p-value = 0.000) for NE monsoon, SW monsoon, and summer seasons, respectively. From these coefficients, the strength levels of correlation between these values were strong correlation for NE monsoon and SW monsoon season, and moderate correlation for summer seasons. The linear relationships obtained by the regression test between the event depositional flux of ^{7}Be and amount rainfall are significant positive relationship all duration of monsoon as shown in the Figure 5: The slopes of linear relationship between these are 0.158, 0.163 and 0.161 for the NE monsoon seasons (R^2 = 0.812, p < 0.001), the SW monsoon seasons (R^2 = 0.429, p < 0.001), and the summer season (R^2 = 0.864, p < 0.001) respectively. These results can be considered that the removing of ^{7}Be-bearing aerosols to the ground surface was dominantly regulated by precipitation.

When the depositional fluxes of ^{7}Be and amount rainfall are normalized by duration of sampling time, and the Pearson's correlation test was used to measure the strength of the relationship between these. These correlation coefficients were 0.651 (p-value = 0.000), 0.418 (p-value = 0.007) and 0.732 (p-value = 0.000) for NE monsoon, SW monsoon, and summer seasons, respectively. From these coefficients, the strength levels of correlation between these values were strong correlation for NE monsoon and summer seasons, and moderate correlation for SW monsoon season. These results can be considered that the daily depositional flux of ^{7}Be was dominantly regulated by precipitation.

In these data, there are some data that more scattered than others as shown in the Figure 6 (blue star), which were cut off in the regression test. Only data which were well grouped as shown in the Figure 6 (filled black circles) were used to investigate the linear relationship by regression test. The linear relationships obtained by the regression test between the daily deposition flux of ^{7}Be and daily rainfall are significant for the NE monsoon seasons (R^2 = 0.514, p < 0.001), the SW monsoon seasons (R^2 = 0.429, p < 0.001), and the summer season (R^2 = 0.864, p < 0.001) as shown in Figure 6. They can be explained that the atmospheric deposition of ^{7}Be is

tightly related to rainfall. Hence, the precipitation was the dominant removal pathway of ^{7}Be out of the atmosphere in Songkhla province. This observation was similar to reports obtained in other regions (e.g., Kim et al., 2000; McNeary and Baskaran, 2003; Zhang et al., 2016)

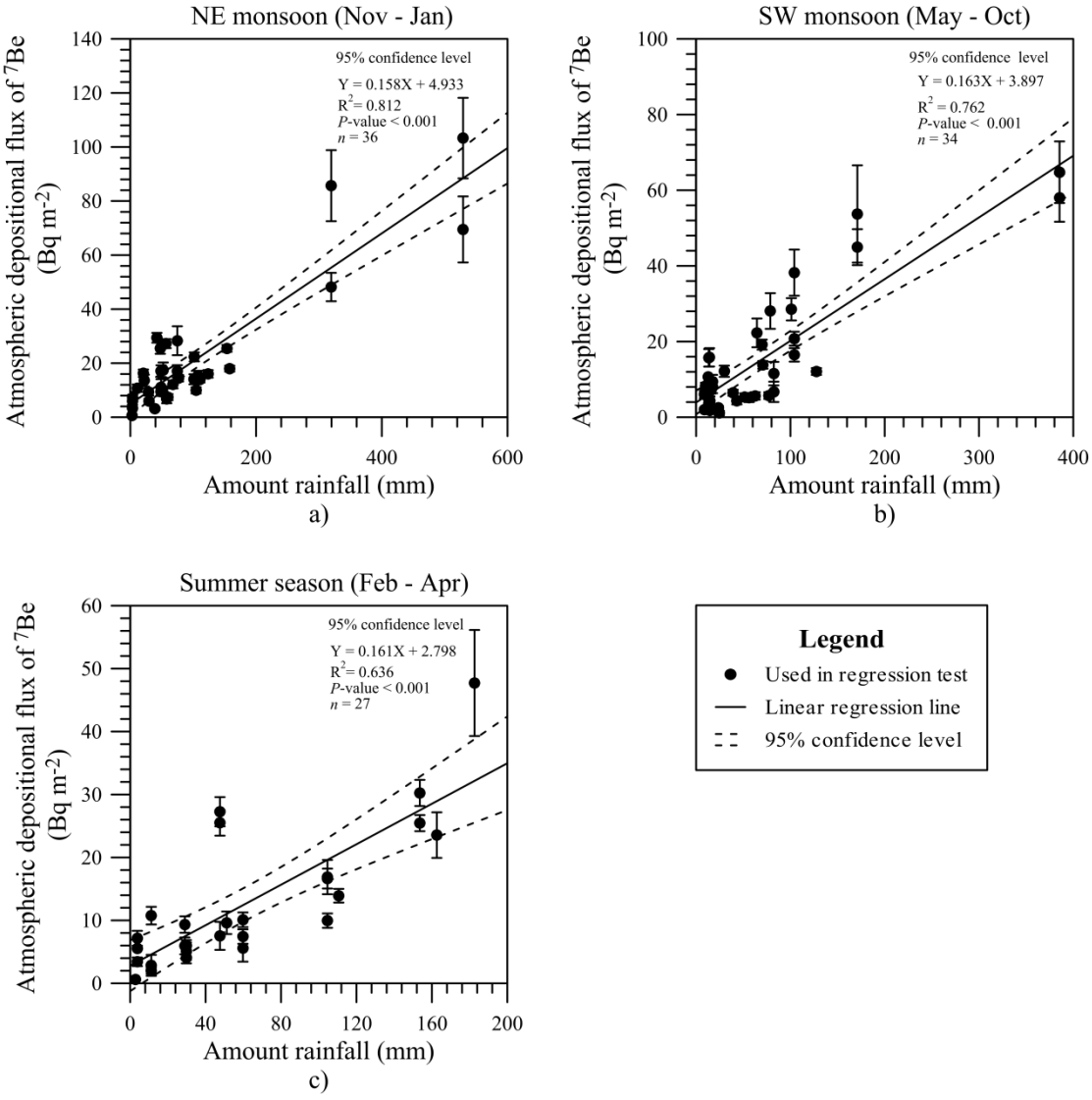

Figure 5 Relationships between the event depositional fluxes of ^{7}Be and amount rainfall classified by duration of monsoon: a) November to January (NE monsoon), b) May to October (SW monsoon) and c) February to April (summer season)

Although the daily deposition of ^{7}Be was dominantly controlled by precipitation, there was an evident difference in the influence of precipitation

magnitude on ^{7}Be deposition between the northeast, southwest monsoon and summer seasons. The slope of the correlation line (0.165) for the northeast monsoon months was two times the slope (0.096) obtained during the southwest monsoon months, indicating more atmospheric ^{7}Be carried by the same amount of rainwater during the northeast monsoon season as shown in Figure 6,.

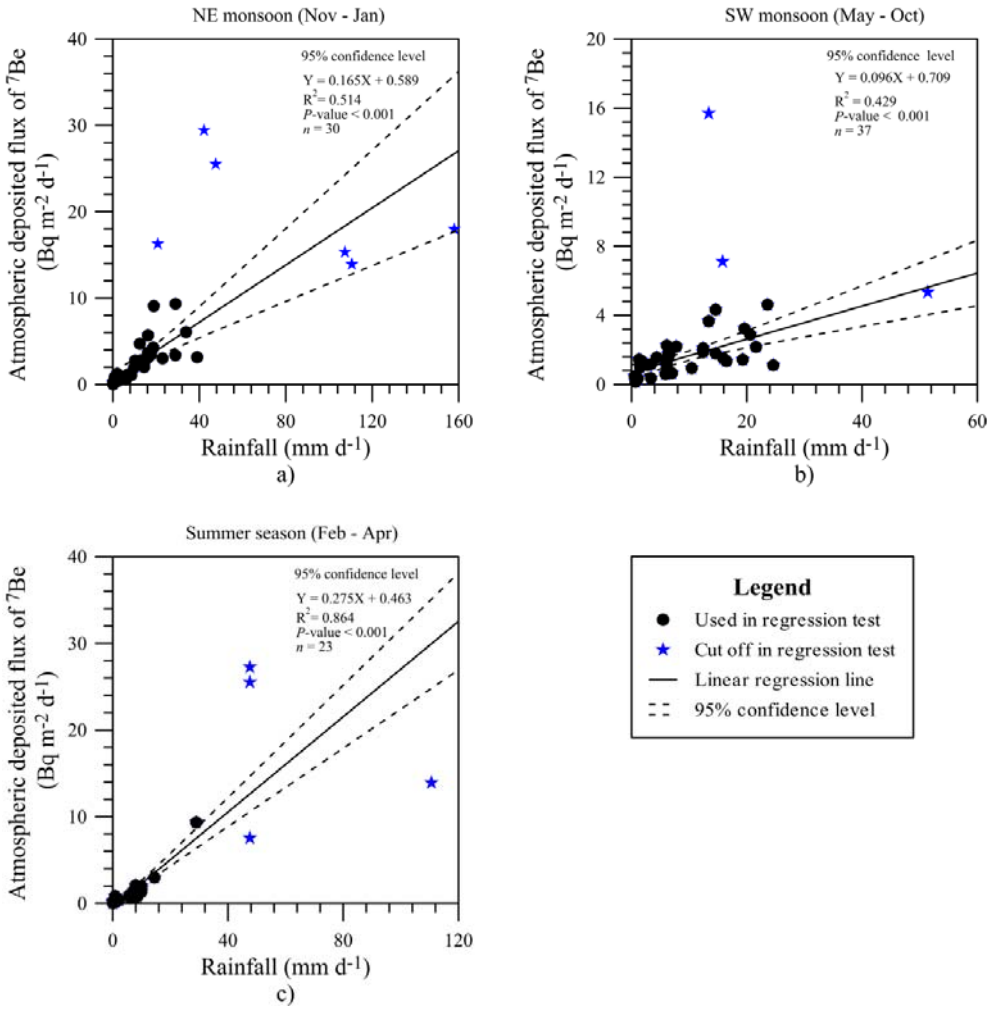

Figure 6 Relationships between the daily depositional fluxes of ^{7}Be and daily rainfall classified by duration of monsoon a) November to January (NE monsoon), b) May to October (SW monsoon) and c) February to April (summer season)

Atmospheric depositional fluxes of ^{7}Be vary with seasonal monsoons as shown in the Figure 6. High values show in the North-East monsoon and summer season months, and low values show in South-West monsoon months. The significant

linear correlations between the daily deposition fluxes of ^{7}Be and precipitation suggested that the atmospheric deposition of ^{7}Be was related to rainfall as shown in Figure 6. Consequently, the precipitation was the dominant removal pathway of ^{7}Be out of the atmosphere in Songkhla. This observation was similar to reports obtained in other regions (e.g. Kim et al., 2000; McNeary and Baskaran, 2003; Zhang et al. 2016; Su et al., 2003).

Such seasonal difference reflected the higher ^{7}Be contents in the atmosphere during the northeast monsoon months. A similar phenomenon was also reported by Su et al. (2003) and Zhang et al. (2016) based on a time-series observation of ^{7}Be deposition in Taiwan and Xiamen, respectively. Since the troposphere usually becomes thinner in the mid-latitude regions in late winter and early spring, the air mass exchange between the troposphere and stratosphere is much active, leading more ^{7}Be to enter into the troposphere.

Table 4 Monthly deposited fluxes of ^{7}Be at sites S01, S02 and S03

Month	Precipitation (mm)	Monthly flux of ^{7}Be (Bq m^{-2})		
		S01	S02	S03
Dec-12	384.8	90 ± 4		
Jan-13	52.2	17 ± 2	23 ± 5	14 ± 4
Feb-13	240.0	55 ± 3	59 ± 18	36 ± 8
Mar-13	3.8	0.6 ± 0.1	3.4 ± 0.7	5.5 ± 0.9
Apr-13	115.8	21 ± 2	17 ± 2	23 ± 9
May-13	238.4	42 ± 2	42 ± 13	58 ± 8
Jun-13	113.0	27 ± 2	16 ± 1	44 ± 7
Jul-13	69.0	16 ± 2	29 ± 8	16 ± 4
Aug-13	253.4	59 ± 3	52 ± 15	65 ± 13
Sep-13	78.7	26 ± 2	38 ± 8	28 ± 4
Oct-13	385.4	58 ± 2	58 ± 6	65 ± 5
Nov-13	509.5	67 ± 3	69 ± 10	103 ± 9
Dec-13	320.7	56 ± 3	48 ± 4	86 ± 7
Annual	2379.9	444.6	454.4	543.5

3.4 Monthly variations of ^{7}Be deposition

Monthly depositional fluxes of ^{7}Be for sites S01, S02 and S03 at Songkhla province are plotted in Figure 3.5 and presented in Table 3.xx. These depositional fluxes ranged 0.6 – 90 Bq m^{-2}, 3.4 – 69 Bq m^{-2}, and 5.5 – 103 Bq m^{-2} for sites S01, S02, and S03, respectively. The maximum and minimum fluxes of ^{7}Be for all sites

occurred in NE monsoon (Oct- Dec) which has the maximum rainfall amounts, and summer season (Feb – Apr) which has the lack of rainfall.

Figure 7 shows that the monthly depositional fluxes of ^{7}Be are changed in the monthly rainfall amounts. The trend of our results is similar to many researchers reported that the ^{7}Be depositional flux is controlled by precipitation (Du et al., 2008). The monthly depositional fluxes of ^{7}Be plotted against monthly rainfall (Figure 8) show that there are strong positive correlations all sampling sites, suggesting that the atmospheric^{7}Be is removed from atmosphere by washout and rainout processes (Narazaki et al, 2003; Yi et al, 2007). This information will be useful for evaluating human impacts on land degradation phenomena as a whole (Ayub et al., 2012).

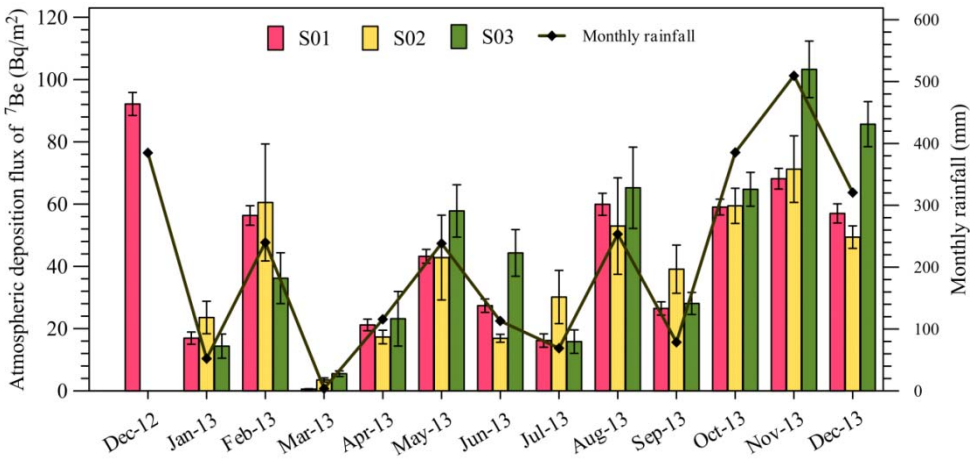

Figure 7 Monthly deposition fluxes of ^{7}Be for sites S01, S02 and S03 contributions to the whole year with precipitation amount

3.5 Annual deposition fluxes of ^{7}Be

From this data, annual deposition fluxes of 444.6, 454.4 and 543.5 Bq m^{-2} for sites S01, S02 and S03, respectively, were calculated by summation of event deposition fluxes during January, 2013 to December, 2013. The average of the annual deposition flux of ^{7}Be in selected sites of the Songkhla province, Thailand is 480.8 Bq m^{-2}. Figure 9 and Table 5 show the annual deposition fluxes collected from around the world. Our result is lower than the annual deposition fluxes reported by researchers in other locations. Generally, high ^{7}Be flux occurs in the mid-latitude region, but this

result shows the lower ^{7}Be flux which may be influenced from the lower latitude of this study site and the topical zone (e.g Baskaran, 1995; Ishikawa et al., 1995; Conaway et al., 2013).

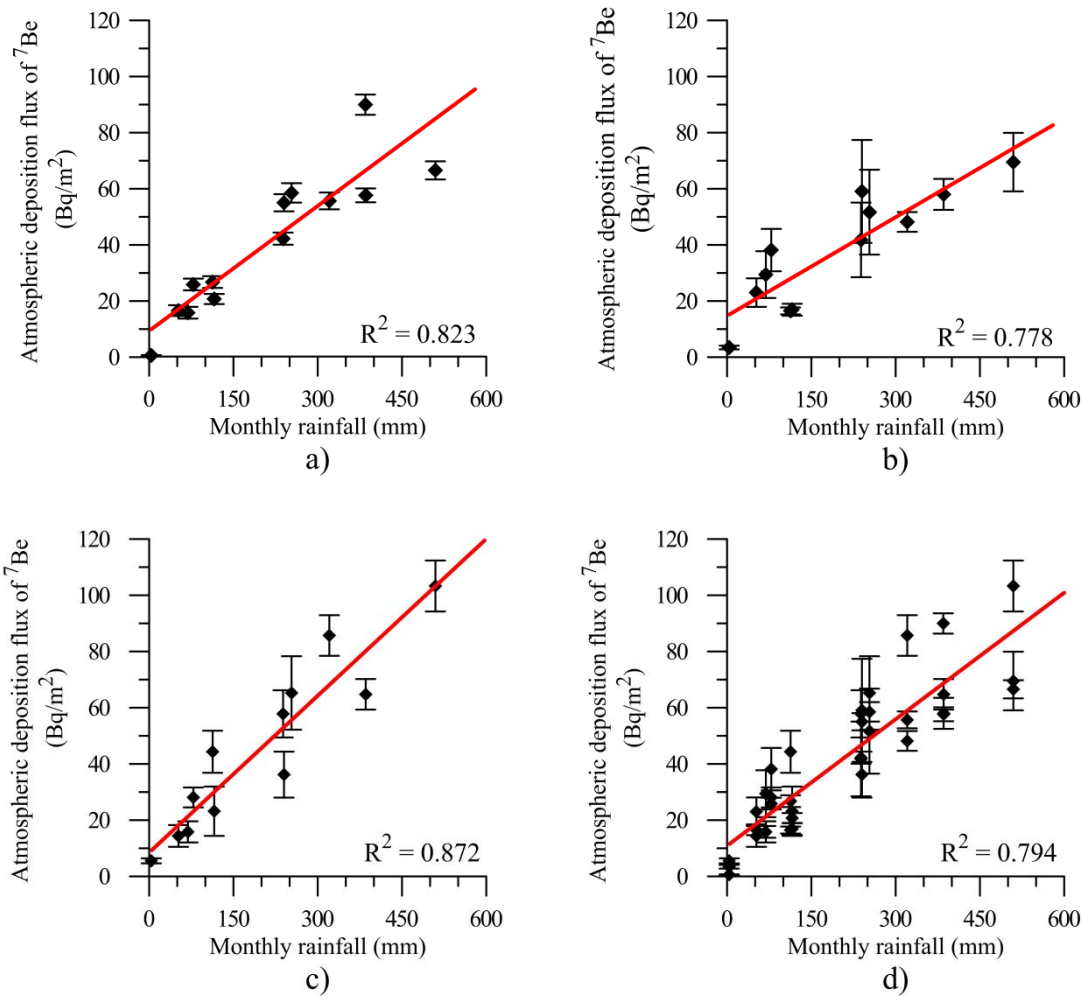

Figure 8 Correlation between monthly precipitation and deposition flux of ^{7}Be for sites S01, S02, S03 and total all sites as shown in a), b), c) and d) respectively.

Table 5 The summarized annual ^{7}Be deposition flux in the world

Locations	Collection period	Position		Annual rainfall	Depositional fluxes of ^{7}Be (Bq m^{-2})	Earth's Magnetic field angle		Earth's Magnetic field intensity			Refference
		Lat.[a]	Long.[b]	(mm)		De.	In.	Horizontal	Vertical	Total	
Hatyai (HY), Thailand	Dec 2012 - Dec 2013	7.12	100.54	2500	480.8	-0.38	-1.52	41479.0	-1102.1	41493.7	**Present study**
Murree (MR), Pakistan	2006 – 2010	33.90	73.38	14500	4832	2.19	51.94	30799.2	39337.3	49960.1	**Ali et al.(2011)**
Islamabad (ID), Pakistan	2009 – 2010	33.72	73.07	1140	3801	2.2	51.77	30859.3	39178.2	49872.1	**Ali et al.(2011)**
Stllpond (SP),USA	Sep 1995 - Sep 1996	39.00	-76.00	126	2167	-11.13	67.7	20434.3	49827.0	53854.4	**Kim et al. (2000)**
Brisbane (BR), Australia	2004 – 2006	-27.48	153.03	718 - 1056	1199	11.1	-57.54	28506.5	-44812.9	53111.3	**Doering and Akber (2008)**
Rokkasho (RK), Japan	2004 – 2006	40.95	141.35	1340 - 1637	2626	-8.57	55.22	27852.1	40108.3	48830.5	**Akata et al. (2008)**
Fuhuoka (FK), Japan	Aug 1995 - Oct 1998	33.58	130.40	1704	1733	-6.91	48.26	31780.3	35615.7	47733.3	**Sugihara et al.(2000)**
Shanghai (SG), China	Nov 2005 - Oct 2006	31.23	121.40	1140	2070	-5.4	46.52	33419.1	35240.1	48566.5	**Du et al. (2008)**
Xiamen (XM), China	Mar 2004 - Apr 2005	24.43	118.08	1135	599	-3.32	35.93	36748.5	26635.4	45386.0	**Yi et al. (2007)**
San Luis (SL), Argentina	Nov 2006 - May 2008	-33.15	-66.30	600 – 800	1140	-1.28	33.96	19545.2	13163.6	23647.4	**Juri Ayub et al. (2009)**
Thessaloniki (TS), Greece	Jan 1987 - Dec 1992	40.63	22.97	337 - 652	736.1	3.85	57.52	25017.1	39304.5	46590.8	**Ioannidou and Papastefanou (2006)**
Thessaloniki (TS), Greece	Jul 1987 - Jun 1994	40.63	22.97	337 - 652	776.3	3.85	57.52	25017.1	39304.5	46590.8	**Papastefanou et al. (1995)**
Geneva (GV), Switzerland	Nov 1997 - Nov 1998	46.27	6.17	1000	2087	0.76	62.12	22087.4	41758.1	47239.7	**Caillet et al. (2001)**
Monterey Bay (MB), USA	Oct 2009 - Sep 2010	36.97	-122.04	763	1450	14.03	60.65	23804.7	42330.7	48564.9	**Conaway et al. (2013)**
IAEA-EL Buildind (IAEA),Monaco	1998 – 2010	43.83	7.5		1260	1.04	59.78	23396.3	40175.4	46493.4	**Pham et al. (2013)**
Tsukuba (TK), Japan	Jan 2000 - Dec 2001	36.05	140.13	1362	1121	-7.0	49.52	30094.2	35265.4	46361.0	**Hirose et al. (2004)**
Tsukuba (TK), Japan	1986 – 1998	36.05	140.13	1362	1322	-6.8	49.09	30075.2	34706.4	45924.4	**Igarashi et al. (1998)**
Nagasaki (NG), Japan	Jan 2000 - Dec 2000	32.75	129.85	1561	1474	-6.35	47.01	32336.6	34687.8	47422.5	**Hirose et al. (2004)**
Massachusetts (MS1),USA	Sep 2000 - Aug 2007	42.32	-71.03		2592	-15.44	68.31	19701.3	49536.1	53310.1	**Zhu and Olsen. (2009)**
Massachusetts (MS2),USA	Mar 1996 - Feb 1998	41.53	-72.65		2133	-14.45	68.85	19467.9	50325.3	53959.6	**Benitez-Nelson and Buesseler. (1999)**
New Hampshire (NH),USA	Mar 1997 - Feb 1998	43.07	-70.7		2767	-16.28	69.59	18917.5	50848.1	54253.1	**Benitez-Nelson and Buesseler. (1999)**
Tatsunokuchi (TS), Japan	1991 – 2002	36.47	136.55		5300	-7.48	50.55	30261.7	36774.1	47624.7	**Yamamoto et al. (2006)**
Ansai (AS), Chaina	Apr 2010 - Dec 2012	36.86	109.32	510	1756	-3.38	55.61	30065.3	44024.9	53349.4	**Zhang et al. (2013)**
Granada (GD), Spain	1995 – 1998	37.18	-0.60	452	469	-2.26	51.47	26764.9	33613.9	42368.0	**Gonzalez-Gomez et al. (2006)**
Malaga (MG), Spain	1992 – 1999	36.73	-4.47	308	412	-3.76	50.8	26899.1	32980.7	42559.2	**Duenas et al. (2002)**
Huelva (HV), spain	Jan 2010 - Dec 2011	37.27	-6.92		740	-2.49	51.1	26991.8	33450.6	42982.6	**Lozano et al.(2013)**
Cadiz (CD), spain	Jan 2010 - Dec 2011	36.53	-6.21		760	-2.25	50.11	27377.4	32758.0	42692.0	**Lozano et al.(2013)**
St. Petersburg (SP), USA	Oct 2003 - Jul 2004	27.76	-82.64	575	1832	-4.0	58.16	24758.7	39864.5	46927.3	**Baskaran and Swarzenshi. (2007)**
Nankang,Taiwan	1996 – 2001	25.0	121.6	1945	1833	-3.83	35.98	36248.7	26318.6	44795.5	**Su et al., 2003**
Peng-Chia Yu, Taiwan	1996 – 2001	25.7	121.1	1929	1117	-3.55	37.20	35905.0	27307.9	45164.8	**Su et al., 2003**
Xiamen, China	2001 – 2003	24.4	118.1	1618	694	-2.94	35.44	36690.6	26151.1	45096.1	**Jia et al. (2003)**
Qingdao,China	2002	36.1	120.3	421	610	-6.08	53.11	30805.8	41047.7	51321.7	**Yi et al. (2005)**
Qingdao,China	2004	36.1	120.3	376	785	-6.16	53.14	30596	41039.6	51296.0	**Yi et al. (2005)**
Nanjing, China	2010.1 – 2011.12	32.1	129.8	1101	1622	-6.42	46.32	32151.1	33883.0	46849.0	**Yang et al. (2012)**
Three gorges reservoir	2009.5 – 2010.5	30.4	108.2	1026	949	-2.60	46.50	34225.0	36068.0	49722.0	**Shi et al, (2011)**

3.6 The effect of ^{7}Be from geomagnetic field

In fact, the ^{7}Be's production rate in the atmosphere depends on the flux of galactic cosmic rays (GCRs) affected by the solar activity or solar magnetic field (Leppänen et al., 2010; Akata et al., 2008; Sakurai et al., 2005), and the geomagnetic field has been influenced the fluxes of the charged GCRs. Therefore, vertical, horizontal, and total intensities of geomagnetic field and absolute geomagnetic latitude were plotted with the annual atmospheric depositions of ^{7}Be reported in the several locations in the world and our result as shown in Figure 9. The calculated geomagnetic fields by using the International Geomagnetic Reference Field (IGRF) model from the National Centers for Environmental Information (NOAA, 2016) were used in this study. The geomagnetic latitude (λ) was calculated from inclination angle (I) as follow $tan(I) = 2\ tan(\lambda)$. The charged GCRs cannot move through to the Earth's atmosphere in area of low geomagnetic latitude because the geomagnetic field can make the magnetic force exerting the charged GCRs in perpendicular of particle motion. Its effect can turn out the charged GCRs. Hence, the low geomagnetic latitude area has the low ^{7}Be's production indicating low annual atmospheric depositions of ^{7}Be (see Figure 9a and b). There are three points of high annual atmospheric depositions of ^{7}Be at the middle latitude which indicate that they may be strongly affected from the exchange between stratosphere and troposphere (Ali et al., 2011; Yamamoto et al., 2006). For discussion of geomagnetic field, we cut out three points of high annual atmospheric depositions of ^{7}Be. Figure 9b shows that geomagnetic latitude have affected with the ^{7}Be depositional fluxes, and the ^{7}Be depositional fluxes are depended on the magnetic field intensities such as horizontal, vertical and total intensities as shown in Figure 9c d and e, respectively. Figure 9c shows the negative correlation between the horizontal magnetic field intensity and the ^{7}Be depositional fluxes. Although, it is poor correlation which may be influenced from other factors such as horizontal movement of atmospheric aerosols carried the ^{7}Be, and folding effect of exchange of aerosols between stratosphere and troposphere.

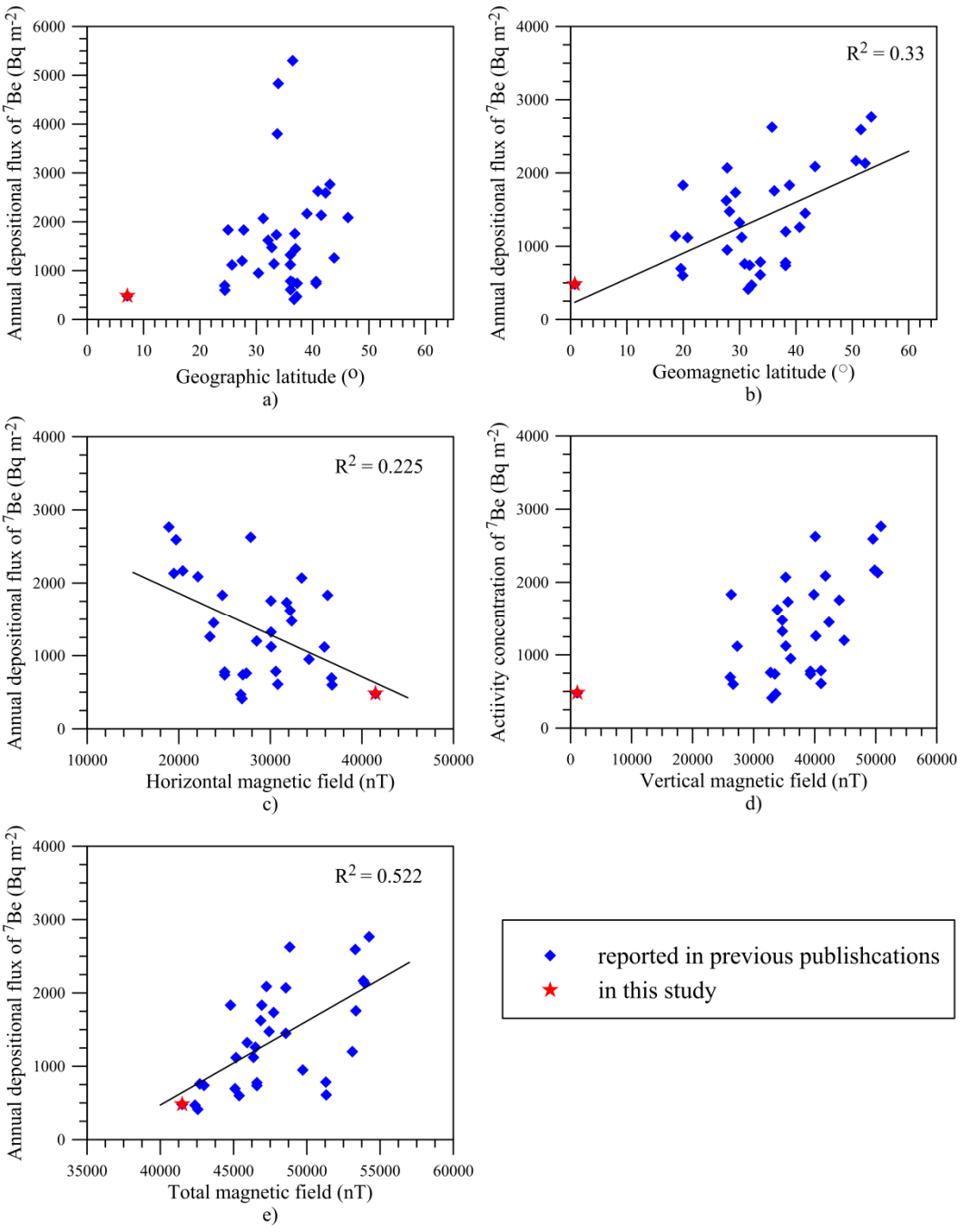

Figure 9 The effect of ^{7}Be depositional fluxes from a) absolute geographic latitude, b) geomagnetic latitude, c) horizontal, d) vertical and e) total geomagnetic field intensities.

The related correlation of these is negative, because the charged GCRs are turned out by high magnetic force from the horizontal magnetic field intensity. The ^{7}Be depositional fluxes as shown in Figure 9d seem that it depends on the vertical

magnetic field intensity, but the vertical magnetic field intensity do not in fact affect to the movement of the GCRs. Therefore, the GCRs can move through to the Earth's atmosphere for interaction of the light particle producing ^{7}Be. The effect of total magnetic field intensity to the ^{7}Be depositional fluxes shows in Figure 9e. It seems that the magnetic field intensity influence the ^{7}Be depositional fluxes because of the total magnetic field intensity including the factors such as geomagnetic latitude, horizontal and vertical magnetic field intensities.

4. Conclusions

The atmospheric concentration and deposition fluxes of ^{7}Be were measured at three sites in the U-Tapao watershed, Songkhla province, South of Thailand during December 2012 – January 2014. This study provides the baseline information and will be helpful to apply and investigate at this site in the future. Based on this study, mean values of specific concentrations of ^{7}Be are influenced by seasonal variations. The average annual depositional flux of ^{7}Be of 480.8 Bq m^{-2} is lower than those reported in other locations in the world. The monthly depositional flux of ^{7}Be did not remain constant but varied between 0.6 and 103 Bq m^{-2} depending on the amount of monthly rainfall. The seasonal variations have been observed that the depositional flux of ^{7}Be in northeast monsoon months was higher than that in the southwest monsoon months indicating more atmospheric ^{7}Be carried by the same amount of rainwater from the middle latitude. From our result and reported data in publications, there are correlations between the depositional flux of ^{7}Be and horizontal, total geomagnetic field intensity.

Acknowledgements

This research was financially supported by the Prince of Songkla University (project code: SCI550111S), the National Research Council of Thailand (project code: SCI560125S), the Physics Department, Geophysics Research Center, Faculty of Science and the graduate fellowship from the Graduate School, Prince of Songkla

University. In addition, the first author would like to thank Prince of Songkla University, Graduate Studies Grant.

References

Akata, N., Kawabata, H., Hasegawa, H., Sato, T., Chikuchi, Y., Kondo, K., Hisamatsu, S., Inaba, J., 2008. Total deposition velocities and scavenging ratios of ^{7}Be and ^{210}Pb at Rokkasho, Japan. J. Radioanal. Nucl. Chem. 277, 347–355.

Ali, N., Khan, E.U., Akhter, P., Rana, M. a., Rajput, M.U., Khattak, N.U., Malik, F., Hussain, S., 2011. Wet depositional fluxes of ^{210}Pb- and ^{7}Be-bearing aerosols at two different altitude cities of North Pakistan. Atmos. Environ. 45, 5699–5709.

Ayub, J.J., Di Gregorio, D.E., Velasco, H., Huck, H., Rizzotto, M., Lohaiza, F., 2009. Short-term seasonal variability in ^{7}Be wet deposition in a semiarid ecosystem of central Argentina. J. Environ. Radioact. 100, 977–81.

Ayub, J.J., Lohaiza, F., Velasco, H., Rizzotto, M., Di Gregorio, D., Huck, H., 2012. Assessment of ^{7}Be content in precipitation in a South American semi-arid environment. Sci. Total Environ. 441, 111–6.

Baskaran, M., 1995. A search for the seasonal variability on the depositional fluxes of Be-7 and Pb-210. J. Geophys. Res. 100, 2833–2840. doi:10.1029/94JD02824

Baskaran, M., Swarzenski, P.W., 2007. Seasonal variations on the residence times and partitioning of short-lived radionuclides (^{234}Th, ^{7}Be and ^{210}Pb) and depositional fluxes of ^{7}Be and ^{210}Pb in Tampa Bay, Florida. Mar. Chem. 104, 27–42.

Benitez-nelson, C.R., Buesseler, K.O., 1999. Phosphorous-32, phosphorous-37, beryllium-7 and lead-210: Atmospheric fluxes and utility in tracing stratosphere/troposphere exchange. J. Geophys. Res. 104, 11745 – 11754.

Blake, W.H., Walling, D.E., He, Q., 1999. Fallout beryllium-7 as a tracer in soil erosion investigations. Appl. Radiat. Isot. 51, 599–605.

Caillet, S., Arpagaus, P., Monna, F., Dominik, J., 2001. Factors controlling ^{7}Be and ^{210}Pb atmospheric deposition as revealed by sampling individual rain events in the region of Geneva , Switzerland. J. Environ. Radioact. 53, 241–256.

Conaway, C.H., Storlazzi, C.D., Draut, A.E., Swarzenski, P.W., 2013. Short-term variability of 7Be atmospheric deposition and watershed response in a Pacific coastal stream, Monterey Bay, California, USA. J. Environ. Radioact. 120, 94–103.

Doering, C., Akber, R., 2008. Beryllium-7 in near-surface air and deposition at Brisbane, Australia. J. Environ. Radioact. 99, 461–7.

Du, J., Zhang, J., Wu, Y., 2008. Deposition patterns of atmospheric ^{7}Be and ^{210}Pb in coast of East China Sea, Shanghai, China. Atmos. Environ. 42, 5101–5109.

Dueñas, C., Fernandez, M.C., Carretero, J., Liger, E., Canete, C., 2002. Atmospheric deposition of ^{7}Be at a coastal Mediterranean station. J. Geophys. Res. 106, 34065 – 34065.

Feely, H.W., Larsen, R.J., Sanderson, C.G., 1989. Factors that cause seasonal variations in Beryllium-7 concentrations in surface air. J. Environ. Radioact. 9, 223–249.

González-Gómez, C., Azahra, M., López-Peñalver, J.J., Camacho-García, a, El Bardouni, T., Boukhal, H., 2006. Seasonal variability in ^{7}Be depositional fluxes at Granada, Spain. Appl. Radiat. Isot. 64, 228–34.

Gourdin, E., Evrard, O., Huon, S., Reyss, J.-L., Ribolzi, O., Bariac, T., Sengtaheuanghoung, O., Ayrault, S., 2014. Spatial and temporal variability of ^{7}Be and ^{210}Pb wet deposition during four successive monsoon storms in a catchment of northern Laos. J. Environ. Radioact. 136, 195–205.

Hirose, K., Honda, T., Yagishita, S., Igarashi, Y., Aoyama, M., 2004. Deposition behaviors of ^{210}Pb, ^{7}Be and thorium isotopes observed in Tsukuba and Nagasaki, Japan. Atmos. Environ. 38, 6601–6608.

Igarashi, Y., Hirose, K., Otsuji-hatori, M., 1998. Beryllium-7 deposition and its relation to sulfate deposition. J. Atmos. Chem. 29, 217–231.

Ioannidou, a, Papastefanou, C., 2006. Precipitation scavenging of ^{7}Be and ^{137}Cs radionuclides in air. J. Environ. Radioact. 85, 121–36.

Ishikawa, Y., Murakami, H., Sekine, T., Yoshihara, K., 1995. Precipitation scavenging studies of radionuclides in air using cosmogenic ^{7}Be. J. Environ. Radioact. 26, 19–36.

Jweda, J., Baskaran, M., van Hees, E., Schweitzer, L., 2008. Short-lived radionuclides (^{7}Be and ^{210}Pb) as tracers of particle dynamics in a river system in southeast Michigan. Limnol. Ocean. 53, 1934–1944.

Kim, G., Hussain, N., Scudlark, J.R., Church, T.M., 2000. Factors Influencing the Atmospheric Depositional Fluxes of Stable Pb , ^{210}Pb , and ^{7}Be into Chesapeake Bay. Juurnal Atmos. Chem. 36, 65–79.

Krmar, M., Radnović, D., Rakic, S., Matavuly, M., 2007. Possible use of terrestrial mosses in detection of atmospheric deposition of ^{7}Be over large areas. J. Environ. Radioact. 95, 53–61.

Krmar, M., Wattanavatee, K., Radnović, D., Slivka, J., Bhongsuwan, T., Frontasyeva, M. V, Pavlov, S.S., 2013. Airborne radionuclides in mosses collected at different latitudes. J. Environ. Radioact. 117, 45–8.

Lecroart, P., Schmidt, S., Jouanneau, J., Weber, O., 2005. Be-7 and Th-234 as tracers of sediment mixing on seasonal time scale at the water-sediment interface of the Thau Lagoon. Radioprot. Suppl. 40, 661–667.

Leppänen, a.-P., Pacini, a. a., Usoskin, I.G., Aldahan, a., Echer, E., Evangelista, H., Klemola, S., Kovaltsov, G. a., Mursula, K., Possnert, G., 2010. Cosmogenic ^{7}Be in air: A complex mixture of production and transport. J. Atmos. Solar-Terrestrial Phys. 72, 1036–1043.

McNeary, D., Baskaran, M., 2003. Depositional characteristics of ^{7}Be and ^{210}Pb in southeastern Michigan. J. Geophys. Res. 108, 4210.

Narazaki, Y., Fujitaka, K., Igarashi, S., Ishikawa, Y., Fujinami, N., 2003. Seasonal variation of ^{7}Be deposition in Japan. J. Radioanal. andNuclear Chem. 256, 489–496.

NOAA. 2016. Magnetic Field Calculators. Available on http://www.ngdc.noaa.gov/geomag-web/?model=igrf#igrfwmm

Papastefanou, C., Ioannidou, A., 1995. Aerodynamic size association of ^{7}Be in ambient aerosols. J. Environ. Radioact. 26, 273–282.

Pham, M.K., Povinec, P.P., Nies, H., Betti, M., 2013. Dry and wet deposition of ^{7}Be, ^{210}Pb and ^{137}Cs in Monaco air during 1998-2010: seasonal variations of deposition fluxes. J. Environ. Radioact. 120, 45–57.

Piñero García, F., Ferro García, M. a., Azahra, M., 2012. ^{7}Be behaviour in the atmosphere of the city of Granada January 2005 to December 2009. Atmos. Environ. 47, 84–91.

Renfro, A.A., Cochran, J.K., Colle, B.A., 2013. Atmospheric fluxes of ^{7}Be and ^{210}Pb on monthly time-scales and during rainfall events at Stony Brook , New York (USA). J. Environ. Radioact. 116, 114–123.

Sakurai, H., Shouji, Y., Osaki, M., Aoki, T., Gandou, T., Kato, W., Takahashi, Y., Gunji, S., Tokanai, F., 2005. Relationship between daily variation of cosmogenic nuclide Be-7 concentration in atmosphere and solar activities. Adv. Sp. Res. 36, 2492–2496.

Schuller, P., Iroumé, A., Walling, D.E., Mancilla, H.B., Castillo, A., Trumper, R.E., 2006. Use of beryllium-7 to document soil redistribution following forest harvest operations. J. Environ. Qual. 35, 1756–1763.

Sepulveda, A., Schuller, P., Walling, D.E., Castillo, A., 2008. Use of ^{7}Be to document soil erosion associated with a short period of extreme rainfall. J. Environ. Radioact. 99, 35–49.

Shi, Z., Wen, A., Yan, D., Zhang, X., Ju, L., 2011. Temporal variation of ^{7}Be fallout and its inventory in purple soil in the Three Gorges Reservoir region, China. J. Radioanal. Nucl. Chem. 288, 671–676.

Su, C.-C., 2003. Factors controlling atmospheric fluxes of ^{7}Be and ^{210}Pb in northern Taiwan. Geophys. Res. Lett. 30, 2018.

Sugihara, S., Osaki, S., Baba, T., Tagawa, Y., Maeda, Y., Inokura, Y., 1999. Distribution and mean residence time of natural radionuclides in the forest ecosystem. J. Radioanal. Nucl. Chem. 239, 549–554.

Taylor, a., Blake, W.H., Smith, H.G., Mabit, L., Keith-Roach, M.J., 2013. Assumptions and challenges in the use of fallout beryllium-7 as a soil and sediment tracer in river basins. Earth-Science Rev. 126, 85–95.

Tositti, L., Brattich, E., Cinelli, G., Baldacci, D., 2014. 12 years of ^{7}Be and ^{210}Pb in Mt. Cimone, and their correlation with meteorological parameters. Atmos. Environ. 87, 108–122.

Usoskin, I.G., Kovaltsov, G. a., 2008a. Production of cosmogenic ^{7}Be isotope in the atmosphere: Full 3-D modeling. J. Geophys. Res. 113, D12107.

Usoskin, I.G., Kovaltsov, G. a., 2008b. Cosmic rays and climate of the Earth: possible connection. Comptes Rendus Geosci. 340, 441–450.

Yamamoto, M., Sakaguchi, A., Sasaki, K., Hirose, K., Igarashi, Y., Kim, C.K., 2006. Seasonal and spatial variation of atmospheric ^{210}Pb and ^{7}Be deposition: features of the Japan Sea side of Japan. J. Environ. Radioact. 86, 110–31.

Yang, Y., Gai, N., Geng, C., Zhu, X., Li, Y., Xue, Y., Yu, H., Tan, K., 2013. East Asia monsoon ' s in fl uence on seasonal changes of beryllium-7 and typical POPs in near-surface atmospheric aerosols in mid-latitude city. Atmos. Environ. 79, 802–810.

Yi, Y., Zhou, P., Liu, G., 2007. Atmospheric deposition fluxes of ^{7}Be, ^{210}Pb and ^{210}Po at Xiamen , China. J. Radioanal. Nucl. Chem. 273, 157–162.

Zhang, L., Yang, W., Chen, M., Wang, Z., Lin, P., Fang, Z., Qiu, Y., Zheng, M., 2016. Atmospheric Deposition of ^{7}Be in the Southeast of China: A Case Study in Xiamen. Areosol Air Qual. Res. 16, 105–113.

Zhu, J., Olsen, C.R., 2009. Beryllium-7 atmospheric deposition and sediment inventories in the Neponset River estuary, Massachusetts, USA. J. Environ. Radioact. 100, 192–197.

Paper II

^{7}Be in Soil Profiles in the Undisturbed Area Using for Reference Site to Estimate the Soil Erosion

Santi Raksawong[1], Miodrag Krmar[2], Tripob Bhongsuwan[1]

[1] Nuclear Physics Research Laboratory and Geophysics Research Center, Department of Physics, Faculty of Science, Prince of Songkla University, Thailand

[2] Department of Physics, Faculty of Science, University of Novi Sad, Trg D. Obradovica 4, Novi Sad, 21000, Serbia

Submitted to Proceeding in International Nuclear Science and Technology Conference (INST 2016), Centara Grand at Central Plaza Ladprao Bangkok, Thailand.

It was received and considered to publish in Journal of Physics: Conference series in International Nuclear Science and Technology Conference (INST 2016)

^{7}Be in soil profiles in the non-disturbed area using for reference site to estimate the soil erosion

S. Raksawong[1], M. Krmar[2], T. Bhongsuwan[1]

[1] Nuclear Physics Research Laboratory and Geophysics Research Center, Department of Physics, Faculty of Science, Prince of Songkla University, Thailand
[2] Department of Physics, Faculty of Science, University of Novi Sad, Trg D. Obradovica 4, Novi Sad, 21000, Serbia

Corresponding author. Tel: +66-0-7428-8761; fax: +66-0-7455-8849.
E-mail address: tripop.b@psu.ac.th (T. Bhongsuwan).

Abstract. The fallout radionuclide ^{7}Be is increasingly being used as a mean of obtaining qualitative information on soil erosion and sedimentation rates within agricultural landscapes. The information of event-related soil erosions is provided by using ^{7}Be measurements. In this presentation, we select two undisturbed and flat areas to calculate the reference inventory and relaxation mass depth for using ^{7}Be technique to document short-term erosion. Our results show that the depth distribution of ^{7}Be in undisturbed soil profiles is 1.0 cm in sites S02 and S03; the initial activities are 31.6 and 38.8 Bq kg^{-1} for the first and the second, respectively. The relaxation mass depths obtained are 5.4 and 7.2 kg m^{-2} and the measured reference ^{7}Be inventories in the sediment are 71 and 110 Bq m^{-2} for sites S02 and S03, respectively. The difference values of the relaxation mass depth and the reference inventory of both sites can imply that for a short term soil erosion and sedimentation study using ^{7}Be, the reference site will be chosen near the study site as close as possible.

1. Introduction

Some agricultural practices such as burning of stubble and crop residues after harvest and subsequent ploughing and disc harrowing for seed bed preparation leave large areas of bare soil have increased the soil erosion problem that relating to the reduction in soil productivity and to the off-site effects of eroded sediments such as transportation of the sediment-associated nutrients and contaminants (e.g. agricultural pesticides) through terrestrial and aquatic ecosystems [1-3]. Therefore, the reliable information on rates of soil loss is important for an improved

understanding of sediment transfer and storage in catchments and river basins to provide a basis for sustainable soil management. The environmental radionuclides ^{137}Cs ($T_{1/2}$ = 30 years) and unsupported ^{210}Pb ($T_{1/2}$ = 22 years) are widely used to document rates of soil redistribution on agricultural land, but both these radionuclides have provided the retrospective estimates in the medium-term (i.e. ca. 50 years for ^{137}Cs and up to 100 years for unsupported ^{210}Pb). The obtained values from both radionuclides are the average rates taking account of inter-annual variability in the magnitude and frequency of erosional events. If the magnitudes of soil loss associated with individual events or periods characterized by specific land use conditions are required, the short-lived radionuclide ^{7}Be is used to calculate the soil erosion rates. This paper reports a preliminary investigation of undisturbed and flat areas aimed at exploring the potential for using ^{7}Be measurements as the reference inventory and relaxation mass depth for using ^{7}Be technique to document the short-term events of soil erosion.

2. Methodology

2.1 Background and initial depth distribution of the beryllium-7 in the soil

^{7}Be is produced by cosmic-rays spallation reactions in the atmosphere. These reactions occur primarily in the stratosphere and upper troposphere, where charged particles (alpha particles, electrons and protons) induce nuclear reactions with oxygen and nitrogen atoms. The ^{7}Be attaches to airborne particles and its deposition is continuously delivered to the earth's surface by wet and dry fallout [2, 4-6]. Although it is quickly sequestered to the Be^{2+} ion by slightly acid rainfall, its ion is rapidly and strongly fixed onto the clay minerals in the soil [2, 7]. Therefore, cosmogenic ^{7}Be has been widely used as a tracer to document both the magnitudes and the spatial patterns associated with short-term or event based soil redistribution on agricultural land [1-2, 8]. The ^{7}Be technique is, principally, based on the comparison of ^{7}Be inventory (Bq m^{-2}) between sampling sites and reference site. The reference site is selected from undisturbed area located near sampling sites. The ^{7}Be inventory for sampling site is depleted relative to the reference inventory that can be referred to occurring erosive

processes, whereas areas of deposition can be located by increased inventories [1-2, 8].

There are three key assumptions for using ^{7}Be measurements to estimate both the soil erosion and sedimentation rates [1-2, 8]. The deposition of ^{7}Be fallout from atmosphere to the ground surface is, first, spatially uniform. Secondly, preexisting ^{7}Be in the surface soil in study area is uniformly distributed across the area. Finally, the ^{7}Be deposited during event is rapidly and strongly absorbed in couple centimeters of surface soil and can be mobilized by erosion. From these assumptions, it can be assumed that the initial vertical distribution of the ^{7}Be activity $C(x)$, Bq kg^{-1}, within the soil will be characterized by an exponential decrease with mass depth x, kg m^{-2}[1-2]. The sample model to estimate the soil erosion and sedimentation rates is described below,

$$C(x) = C(0)\exp(-x/h_o) \tag{1}$$

where $C(0)$ is the initial activity of the surface soil (at $x = 0$) and h_o, kg m^{-2}, is the relaxation mass depth.

The reference inventory of ^{7}Be , A_{ref}, Bq m^{-2}, is defined as the initial total areal activity at an uneroded stable site or reference site in the study area:

$$A_{ref} = A(0) = \int_0^\infty C(x)dx = h_o C(0) \tag{2}$$

The areal activity of ^{7}Be below depth x, $A(x)$, Bq m^{-2}, for the initial distribution is therefore:

$$A(x) = \int_x^\infty C(x)dx = A_{ref}\exp(-x/h_o) \tag{3}$$

The relaxation mass depth describes the shape of the initial depth distribution of both the activity as shown in Eq. (1) and areal activity as shown in Eq. (3) in the soil.

By measuring the activity of ^{7}Be, C, in different depth increments of soil collected from the reference site and establishing the mass depth of each depth increment, the values of $A(x)$ for corresponding mass depths x down the reference profile can be calculated. Logarithmically transforming Eq. (3), h_o and the reference inventory A_{ref} can be deduced from a linear regression between $ln[A(x)]$ and x.

2.2 Study site

Atmospheric deposition fluxes of ^{7}Be in the study areas, the fallout samples during December, 2012 to December, 2013 were collected at the top roof of the Physics building called S01 site (7°00′24.6″ N, 100°29′57.8″ E) where is the control site to estimate the running inventory of ^{7}Be. Two sites for the collected rain water samples were at selected reference sites 7°00′30.9″ N, 100°30′22.0″ E and 6°59′32.1″ N, 100°33′04.8′ E named S02 and S03, respectively. Rain water samples were collected after rainfall event. The water sample was filtered through the MnO_2-fiber (5 g) in the cylinder of 15 cm long and 1.8 cm inner diameter.

a) b)

Figure. 1 *photographs showing **a)** soil core sampling; **b)** cutting the cover grasses*

Soil samples were collected from two selected reference sites S02 and S03 in the U-Tapao subcatchment, Songkhla province, South of Thailand. Using a hand-operated corer equipped with the PVC core tubes (8.5 cm internal diameter, 20 cm length), 8 soil cores were collected from two selected reference sites S02 and S03 on

January 10, 2014. **Figure. 1** shows the soil core sampling and cutting the cover grasses. All the soil cores were kept vertically and returned to the laboratory, and then sliced at 0.5 cm intervals through its depth using the hand-held extruder. All the cut samples were dried at 105 °C for 24 hours by electric oven, grinded by ceramic mortar, sieved to < 2 mm fraction, homogenized, weighed and put into a polyethelene bottle.

2.3 Measurement and analyze method

Beryllium-7 activity concentrations in fallout (wet and dry) samples, soil samples and grass were determined by measuring its gamma line at 477.6 keV. The gamma-ray measurements were performed using gamma spectrometer with an HPGe detector (GC7020, Canberra Industries, USA) in a low-background cylindrical shield (Model 747, Canberra, USA). Data were accumulated in a multichannel analyzer (DSA1000, Canberra, USA) based on a personal computer. The energy resolution was 0.88 keV (FWHM) at 122 keV (^{57}Co), and 1.77 keV (FWHM) at 1332 keV (^{60}Co). The minimum counting-time for each sample was set in 40,000s. For samples having an analytical error more than 1σ, the counting-time will be added until 100,000s to provide reasonable analytical error (less than 25% or 1σ). The spectrum analysis was performed by the computer software Genie 2000 (Canberra, USA). The absolute efficiency curve of detector used in this work was fitted from activity concentrations of discrete gamma-ray lines in the IAEA TEL 2011-03 WWOPT soil-04 sample with certified radionuclide activities, and it was used to calculate the relative efficiency of ^{7}Be at 477.7 keV. The ^{7}Be activities were corrected for decay to the sampling time on January 10, 2014.

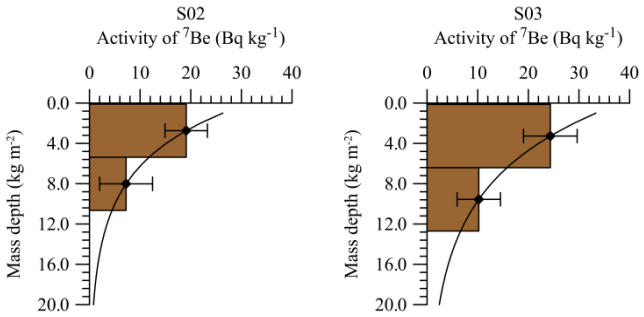

Figure 2. The depth distribution of ^{7}Be in the soil profiles within the selected reference site.

3. Results and Discussions

The results reported in this paper were obtained from the selected reference sites (S02 and S03) where located in the undisturbed, non-tilled areas at the U-Tapao subcatchment, Songkhla province, South of Thailand. Our results obtained that the depth distribution of ^{7}Be in undisturbed soil profiles is 1.0 cm in both sites (S02 and S03), the initial activities are 31.6 and 38.8 Bq kg^{-1} for S02 and S03 sites, respectively. The ^{7}Be activities for both locations declined exponentially with mass depth as shown in **Figure 2**. Following from Eq.(1), the relaxation mass depths were, therefore, calculated from linear regression between $ln[C(x)]$ and x. These obtained results are 5.4 and 7.2 kg m^{-2} for S02 and S03 sites, respectively.

The measured reference inventories of ^{7}Be in soil profiles are 71 and 110 Bq m^{-2} for S02 and S03 sites, respectively. The calculated reference inventories from Eq. (2) are 170 and 279 Bq m^{-2} for sites S02 and S03, respectively. Both important parameters, relaxation mass depth and reference inventory, can be used to estimate the magnitudes of soil loss or deposition. The soil mass eroded per unit area, R, kg m^{-2}, or soil erosion rate as provided from Blake et al. [1] can be calculated by using both values as:

$$R = h_o \ln\left[A_{ref} / A\right] \tag{4}$$

Moreover, the magnitude of deposited sediment rate, R', kg m^{-2}, can be calculated by:

$$R' = \left(A' - A_{ref}\right)/C_d \quad (5)$$

when A', Bq m^{-2}, is the areal activity of ^{7}Be at a sampling point located in in sediment deposition zone, C_d is the mean ^{7}Be activity of deposited sediment that can be estimate by

$$C_d = \int_S C_e R dS \Big/ \int_S R dS \quad (6)$$

when C_e, Bq kg^{-1}, is the weighted mean ^{7}Be activity of mobilized sediment from eroding area S, m^{-2}, which can be:

$$C_e = (A_{ref} - A)/R = A_{ref}\left[1 - \exp(-R/h_o)\right]/R \quad (7)$$

From procedure outlined above, the h_o and A_{ref} are crucial important for calculating the magnitudes of soil erosion and deposition rates at sampling points for study area. The relaxation mass depths and ^{7}Be inventories in the soil obtained from selected reference sites are different because the atmospheric depositional fluxes of ^{7}Be are controlled by several factors depending on location, precipitation, the cover crops etc. Lohaiza et al. [7] reported the monthly relaxation mass depths and inventory of ^{7}Be from one reference site changing with season, the maximum value in heavy rain period and low value in dry period. Moreover, the relaxation mass depths in some locations where selected reference site are significantly higher than that in others. Therefore, the running atmospheric deposition flux of ^{7}Be and the ^{7}Be activity in the covered grasses were used to compare with the inventory in soil for the reference study site.

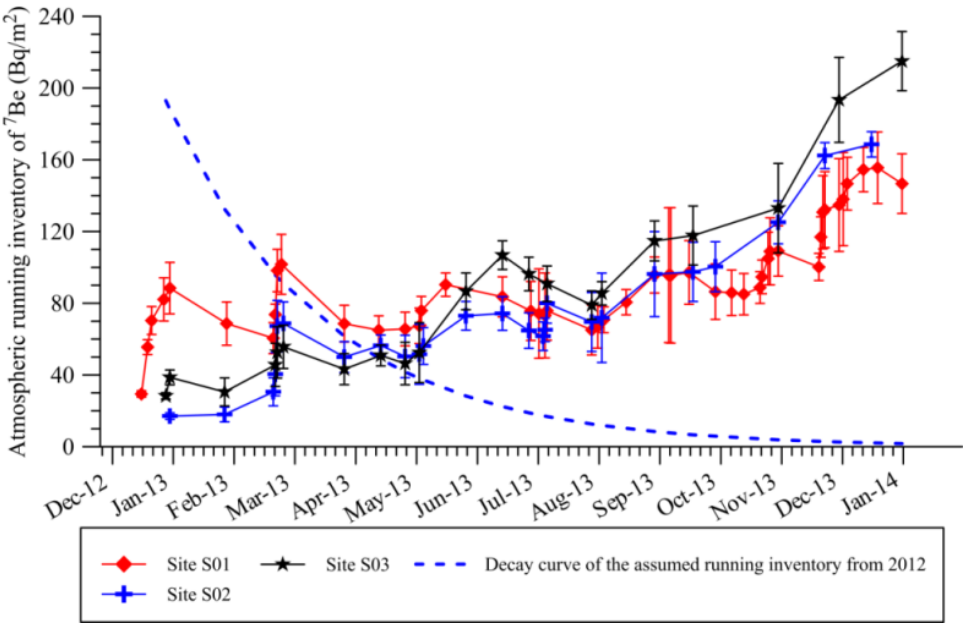

Figure 3. Atmospheric running inventory of ^{7}Be collected from S01, S02 and S03 sites.

In this study, the atmospheric depositional fluxes of ^{7}Be have been decay-corrected to the collecting time of rainfall sample, and the results are shown in **Figure 3**. In order to calculate the atmospheric deposition running inventory of ^{7}Be following Zhu and Olsen [9], the calculated running inventory values range 29 ± 1 to 156 ± 14 Bq m^{-2}, with an average value of 92.2 Bq m^{-2} for site S01, 2.0 ± 0.5 to 96 ± 12 Bq m^{-2}, with an average value of 19.6 Bq m^{-2} for site S02, and 2.9 ± 1 to 103 ± 15 Bq m^{-2}, with an average value of 27.1 Bq m^{-2} for S03. The estimated ^{7}Be running inventories at the time of sediment sampling are 156 ± 20 Bq m^{-2}, 169 ± 7 Bq m^{-2} and 215 ± 17 Bq m^{-2} for S01, S02 and S03, respectively. Atmospheric running inventories for the selected reference sites S02 and S03 are shown in the **Table 1** and **Figure 4**.

Table 1. ^{7}Be inventories in soil cores, areal activities in cover grasses and atmospheric running inventories which were corrected to the soil sampling time on January 10, 2014.

Type/Location	S02	S03
Measured sediment inventory (Bq m^{-2})	71 ± 18	110 ± 26
Areal activity in grasses (Bq m^{-2})	112 ± 9	108 ± 9
Atmospheric running inventory (Bq m^{-2})	169 ± 7	215 ± 17

The measured ^{7}Be inventories in soil cores of 71 ± 18 and 110 ± 26 Bq m^{-2} were stacked with the areal activities in cover grasses of 112 ± 9 and 108 ± 9 Bq m^{-2} for the selected reference sites S02 and S03, respectively. The atmospheric running inventories are similar to the stacked activities between the areal activities in cover grasses and the measured ^{7}Be inventories in soil cores for both sites S02 and S03 as shown in **Figure 4.**

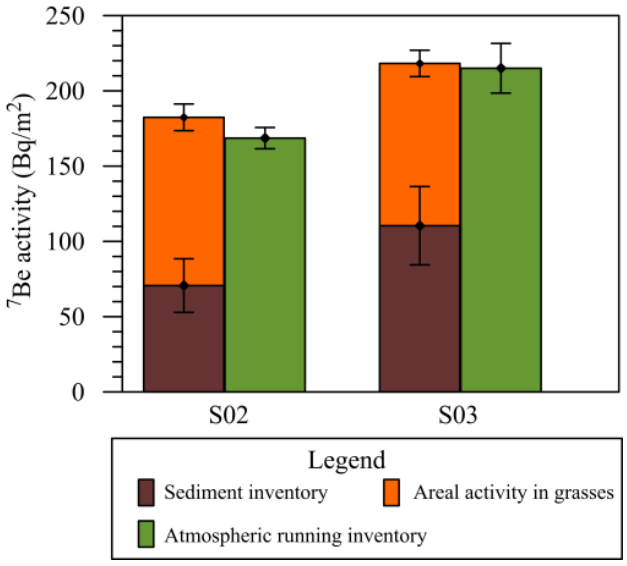

Figure 4. the bar charts comparing the atmospheric running inventory and the stacked columns between measured sediment inventory and areal activity in grasses.

Event though, the calculated reference inventories, 170 and 279 Bq m^{-2}, are larger than the measured inventories. The measured inventories in soil cores, 71 ± 18 and 110 ± 26 Bq m^{-2} for both sites S02 and S03, may be used as the reference inventories, A_{ref}, in the model to calculate the soil erosion and deposition rates in

study area. This is in fact the calculated reference inventories are not possible to be larger than the atmospheric running inventory. This problem may occur due to the thicker section of soil cores. In the future work, the thin sliced section of soil cores will be made, because there will be more than two points in the ^{7}Be profiles with mass depth to estimate the calculated reference inventory and relaxation mass depth.

4. Conclusions

This preliminary study is successful to detect ^{7}Be in the soil and atmospheric deposition in the South of Thailand located near equatorial zone where is known that very low ^{7}Be activity and the ^{7}Be measurement in soil can be used to estimate important parameters (relaxation mass depth and reference inventory) for approached model of the soil erosion and deposition. Further work, we will investigate the magnitudes of both soil erosion and deposition obtained from the ^{7}Be measurement technique in this study area.

Acknowledgments

This research was financially supported by the Prince of Songkla University (project code: SCI550111S), the National Research Council of Thailand (project code: SCI560125S), the Physics Department, Geophysics Research Center, Faculty of Science and the graduate fellowship from the Graduate School, Prince of Songkla University. In addition, the first author would like to thank Prince of Songkla University, Graduate Studies Grant.

References

1. Blake, W.H., Walling, D.E., He, Q., 1999. Fallout beryllium-7 as a tracer in soil erosion investigations. Appl. Radiat. Isot. 51, 599–605.
2. Schuller, P., Iroumé, A., Walling, D.E., Mancilla, H.B., Castillo, A., Trumper, R.E., 2006. Use of beryllium-7 to document soil redistribution following forest harvest operations. J. Environ. Qual. 35, 1756–1763.

3. Sepulveda, A., Schuller, P., Walling, D.E., Castillo, A., 2008. Use of ^{7}Be to document soil erosion associated with a short period of extreme rainfall. J. Environ. Radioact. 99, 35–49.

4. Ioannidou, a, Papastefanou, C., 2006. Precipitation scavenging of ^{7}Be and ^{137}Cs radionuclides in air. J. Environ. Radioact. 85, 121–36.

5. Ishikawa, Y., Murakami, H., Sekine, T., Yoshihara, K., 1995. Precipitation scavenging studies of radionuclides in air using cosmogenic ^{7}Be. J. Environ. Radioact. 26, 19–36.

6. Papastefanou, C., Ioannidou, A., 1995. Aerodynamic size association of ^{7}Be in ambient aerosols. J. Environ. Radioact. 26, 273–282.

7. Lohaiza, F., Velasco, H., Juri Ayub, J., Rizzotto, M., Di Gregorio, D.E., Huck, H., Valladares, D.L., 2014. Annual variation of ^{7}Be soil inventory in a semiarid region of central Argentina. J. Environ. Radioact. 130, 72–7.

8. Zapata, F., Garcia-Agudo, E., Ritchie, J.C., Appleby, P.G., 2002. Introduction, in: Zapata F. (Ed.), Handbook for the Assessment of Soil Erosion and Sedimentation Using Environmental Radionuclides. Kluwer Academic Publishers, Dordrecht, Netherlands, pp. 1–13.

9. Zhu, J., Olsen, C.R., 2009. Beryllium-7 atmospheric deposition and sediment inventories in the Neponset River estuary, Massachusetts, USA. J. Environ. Radioact. 100, 192–197.

Paper III

Measurement of ^{7}Be inventory in the Outer Songkhla Lagoon, Thailand

Santi Raksawong[1], Miodrag Krmar[2], Tripob Bhongsuwan[1*]

[1]Nuclear Physics Research Laboratory and Geophysics Research Center, Department of Physics, Faculty of Science, Prince of Songkla University, Hat Yai, 90112, Thailand

[2]Department of Physics, Faculty of Sciences, University of Novi Sad, Trg D. Obradovica 4 , Novi Sad, 21000, Serbia

E-mail address of the corresponding author: tripop.b@psu.ac.th (T. Bhongsuwan).

Published in Journal of Radioanalytical and Nuclear Chemistry:(2016) Vol 310, p 33 – 44 :DOI 10.1007/s10967-016-4851-0.

J Radioanal Nucl Chem (2016) 310:33–44
DOI 10.1007/s10967-016-4851-0

Measurement of ^{7}Be inventory in the outer Songkhla lagoon, Thailand

Santi Raksawong[1] · Miodrag Krmar[2] · Tripob Bhongsuwan[1]

Received: 19 August 2015 / Published online: 29 April 2016

Abstract The main objective of this study is to estimate the sediment distribution pattern in the outer part of the Songkhla Lagoon, in southern Thailand, by measuring the cosmogenic ^{7}Be in the lake bottom sediment cores. The results indicate that ^{7}Be inventories are larger in the areas where channels collecting water from large subcatchments flow into the lake (mouths of Pak Ro, U-Tapao, Ro-1, and Ro-3 canals). Lower ^{7}Be inventory areas are observed near mouth of channel transporting eroded materials from smaller subcatchments and at the northern tip of Koh Yo island, which is strongly influenced by tidal currents and wind waves which can probably cause sediment re-suspension.

Keywords Atmospheric ^{7}Be · ^{7}Be running inventory · ^{7}Be inventory · Songkhla lagoon · Sediment

Introduction

In recent decades, the pollution problems in the Songkhla lagoon have continuously become worse [1–10]. The main sources of the pollutants for the outer part of the Songkhla lagoon include sewage from the Songkhla and the Hat Yai urban areas, waste from the Songkhla harbor, near shore drainage, and effluents from the large factories around the lake and the watershed [5, 8, 9, 11–14]. Moreover, the fine sediment eroded with the pullutants from the lake watershed among the pollutants damaging the ecosystems in the lake [15, 16]. This sediment erosion is usually caused by human activities (non-sustainable farming practices, overgrazing, deforestation, and change in land use from farm to urban), as well as by natural processes (runoff, flooding). Because of these increasing problems, it is essential to obtain reliable quantitative data, and to comprehensively assess the problems. The actions should then be steered towards effective sustainability, based on both economic and environmental impacts. The current study of sedimentation dynamics and its patterns in this lake will provide understanding of the dynamics of pollutants, and aids in developing sustainable effective management.

The environmental radionuclides ^{137}Cs, ^{210}Pb, and ^{7}Be, have been widely used to determine the dynamics of sediment, namely deposition, erosion, and distribution patterns [e.g. 17–19]. In particular, the cosmogenic radionuclide ^{7}Be has been used to determine recent (short-term) soil erosion/sedimentation in watersheds that have been degraded by natural processes or human activities [e.g. 17, 18, 20–26]. This technique may also be used to estimate recent sedimentation patterns in lakes, rivers, and marine shores [e.g.27–34].

The nuclide ^{7}Be is naturally produced by the spallation reactions of cosmic particle rays (protons and neutrons) with the nuclei of light elements (carbon, oxygen and nitrogen), in the stratosphere and the troposphere. These cosmogenic ^{7}Be atoms are readily attached to airborne particulates, and settle to the earth's surface by precipitation and by dry deposition [e.g. [35]]. Therefore, the ^{7}Be in a lake is supplied by two incoming streams, the one directly entering from the atmosphere into the water column and lake-bottom, and the other transported from the

✉ Tripob Bhongsuwan
tripop.b@psu.ac.th

[1] Nuclear Physics Research Laboratory and Geophysics Research Center, Department of Physics, Faculty of Science, Prince of Songkla University, Hat Yai 90112, Thailand

[2] Department of Physics, Faculty of Sciences, University of Novi Sad, Trg D. Obradovica 4, Novi Sad 21000, Serbia

Table 1 Event of total rainfall, ^{7}Be atmospheric deposition flux, and the calculated running inventory of ^{7}Be atmospheric deposition during December 21, 2012 to December 31, 2013 at the top roof of Physics Building, Prince of Songkla University

Collecting date	Exposure time (day)	Total rainfall (mm)	^{7}Be depositional flux (Bq m^{-2})	Running inventory (Bq m^{-2})
21-Dec-12	1	42.2	29 ± 2	29 ± 1
24-Dec-12	3	56.8	27 ± 2	56 ± 3
26-Dec-12	1	20.8	16 ± 1	70 ± 6
1-Jan-13	4	74.7	17 ± 2	82 ± 9
4-Jan-13	3	48.8	9 ± 2	88 ± 10
1-Feb-13	27	3.8	7 ± 1	69 ± 9
24-Feb-13	23	51.2	10 ± 2	61 ± 6
25-Feb-13	1	110.6	14 ± 1	74 ± 4
26-Feb-13	1	47.6	25 ± 2	98 ± 8
28-Feb-13	3	29.8	6.0 ± 0.9	102 ± 12
31-Mar-13	31	2.8	0.6 ± 0.1	69 ± 7
17-Apr-13	17	104.6	10 ± 1	65 ± 6
30-Apr-13	13	11.2	11 ± 1	66 ± 7
7-May-13	7	59.8	7 ± 1	67 ± 7
8-May-13	1	29.0	9 ± 1	76 ± 6
20-May-13	22	153.6	25 ± 1	90 ± 5
17-Jun-13	17	104.1	21 ± 2	84 ± 8
1-Jul-13	13	8.8	6 ± 1	76 ± 12
5-Jul-13	4	23.6	2.4 ± 0.6	74 ± 18
8-Jul-13	1	14.6	1.8 ± 0.7	73 ± 17
9-Jul-13	1	13.4	3.7 ± 0.8	76 ± 12
31-Jul-13	24	17.4	8 ± 2	65 ± 10
3-Aug-13	2	43.2	4.3 ± 0.9	67 ± 8
6-Aug-13	2	39.2	6.5 ± 0.8	71 ± 5
17-Aug-13	11	70.0	19 ± 1	81 ± 5
31-Aug-13	13	101.0	29 ± 3	96 ± 7
7-Sep-13	6	10.0	8.2 ± 0.9	96 ± 27
8-Sep-13	1	24.6	1.1 ± 0.6	96 ± 27
17-Sep-13	11	29.9	12 ± 1	97 ± 13
30-Sep-13	13	14.2	4 ± 1	86 ± 11
8-Oct-13	8	12	7.9 ± 0.9	86 ± 9
14-Oct-13	6	62.6	6 ± 1	85 ± 8
22-Oct-13	8	127.6	12.1 ± 0.9	89 ± 6
23-Oct-13	1	15.8	7.1 ± 0.8	95 ± 7
26-Oct-13	3	70.8	14 ± 1	105 ± 10
27-Oct-13	1	51.4	5 ± 1	109 ± 13
31-Oct-13	4	77.2	5.7 ± 0.9	109 ± 10
20-Nov-13	20	123.6	16 ± 1	100 ± 5
21-Nov-13	1	158	18 ± 1	117 ± 8
22-Nov-13	1	107.4	15 ± 2	131 ± 14
23-Nov-13	1	39	3.1 ± 0.6	132 ± 15
30-Nov-13	7	101.3	14 ± 2	135 ± 18
2-Dec-13	2	57.8	7 ± 2	138 ± 18
4-Dec-13	2	67.7	12 ± 1	147 ± 10
12-Dec-13	8	101.8	22 ± 2	155 ± 9
19-Dec-13	*5*	*76.6*	*14 ± 1*	*156 ± 14*
31-Dec-13	11	22.2	14 ± 2	147 ± 12

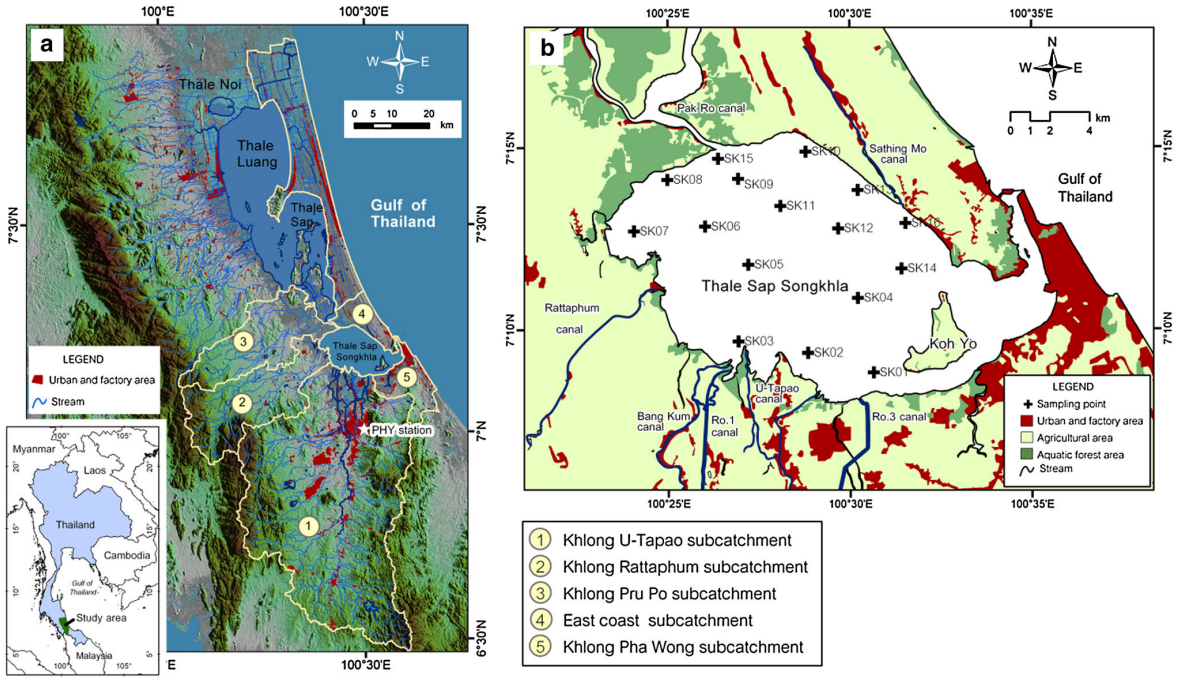

Fig. 1 Location maps of the study area, **a** Thale Sap Songkhla subcatchment, **b** sampling points

watershed through streams and overland flow [e.g.17, 36–38].

Although ^{7}Be was frequently used in environmental studies, most of those research activities were focused to exploration of soil erosion. Published results concerning ^{7}Be content in lake and lagoon sediments involving its spatial distribution are not so abundant in scientific literature. The most important goal in this pilot study was to establish range of ^{7}Be inventory at Songkhla Lagoon, compare it with results of other similar studies and check if there is some heterogeneity in ^{7}Be inventory pattern. Moreover, vertical distribution and the maximum penetration depths of ^{7}Be were determined to estimate recent sedimentation patterns. Comparison of the ^{7}Be sediment inventories with the running inventory of ^{7}Be atmospheric deposition measured in the period of 12 months before the time of sample collection of lake-bottom material, can help us to gain rough indication concerning sediment accumulation or resuspension/erosion. As the studied lagoon lake is shallow, the hydrodynamic properties (including runoff,

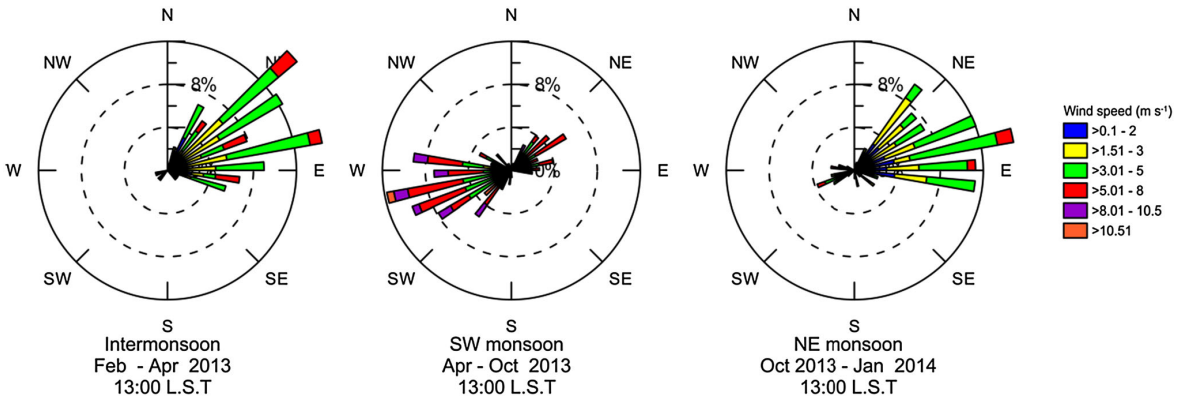

Fig. 2 Wind diagram showing percentage of wind direction at the Songkhla meteorological station (WMO Index: 568501/48568, located 7°12′14″N 100°36′11″E) during January 2013–January 2014. (data from Thai Meteorological Department)

diurnal variation of tides, and wind waves) probably have significant influence to the sedimentation processes. Obtained results of this pilot study can suggest if ^{7}Be technique has potential as a tool for assessing of some environmental parameters related to sediment in one very interesting water system—Songkhla lagoon highly influenced by heavy tropical rains, winds and tidal activities.

Experimental

In this study, we assume that the direct deposition of ^{7}Be is a constant, because the precipitation of ^{7}Be from the atmosphere is relatively uniform regionally. However, its value can vary by up to an order of magnitude by location, depending on factors such as rainfall and geography [e.g.17, 23–25, 34, 39]. The principal hypothesis applied in this pilot study is as follows; ^{7}Be reaches the soil surface and attaches strongly to fine particles [23–25, 33]. The ^{7}Be and attached soil are then eroded from the watershed and transported to the lake, and the ^{7}Be inventory is thereby related to the sediment deposition. The highest ^{7}Be inventory activity corresponds to the greatest sedimentation rates as well as the depth distribution processes. Low ^{7}Be inventories correspond to the low sedimentation rate or increased effects of erosion and redistribution. However short-living ^{7}Be can be used to indicate the short-term sedimentation patterns, and the distribution of ^{7}Be inventory can reveal the sedimentation/erosion in the moment of the sampling.

Study area

The Songkhla lagoon is the largest lagoon in South–East Asia, located in southern Thailand and on the east coast of Malay Peninsula (Fig. 1a). It has a total catchment area of 7460 km^2 and a total water surface of 1050 km^2. The Songkhla lagoon consists of four parts: Thale Noi (swamp), Thale Luang (inner part), Thale Sap (middle part) and Thale Sap Songkhla (outer part) as illustrated in Fig. 1a. This study focused on Thale Sap Songkhla, the outer part of the Songkhla lagoon (Fig. 1b.), which is located between latitudes 7°05′ and 7°50′N and longitudes 100°05′ and 100°37′E. The Thale Sap Songkhla catchment can be further subdivided into five parts. The two parts in the South and South-West side are the Khlong U-Tapao subcatchment (2357 km^2) and the Khlong Rattaphum subcatchment (625 km^2), while the Khlong Pru Po subcatchment (487 km^2) is in the North–West side, and the East coast subcatchment (205 km^2), the Khlong Pha Wong subcatchment (137 km^2) are located on the East side see Fig. 1a.

The majority of Songkhla lagoon subcatchments, 5660 km^2, is agricultural areas that consist of rubber plantation (60 %), paddy field (30 %) and others (10 %). There are rain forest, crop area and mangrove forest (ca. 940, 694, and 168 km^2, respectively). Urban area is 126 km^2 (1.5 %). There are mainly sandy clay in the Khlong U-Tapao subcatchment, Khlong Rattaphum subcatchment, and silty clay in the east coast subcatchment (data from GEO-informatics center for natural resource and environment and Land development department). The annual runoff of Khlong U-tapao subcatchment and Khlong Rattaphum subcatchment is 1664×10^6 and 249×10^6 m^3, respectively. There is the runoff from subcatchments of upper and middle parts of Songkhla lagoon about 1305×10^6 m^3 (data from Hydrology and water management center, Royal irrigration department).

The climate of the Songkhla lagoon is controlled by tropical monsoons, namely the South–West (May–October) and the North–East (October–February) monsoons. There are generally two seasons—the rainy season and the dry season. The rainy season (May–September) is influenced by the South–West monsoon that brings moist and warm air from the Indian Ocean, whereas the North–East monsoon brings moist air from the Gulf of Thailand (October–January). Meteorological data were provided by the Thai Meteorological Department at the Songkhla Meteorological station (WMO Index: 568501/48568, located 7°12′14″N 100°36′11″E). During the period A.D. 2003–2013, the mean annual rainfall was 2451 mm and rains were frequent in October to December. The mean of total rainfall in these 3 months was 1441 mm. The monsoon system affects the wind speed and direction in the Songkhla lagoon. The wind was predominantly from ENE during the inter-monsoon (February–April), from WSW during the SW monsoon (April–October), and from ENE during the NE monsoon (October–January) as shown in Fig. 2.

Thale Sap Songkhla is a shallow coastal lagoon and has an average depth ca. 2.0 m in the rainy season, and about 1.5 m in the summer season. There is a narrow deep channel (5–12 m depth) near the Songkhla harbor connecting the lagoon with the sea of the Gulf of Thailand, and allowing the tides to propagate into the lagoon. The aquatic environment in the Thale Sap Songkhla is therefore a mixture of seawater and freshwater, and the hydrodynamics of this system are mainly controlled by tides, runoff, winds and waves. The salinity of the lake water has reached about 31 ppt in the dry season, when the saline water is brought into the lagoon by the tidal effects and there is less runoff water from the subcatchments. The salinity reaches zero ppt (freshwater) in the season with heavy rains (October–January) as the rain water drains from the catchments in two main streams; Rattaphum and

Fig. 3 Photographs showing **a** panoramic scenery of the study lake during sediment core sampling and **b** slicing the extruded piece of sediment core 0.5 cm thick using a metal blade in the laboratory

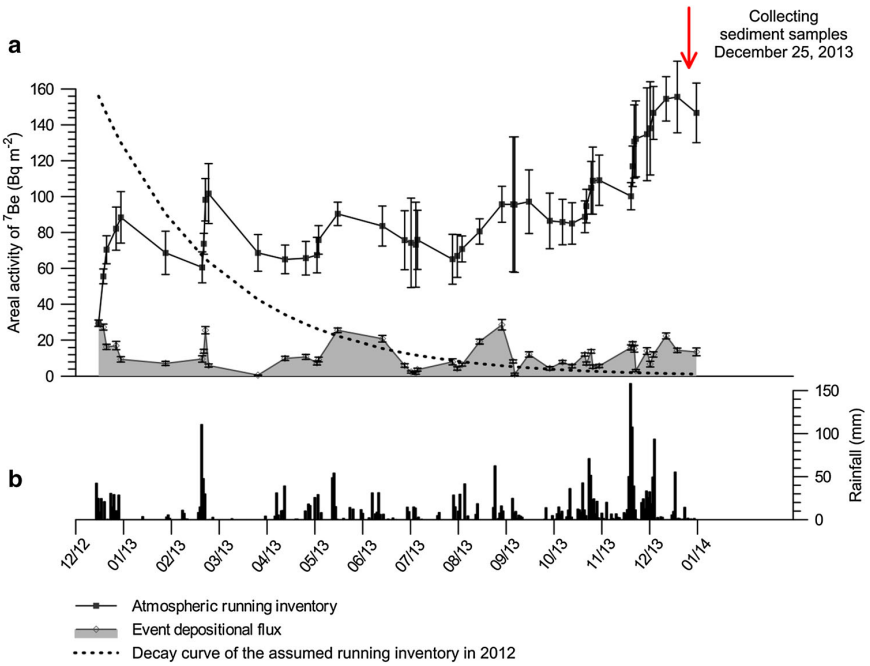

Fig. 4 **a** Atmospheric deposition flux and running inventory of ^{7}Be. **b** rainfall at the Kho Hong agrometeorological station (WMO Index: 568301/48571, located 7°N 100°30′E) (data from Thai Meteorological Department)

U-Tapao canals, and there is also inflow at the Pak Ro canal from the middle lake [40–42]. The current velocity of water in the inner lake (Thale Luang; Fig. 1a) is quite slow, 0.01–0.10 m/s, whereas strong flows from 0.40 to 0.75 m/s occur at the tidal inlet during the maximum outflow in the low tide or the maximum inflow in the high tide [40, 43].

Rain water samples for estimation of the total inventory flux of ^{7}Be

In order to estimate the total inventory flux of ^{7}Be in the study area, the wet and dry deposited samples were collected by using three polyethelene buckets that is a surface area of 0.13 m^{2}. All of the buckets was exposed to atmosphere continuously on the top roof of the Physics building (PHY station) situated ca.15 km away from the study lake, from December, 2012, to December, 2013. The collection procedure for wet deposition, firstly, the large rainwater samples were collected into the tanks after rainfall events. Secondly, the inside of the buckets was rinsed with 1.5 L acidified distilled water by 30 mL 6 N nitric acid, and the rinsing water was combined with the rainwater sample. Finally, 20 L rainwater sample was justified to pH 7 by 2 N NaOH and filtered through MnO_2-

fiber (5 g) in a 15 cm long and 1.8 cm inner diameter cylinder. During periods without rainfall event, the acidified distilled water was added in the buckets to prevent any loss atmospheric deposited material. The distilled water was processed like rainwater sample. After filtering, the MnO_2-fibers in distilled water medium were measured by a gamma spectrometer with an HPGe detector (GC7020, Canberra Industries, USA) in a low-background cylindrical shield (Model 747, Canberra, USA) and coupled to a multichannel analyzer (DSA1000, Canberra, USA). The energy resolution was 0.88 keV (FWHM) at 122 keV (^{57}Co), and 1.77 keV (FWHM) at 1332 keV (^{60}Co). The efficiency calibration of the detection system was done with a certified Europium-152 solution (Gammadata Instrument AB, Sweden), at 477.7 keV gamma energy. The counting-time was set to 21600 s for each sample, to provide a reasonably low analytical error (less than 25 % or 1σ). The prominent point in using MnO_2-fibers to absorb the ^{7}Be in rain water are (1) quick sample preparation, and (2) comparatively short counting-time in gamma spectrometry relative to other methods.

Sampling of the lake-bottom sediment cores

A total of 16 bottom sediment cores were collected using a hand-operated corer equipped with PVC core tubes (8.5 cm internal diameter, 30 cm length), sampled from Thale Sap Songkhla on December 25, 2013. Figure 3a shows the panoramic scenery of the study lake during the sampling of sediment cores. All the sediment cores were kept vertical and transported to the laboratory, then sliced at 0.5 cm intervals in depth direction, using a hand-held extruder (Fig. 3b). These specimens were dried at 105 °C for 24 h in an electric oven, ground in a ceramic mortar, sieved to <2 mm fraction, weighed, and stored in polyethelene bottles. The ^{7}Be activities were measured using gamma spectrometry (as described above). The minimum counting-time for each specimen was set in 40,000 s to get overall uncertainty of ^{7}Be concentration (in Bq kg^{-1}) less than 25 % at 1 σ. However, for some specimens having low content of ^{7}Be, we added to the counting-time up to 100,000 s to provide reasonable analytical error (less than 25 % or 1 σ). Gamma ray energy at 477.7 keV was used

Table 2 The ^{7}Be areal activity, total inventory in sediment cores and percentage of classified sediment

Cores	^{7}Be activity of penetration layer (Bq m^{-2})				^{7}Be inventory[a]	Expected running inventory[b]	Difference[c]	Percentage of classified sediment		Zone
	Depth (cm)							Medium to fine sand (0.1–0.3 mm)[d]	Very fine sand to silt and clay (<0.1 mm)[d]	
	0.0–0.5	0.5–1.0	1.0–1.5	1.5–2.0	(Bq m^{-2})	(Bq m^{-2})	(Bq m^{-2})			
SK01	221 ± 80	238 ± 71	156 ± 72		615 ± 135	156 ± 14	+459	41.1	58.9	B
SK02	217 ± 65	105 ± 61	98 ± 58	55 ± 62	420 ± 141	156 ± 14	+264	42.1	57.9	
SK03	49 ± 22	38 ± 17	26 ± 17		114 ± 34	156 ± 14	−42	65.1	34.9	
SK05	164 ± 46	91 ± 45	102 ± 46		358 ± 86	156 ± 14	+202	34.6	65.4	
SK06	174 ± 57				174 ± 57	156 ± 14	+18	28.9	71.1	C
SK07	173 ± 29	111 ± 30			284 ± 30	156 ± 14	+128	16.9	83.1	
SK08	111 ± 23	70 ± 30	56 ± 27	96 ± 33	237 ± 76	156 ± 14	+81	18.5	81.5	
SK09	388 ± 51	174 ± 49	156 ± 49		718 ± 105	156 ± 14	+562	29.3	70.7	A
SK10	239 ± 52	136 ± 50	106 ± 53		482 ± 105	156 ± 14	+326	34.9	65.1	
SK11	201 ± 32	104 ± 28	34 ± 28		340 ± 98	156 ± 14	+184	25.8	74.2	
SK13	225 ± 76	139 ± 69	106 ± 62		470 ± 132	156 ± 14	+314	49.2	50.8	
SK15	219 ± 29	127 ± 18	167 ± 29	74 ± 35	587 ± 51	156 ± 14	+431	66.3	33.7	
SK04	224 ± 69	84 ± 70			308 ± 137	156 ± 14	+152	48.4	51.6	D
SK12	80 ± 57	228 ± 51			307 ± 116	156 ± 14	+151	46.2	53.8	
SK14	184 ± 81				184 ± 81	156 ± 14	+28	24.9	75.1	
SK16	175 ± 69				175 ± 69	156 ± 14	+19	28.8	71.2	
Avg.					370					
S.D.					174					

[a] The ^{7}Be inventory is the summation of ^{7}Be activity for all layer in a sediment core

[b] The expected running inventory is the atmospheric depositional running inventory at the time of sampling (December 25, 2013)

[c] The differences between the ^{7}Be inventory and the expected running inventory for each sediment core. Positive values (+) indicate sediment accumulation and negative values (−) indicate sediment erosion. (followed the method in Zhu and Olsen [34])

[d] Particle size of sediment classified by sieve analysis

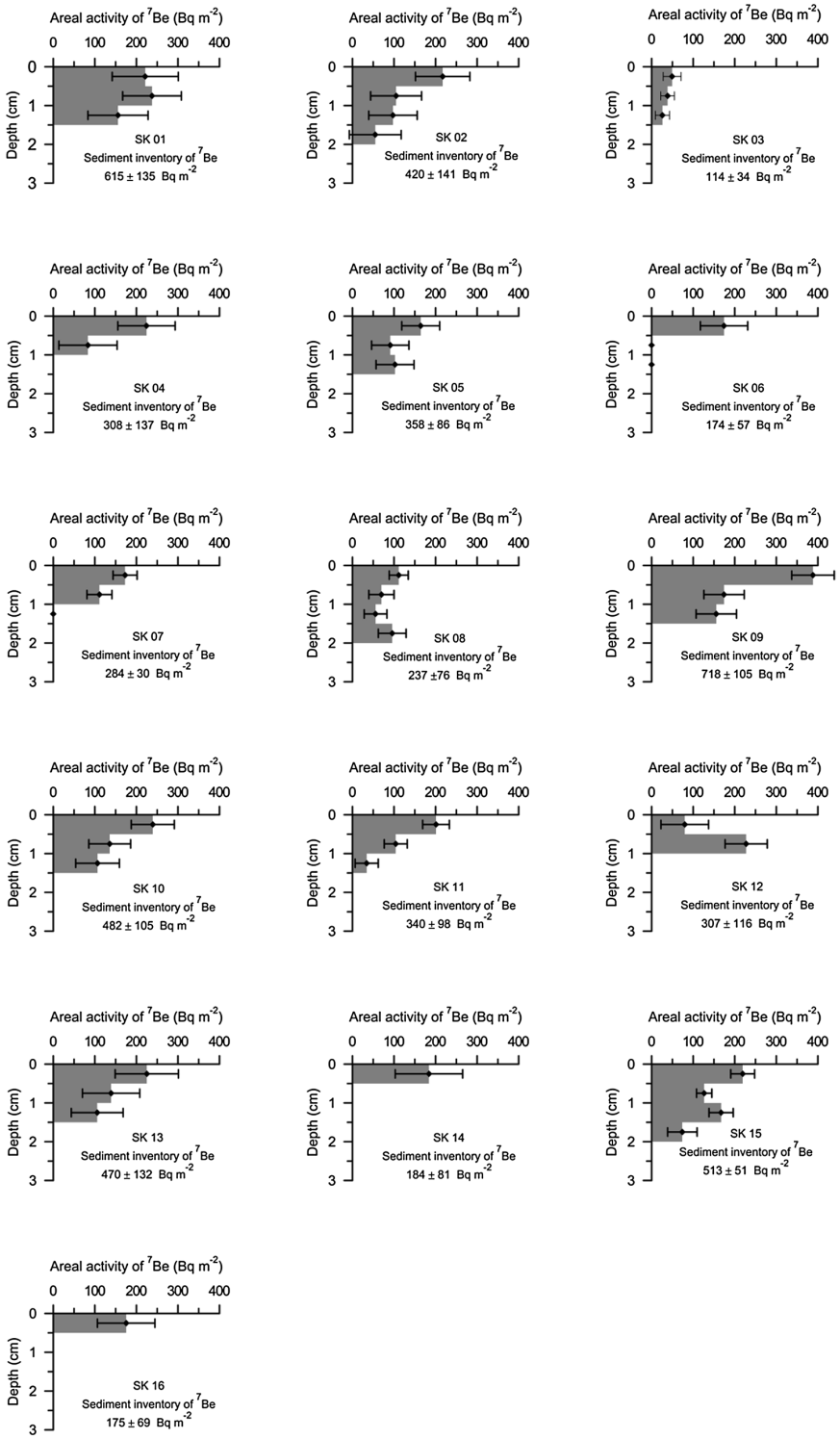

Fig. 5 The vertical profiles of areal activity of ^{7}Be in lake sediment versus sample depth, the measured sediment inventory of ^{7}Be in these cores in the outer part of the Songkhla Lagoon

for the ^{7}Be determination. The IAEA TEL 2011-03 WWOPT soil-04 sample with certified radionuclide activities was used to calculate the relative efficiency of ^{7}Be detection at 477.7 keV. The ^{7}Be activities were corrected for decay from the sampling time on December 25, 2013.

Results and discussion

Atmospheric deposition flux of ^{7}Be

In this study, due to varying rainfall periods and their frequency, the atmospheric deposition flux of ^{7}Be was decay-corrected to the collection time of the rainfall sample. The results are shown in Table 1 and Fig. 4a for sampling from December 21, 2012 to December 31, 2013. The minimum, maximum and mean daily depositional fluxes of ^{7}Be during this period were 0.02 ± 0.01, 29 ± 3, and 4.6 Bq m^{-2}, respectively. This result also is comparable to the the daily atmospheric deposition fluxes of ^{7}Be at Xiamen, China during March 2004 to April 2005 varied between 0.11 and 2.93 Bq m^{-2} that reported by Yi et al. [44]. However, the annual atmospheric deposition flux of ^{7}Be, 0.52 kBq m^{-2}, is in low range comparing to those reported from Japan during period of 1989–1995 (0.325–4.94 kBq m^{-2}) [45, 46]. This is probably because Thailand is located in the magnetic equator zone.

In order to calculate the atmospheric deposition running inventory of ^{7}Be following Zhu and Olsen [34], all the preceding atmospheric deposition fluxes were decay-corrected to the current time and summed to the present value, shown in Table 1 and Fig. 4a. Running inventory of ^{7}Be is a result of very non-uniform atmospheric deposition and decay. In our study this quantity will be used as some kind of index showing us inventory of ^{7}Be which could be expected in the simplest possible case where just deposition and decay (without transport processes) have influence on ^{7}Be presence. The calculated ^{7}Be running inventory of 156 ± 14 Bq m^{-2} at the time of sediment-core sampling in 2013, on December 25. Because atmospheric ^{7}Be samples were collected in short period (about 1 year), the estimated ^{7}Be running inventory from the year 2012 was assumed to equal that of the year 2013 (156 Bq m^{-2}) as shown with exponential decay to less than 2.0 Bq m^{-2} in 6 half-lives of ^{7}Be (about 321 days; dashed line in Fig. 4a). It can be concluded that the running inventory of ^{7}Be from the year 2012 had little influence on the expected running inventory of ^{7}Be at the time of sediment sampling in 2013. Therefore, the expected running inventory of 156 ± 14 Bq m^{-2} in the study lake was considered a good estimate (italicized in Table 1).

Considering that half-life of ^{7}Be is relatively short, time necessary to transport ^{7}Be from surrounding catchments or through water column can have influence on ^{7}Be activity in sediment. There are several factors affecting mixing of water in lagoon: five tributaries from subcatchments, strong wind, tidal activities and currents inside lake, it was reasonable to suppose that in lake can be find region having sedimentation rate and residence time significantly different (in the time scale of ^{7}Be half-life) than in other parts of lake. Therefore, we can expect that possible differences in timing of sedimentation at different locations of the lake do not significantly influences spatial distribution of ^{7}Be measured in this study.

^{7}Be inventories and depth profiles

Obtained results of ^{7}Be sediment inventories are depicted on Table 2. It can be seen that measured inventories are ranging from 114 ± 34 to 718 ± 105 Bq m^{-2}. Similar values were obtained by Bai et al. [27]. They have measured ^{7}Be inventories from 237 ± 73 to 783 ± 44 Bq m^{-2} in lake sediments collected at the deepest part of the lake (overlying water depth up to 60 m). In some river estuaries characteristic ^{7}Be inventories can be significantly higher at locations exposed to intensive deposition (5460 ± 54 Bq m^{-2}, as reported by Zhu and Olsen [34]). Minimal value of ^{7}Be inventory (core SK03) is just 73 % of what would be expected from the running inventory at the time of sampling. This probably indicates a slower rate of net sediment accumulation at this site in this period, but may also reflect some sediment redeposition or erosion, what should be confirmed by further studies. The maximal ^{7}Be sediment inventory measured at the site SK09 is 4.6 times higher than running inventory.

The depth profiles of ^{7}Be areal activity in each sediment core are presented in Table 2 and Fig. 5. The maximum depths at which ^{7}Be activities were still measurable in the cores ranged from 0.5 cm (sites SK06, SK14 and SK16) to 2.0 cm (sites SK02 and SK15). It is comparable with results obtained by Bai et al. [27]. In their study ^{7}Be was mainly distributed within top of 2 cm of lake-bottom. The maximum of ^{7}Be depth penetration in another one fresh water lake [47] is between 2 and 3 cm, however there are examples that measurable values of ^{7}Be activities were obtained in river estuaries at depths of 10 cm [34]. For the topmost sediment layer at 0–0.5 cm depth, the minimum and maximum areal activities of ^{7}Be were 49 ± 22 and 338 ± 51 Bq m^{-2}, found at sites SK03 and SK09 respectively.

If we suppose that a continuously and non-perturbed accumulating sediment is governed by two most important processes: its supply via sedimentation and radioactive decay, depth distribution of ^{7}Be activity should be described by uniformly decreasing exponential function of depth. Depth profiles depicted at Fig. 5 show that sediments at several cores (SK10, SK11, SK13, for example) appears to

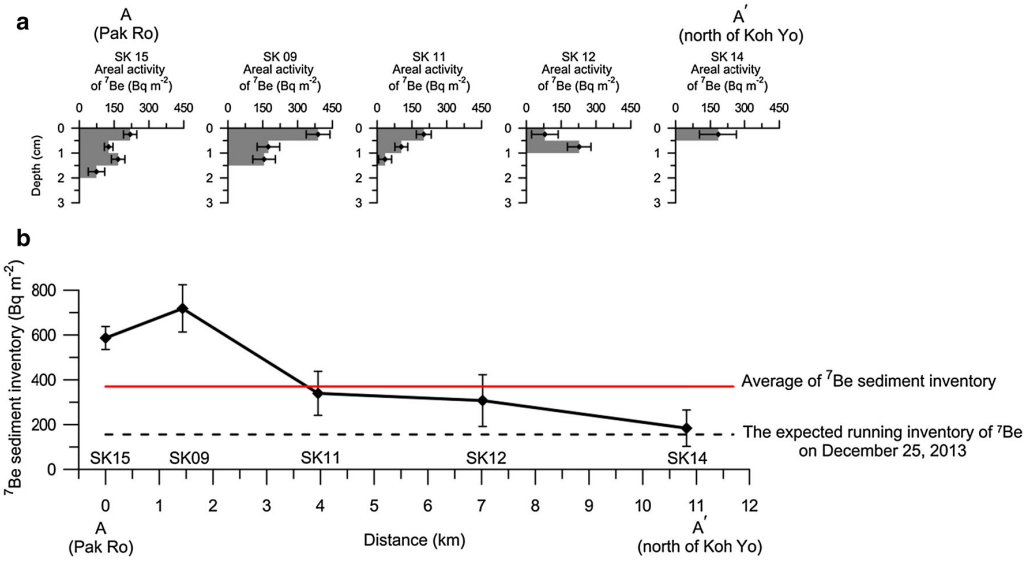

Fig. 6 **a** The vertical profiles of ^{7}Be areal activity and **b** The ^{7}Be sediment inventory from Pak Ro canal to North of Koh Yo along the line *AA′*

reflect what would be expected from radioactive decay with continuous sediment deposition without mixing. In some of other location we have reduced thickness of the bottom containing ^{7}Be (SK6, SK14). It indicates the locations exposed to erosion or with reduced rate of sedimentation. It is interesting to notice that there are several depth profiles which exhibits a prominent sub-surface peaks (SK12 is one of them) which may reflect some redistribution mechanisms or perhaps some nonuniform deposition of sediment on the lake bottom.

It is interesting to notice that the maximum depth of ^{7}Be in SK09 core is less than 2 cm. Moreover, at this core maximal ^{7}Be inventory was detected in topmost sediment layer, almost 400 Bq m^{-2}. Subsurface peak at the depth distribution of ^{7}Be in SK15 core indicates that sediment deposition in this area is not stable. Both mentioned locations are close to of Pak Ro channel delta and when heavy rainfall events occurred in subcatchments of the upper and the middle lake, large amounts of sediment were eroded and then redeposited in this area. Chittrakarn et al. [2] reported pretty high mean sediment accumulation rate of 0.57 cm y^{-1} in this zone, from ^{137}Cs measurements. So high ^{7}Be inventory and specific depth distribution could be result of hydrodynamic changes in this area. Nonuniform depth distribution and high ^{7}Be inventory measured at SK01 core could be explained by similar way. In the area of SK01 core large U-Tapao subcatchments contributes with eroded material from cultivated soil. Moreover, this zone is influenced by the slack tides when the maximum ebb or flood currents occur, with slow flow rates [40, 43, 48].

Considering that tributary channels transport sediment from subcatchment, it should be interesting to compare ^{7}Be inventories and depth distribution patterns along one line which can coincide with some water currents in lake. The depth profiles of ^{7}Be areal activity and the sediment inventories along line AÁ, connecting the sites near Pak Ro canal to the northern tip of Koh Yo island, are shown in Fig. 6a and b, respectively. It can be seen that maximal ^{7}Be inventory is observed at core SK09, about 1.5 km far from Pak Ro channel mouth, and the ^{7}Be sediment inventories were lower at the sites SK11, SK12 and SK14. The depth profile of ^{7}Be areal activity at the site SK11 decreased uniformly, and the ^{7}Be sediment inventory was close to average indicating that this area could be a uniform deposition zone with only slight disturbances. The depth profiles of ^{7}Be areal activity and ^{7}Be sediment inventories at the sites SK12 and SK14 indicate possible erosion, probably caused by strong tidal currents.

The areal pattern of ^{7}Be inventory in the outer part of Songkhla Lagoon

We assumed that most of the ^{7}Be measured in sediment comes by dry and wet precipitation falling directly on the surface of the lake and from soil particles transported by surface runoffs. We should keep in mind that some amount of ^{7}Be dissolved in water, or transported by streams, especially in period of heavy rains, avoid sedimentation, however this process is not analyzed in this work.

In this study, the ^{7}Be sediment inventories ranged from 114 ± 34 Bq m^{-2} at the site SK03 to 718 ± 105 Bq m^{-2} at the site SK09. The spatial distribution of ^{7}Be sediment inventory is illustrated with a colored contour map in Fig. 7b. It can be seen that two highest ^{7}Be inventory areas

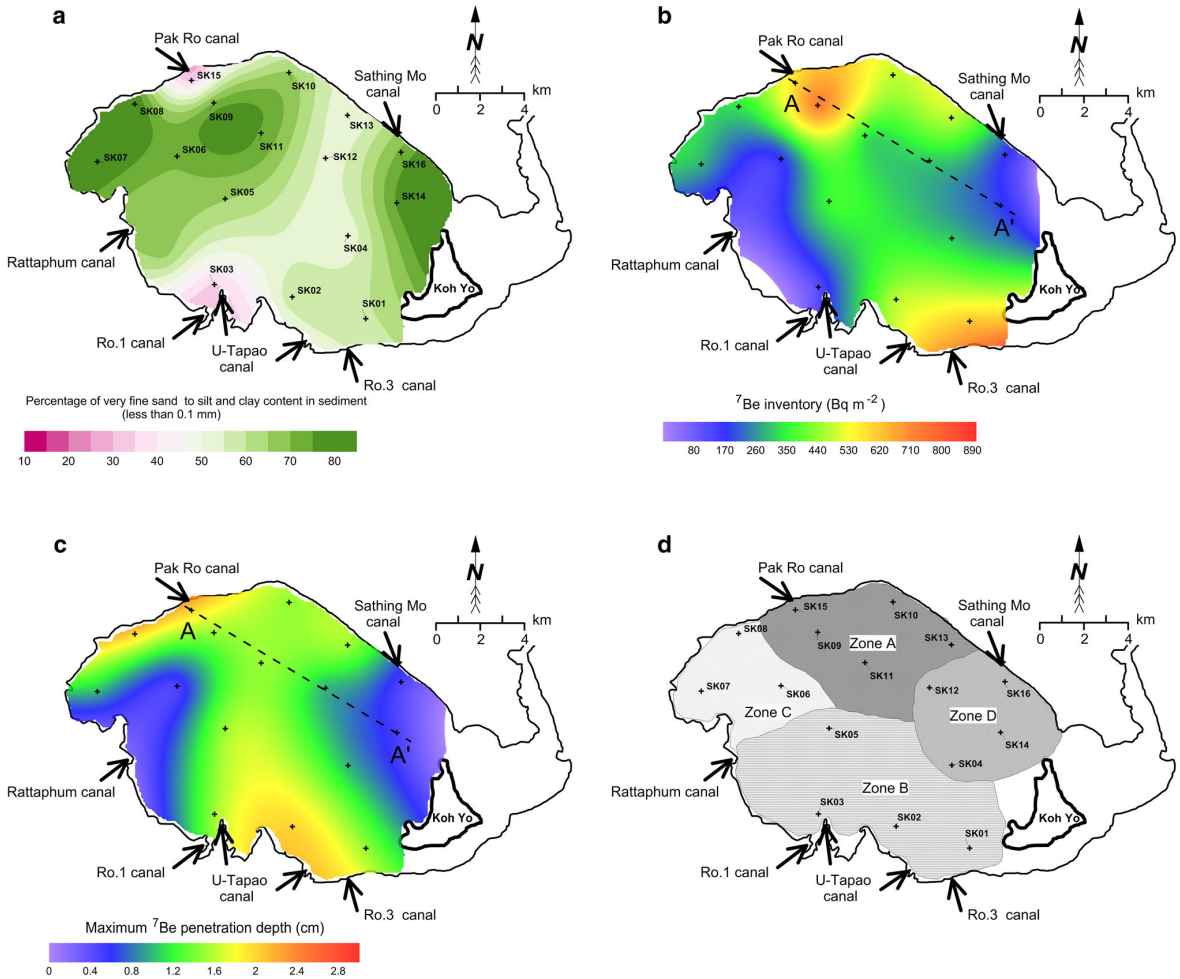

Fig. 7 *Shaded color* map of **a** percentage of very fine sand to silt and clay content in sediment, **b** ^{7}Be inventory, **c** maximum penetration depth of ^{7}Be, and **d** separated zones of sedimentation/erosion pattern

are at the northern part of the lagoon (Pak Ro delta; Zone A) and at the southern part of the lagoon (U-Tapao, Ro-1, Ro-3 deltas; Zone B). The two lowest ^{7}Be inventory zones are the southwest of the lagoon (Ratthaphum delta; zone C) and the northern tip of the Koh Yo island (zone D).

It can be expected that the runoff water or flood carrying eroded sediments from their subcatchment through river or channel tributaries after flow into the lake deposit sediments near the mouth. The location of sedimentation also depends on grain size, affecting distance from the mouth. At the Pak Ro delta area (zone A in Fig. 7d), the main type of sediment is the very fine sand, silt and clay, which is more abundant than medium and fine sand fraction, except at the mouth (SK15) as shown in the Table 2 and Fig. 7a. The ^{7}Be sediment inventory was high ranging between 340 and 718 Bq m^{-2}. This indicates that the sediment is transported from the middle of Songkhla Lagoon and from the nearby subcatchment before finally deposited near the mouth of Pak Ro canal. A large portion of the eroded sediments probably comes from the modern rubber and oil-palm plantations, and from cultivated rice fields in the subcatchment of the upper and middle part of Songkhla Lagoon.

In zone B or U-Tapao delta high values of ^{7}Be inventories (up to 615 Bq m^{-2}) were observed. High values of ^{7}Be deposition can be explained by the fact that U-Tapao subcatchment is the largest area of 2,357 km^{2}. The eroded sediment from U-Tapao subbasin was transported to this area by the Ro-1 and Ro-3 canals that were constructed to bypass the overflow, and to protect Hat Yai city against flooding in the rainy season.

Although, the very small sediment fraction (very fine sand, silt and clay) in Zone C were found more abundant than larger sizes, but the inventory of ^{7}Be was low,

indicating small ^{7}Be input in the lagoon zone C, matching the smaller size of Khlong Ratthapum sub-catchment (625 km^2) than the much bigger U-Tapao sub-catchment (2357 km^2).

In zone D, the very small size particles fraction was found more abundant than the larger sizes particles (in the Table 2 and Fig. 7a). The sediment inventories of ^{7}Be for the sites SK04, SK12, SK14 and SK16 were below those of zones A and B, and were comparable to the atmospheric running inventory. Moreover, the depth of ^{7}Be penetration in sediment cores in zone D is significantly lower than in other parts of lagoon. This fact can indicate effects of erosion because this zone is strongly influenced by the tidal currents and wind waves coming from the Gulf of Thailand. Effects of increasing salinity upon ^{7}Be desorption [26] should be tested in this zone in some further research.

Conclusions

The most important objective of this study was to use ^{7}Be as a tracer to examine recent accumulation pattern in the outer part of Songkhla Lagoon. In this study inventories as well as depth distributions of ^{7}Be in soil samples taken in Songkhla Lagoon were measured. These measurements indicate sediment accumulation zones at the Pak Ro zone and the U-Tapao zone, while the northern tip of Koh Yo is probably an erosion zone. Obtained results of ^{7}Be inventories are spread in the relative large region, from 114 to 718 Bq m^{-2}. Variations in the ^{7}Be inventories in sediment cores collected in the Songkhla Lagoon indicate a high degree of spatial heterogeneity in sediment accumulation patterns. These results suggest that ^{7}Be can serve as a useful tool for quantifying short-term changes in sediment dynamics.

The depth distributions of ^{7}Be in cores from Songkhla Lagoon showed that ^{7}Be was present only in the top 2 cm or less. The vertical profile of ^{7}Be in the sediment cores indicating continuous sediment deposition without mixing (exponential uniformly decreasing) was observed at just a few locations. At other sampling sites vertical distributions of ^{7}Be inventories were not uniform or maximal penetration depth was less than 2 cm. This fact indicates high dynamic and changes in sedimentation process, probably caused by hydrodynamical properties of lagoon water system.

Our measurements indicate that the phenomena in this area are complicated, and a good understanding of the hydrodynamic systems in this lagoon would require further studies. Obtained results are very encouraging and complete understanding of sedimentation can be gained after repeated measurements and comparison of measured short-term changes in the ^{7}Be sediment inventories and depth profiles with respect to characteristic seasonal and hydrological conditions in this area.

Acknowledgments This research was financially supported by the Prince of Songkla University (project code: SCI550111S), the National Research Council of Thailand (project code: SCI560125S), the Physics Department, Geophysics Research Center, Faculty of Science and the graduate fellowship from the Graduate School, Prince of Songkla University. In addition, the first author would like to thank the Prince of Songkla University Graduate Studies Grant. We thank Associate Professor Seppo Karrila, Faculty of Science and Industrial Technology, Prince of Songkla University and the Research and Development Office of the Prince of Songkla University, for English proof reading service. The Thai Meteorological Department is acknowledged for providing the meteorological data at the Songkhla station.

References

1. Bhongsuwan T, Bhongsuwan D (2002) Concentration of heavy metals Mn, Fe, Ni, Pb, Cr and Cd in bottom sediments of the Outer Songkhla Lake deposited between the year B.E. 2520-2538. Songklanakarin. J Sci Technol 24(1):89–106
2. Chittrakarn T, Pornpinatepong S, Bhongsuwan T, Nuannil P (1998) Mathematical model study for determination of sedimentation rate in Thale Sap Songkhla, Final report; Dept. of Physics, Prince of Songkla University, Songkhla
3. Gyawali S, Techato K, Yuangyai C, Musikavong C (2013) Assessment of relationship between land uses of riparian zone and water quality of river for sustainable development of river basin, A case study of U-Tapao river basin, Thailand. Procedia Environ Sci 17:291–297
4. Ladachart R, Suthirat C, Hisada K-I, Charusiri P (2011) Distribution of heavy metals in core sediments from the Middle part of Songkhla Lake, Southern Thailand. J Appl Sci 11(17):3117–3129
5. Pornpinatepong K, Kiripat S, Treewanchai S, Chongwilaikasaem S, Pornsawang C, Chantarasap P,Chandee C,Jantrakul P (2010) Pollution control and sustainable fisheries management in Songkhla Lake. Report No 2010-RR5, Dept. of Economics, Prince of Songkla University, Songkhla
6. Pradit S, Wattayakorn G, Angsupanich S, Baeyens W, Leermakers M (2010) Distribution of trace elements in sediments and biota of Songkhla Lake, Southern Thailand. Water Air Soil Poll 206:155–174
7. Pradit S, Pattarathomrong MS, Panutrakul S (2013) Arsenic Cadmium and Lead concentrations in sediment and biota from Songkhla Lake: a review. Procedia Soc Behav Sci 91:573–580
8. Sirinawin W, Turner DR, Westerlund S, Kanatharana P (1998) Trace metals study in the Outer Songkla Lake, Thale Sap Songkla, a southern Thai estuary. Mar Chem 62:175–183
9. Sirinawin W, Sompongchaiyakul P (2005) Nondetrital and total metal distribution in core sediments from the U-Tapao canal, Songkhla, Thailand. Mar Chem 94:5–16
10. Tanavud C, Yongchalermchai C, Bennui A, Densrisereekul O (2001) The expansion of inland shrimp farming and its environmental impacts in Songkla Lake Basin. Kasetsart J (Nat Sci.) 35:326–343
11. Angsupanich S, Kuwabara R (1999) Distribution of macrobenthic fauna in Phawong and U-Taphao canals flowing into a lagoonal lake, Songkhla, Thailand. Lakes Reserv Res Manage 4:1–13
12. Chevakidagarn P (2006) Operational problems of wastewater treatment plants in Thailand and case study: wastewater pollution

problems in Songkhla Lake Basin. Songklanakarin J Sci Technol 28(3):633–639
13. Maneepong S (1996) Distribution of heavy metals in sediments from outer part of Songkhla Lagoon, southern Thailand. Songklanakarin J Sci Technol 18(1):87–97
14. Maneepong S, Angsupanich S (1999) Concentrations of arsenic and heavy metals in sediments and aquatic fauna from the outer part of Songkhla Lagoon, Phawong and U-Taphao canals. Songklanakarin J Sci Technol 21(1):111–121
15. Environmental Protection Agency (2000) National Water Quality Inventory. Report No EPA-841-R-02-001, EPA Office of Water, Washington, DC
16. Donohue I, Molinos JG (2009) Impacts of increased sediment loads on the ecology of lake. Biol Rev 84:517–531
17. Walling D E (2004) Using environmental radionuclides to trace sediment mobilisation and delivery in river basins as an aid to catchment management. Proceeding Ninth International Symposium on River Sediment. October 18–21, Yichang, China 121–135
18. Zapata F, Garcia-Agudo E, Ritchie JC, Appleby PG (2002) Introduction. In: Zapata F (ed) Handbook for the assessment of soil erosion and sedimentation using environmental radionuclides. Kluwer Acad, Dordrecht
19. Uğur A, Saç MM, Yener G, Altmbaş Ü, Kurucu Y, Bolca M, Özden B (2004) Vertical distribution of the natural and artificial radionuclides in various soil profiles to investigation soil erosion. J Radioanal Nucl Chem 259(2):265–270
20. Blake WH, Walling DE, He Q (1999) Fallout beryllium-7 as a tracer in soil erosion investigations. Appl Radiat Isotopes 51:599–605
21. Blake WH, Walling DE, He Q (2002) Using cosmogenic beryllium-7 as a tracer in sediment budget investigations. Geogr Ann 84A(2):89–102
22. Mabit L, Benmansour M, Walling DE (2008) Comparative advantages and limitations of the fallout radionuclides ^{137}Cs, $^{210}Pb_{ex}$ and ^{7}Be for assessing soil erosion and sedimentation. J Environ Radioact 99:1799–1807
23. Schuller P, Iroumé A, Walling DE, Mancilla HB, Castillo A, Trumper RE (2006) Use of beryllium-7 to document soil redistribution following forest harvest operations. J Environ Qual 35:1756–1763
24. Schuller P, Walling DE, Iroumé A, Castillo A (2010) Use of ^{7}Be to study the effectiveness of woody trash barriers in reducing sediment delivery to streams after forest clearcutting. Soil Tillage Res 110:143–153
25. Sepulveda A, Schuller P, Walling DE, Castillo A (2008) Use of ^{7}Be to document soil erosion associated with a short period of extreme rainfall. J Environ Radioact 99:35–49
26. Taylor A, Blake WH, Smith HG, Mabit L, Keith-Roach MJ (2013) Assumptions and challenges in the use of fallout ^{7}Be as a soil and sediment tracer in river basins. Earth Sci Rev 126:85–95
27. Bai ZG, Wan GJ, Huang RG, Liu TS (2002) A comparison on the accumulation characteristics of ^{7}Be and ^{137}Cs in lake sediments and surface soils in western Yunnan and central Guizhou, China. Catena 49:253–270
28. Belmaker R, Stein M, Beer J, Christl M, Fink D, Lazar B (2014) Beryllium isotopes as tracers of Lake Lisan (last Glacial Dead Sea) hydrology and the Laschamp geomagnetic excursion. Earth Planet Sci Lett 400:233–242
29. Ciffroy P, Reyss J-L, Siclet F (2003) Determination of the residence time of suspended particles in the turbidity maximum of the Loire estuary by ^{7}Be analysis. Estuar Coast Shelf Sci 57:553–568
30. Feng H, Cochran JK, Hirschberg DJ (1999) ^{234}Th and ^{7}Be as tracers for the transport and dynamics of suspended particles in a partially mixed estuary. Geochim Cosmochim Acta 63(17):2487–2505
31. Matisoff G, Wilson CG, Whiting PJ (2005) The $^{7}Be/^{210}Pb_{xs}$ ratio as an indicator of suspended sediment age or fraction new sediment in suspension. Earth Surf Process Landforms 30:1191–1201
32. Palinkas CM, Nittrouer CA, Wheatcroft RA, Langone L (2005) The use of ^{7}Be to identify event and seasonal sedimentation near the Po River delta, Adriatic Sea. Mar Geol 222–223:95–112
33. Schmidt S, Jouanneau J-M, Weber O, Lecroart P, Radakovitch O, Gilbert F, Jézéquel D (2007) Sedimentary processes in the Thau Lagoon (France): from seasonal to century time scales. Estuar Coast Shelf Sci 72:534–542
34. Zhu J, Olsen CR (2009) Beryllium-7 atmospheric deposition and sediment inventories in the Neponset River estuary, Massachusetts, USA. J Environ Radioact 100:192–197
35. Papastefanou C, Ioannidou A (1995) Aerodynamic size association of ^{7}Be in ambient aerosols. J Environ Radioact 26:273–282
36. Appleby P G (2001) Chronostratigraphic techniques inrecent sediments. In: Last W. M., Smol, J. P. (Eds.). Tracking environmental change using lake sediments. Volume 1: Basin analysis, coring, and chronological techniques. Kluwer Academic Publishers, Dordrecht
37. Jweda J, Baskaran M, Hees EV, Schweitzer L (2008) Short-lived radionuclides (^{7}Be and ^{210}Pb) as tracers of particle dynamics in a river system in southeast Michigan. Limnol Oceanogr 53(5):1934–1944
38. Matsunaga T, Amano H, Ueno T, Yanase N, Kobayashi Y (1995) The role of suspended particles in the discharge of ^{210}Pb and ^{7}Be within the Kuji River watershed, Japan. J Environ Radioact 26:3–17
39. Steinmann P, Billen T, Loizeau J-L, Dominik J (1999) ^{7}Be as a tracer to study mechanisms and rates of metal scavenging from lake surface waters. Geochim Cosmochim Acta 63(11/12):1621–1633
40. Ganasut J, Weesakul S, Vongvisessomjai S (2005) Hydrodynamic modeling Thailand Lagoon, Thailand. ThammasatInt J Sci Technol 10(1):32–46
41. Phasook S, Sojisuporn P (2005) Numerical model application on water circulation and salt dispersion in the Songkhla Lake Basin. J Sci Res (Sect T) 4(2):111–130
42. Pornpinatepong S (2005) Salt transport in Songkhla Lake. Songklanakarin J Sci Technol 27(4):889–900
43. Pornpinatepong S, Tanaka H, Takasaki M (2006) Application of 2-D vertically averaged boundary-fitted coordinate model of tidal circulation in Thale Sap Songkhla. Thailand. Walailak J Sci Technol 3(1):105–118
44. Yi Y, Zhou P, Liu G (2007) Atmospheric deposition fluxes of ^{7}Be, ^{210}Pb and ^{210}Po at Xiamen, Chaina. J Radioanal Nucl Chem 273(1):157–162
45. Narazaki Y, Fujitaka K, Igarashi S, Ishikawa Y, Fujinami N (2003) Seasonal variation of ^{7}Be deposition in Japan. J Radioanal Nucl Chem 256(3):489–496
46. Akata N, Kawabata H, Hasegawa H, Sato T, Chikuchi Y, Kondo K, Hisamatsu S, Inaba J (2008) Total deposition velocities and scavenging ratios of ^{7}Be and ^{210}Pb at Rokkasho, Japan. J Radioanal Nucl Chem 277(2):347–355
47. Krishnaswami S, Benninger LK, Aller RC, Von Damm KL (1980) Atmospherically-derived radionuclides as tracers of sediment mixing and accumulation in near-shore marine and lake sediments:evidence from ^{7}Be, ^{210}Pb and $^{239,240}Pu$. Earth planet Scilett 47:307–318
48. Primo de Siqueira B V (2011) Climate change impacts no mixing and circulation at Songkhla Lagoon, Thailand. M.S. Thesis, Delft University of Technology

Paper IV

Preliminary study of sediment mixing in the outer Songkhla lagoon, Southern Thailand as observed from ^{7}Be and ^{210}Pb profiles

Santi Raksawong[a], Miodrag Krmar[b], Tripob Bhongsuwan[a*]

[a] Nuclear Physics Research Laboratory, Department of Physics, Faculty of Science, Prince of Songkla University, Hat Yai, Songkhla, 90112, Thailand

[b] Department of Physics, Faculty of Science, University of Novi Sad, Trg D. Obradovica 4, Novi Sad, 21000, Serbia

* Corresponding author. Tel: +66-0-7428-8761; fax: +66-0-7455-8849.

E-mail address: tripop.b@psu.ac.th (T. Bhongsuwan).

Estuarine, Coastal and Shelf Science Journal (**Submitted** August 9, 2016)

(**Revising process** after received referee's comments, It was submitted in February 24, 2017)

Preliminary study of sediment mixing in the outer Songkhla lagoon, Southern Thailand as observed from ^{7}Be and ^{210}Pb profiles

Santi Raksawong[a], Miodrag Krmar[b], Tripob Bhongsuwan[a*]

[a] Nuclear Physics Research Laboratory, Department of Physics, Faculty of Science, Prince of Songkla University, Hat Yai, Songkhla, 90112, Thailand

[b] Department of Physics, Faculty of Science, University of Novi Sad, Trg D. Obradovica 4, Novi Sad, 21000, Serbia

Abstract

Studying the particle exchange processes at the sediment-water interface provides new insights into benthic processes in the Outer Songkhla lagoon. In this contribution, we present the sediment mixing rates derived from $^{210}Pb_{ex}$ and ^{7}Be depth profiles in the lagoon sediment. The long-term sediment mixing rates estimated from $^{210}Pb_{ex}$ profiles range from 8.7 to 41.9 cm^2 y^{-1}. In addition, these $^{210}Pb_{ex}$ profiles indicate sedimentation rates between 0.37 and 0.81 cm y^{-1}. The ^{7}Be activity profiles show the maximum penetration depth or the thickness of particle mixing layer ranging from 0.5 cm to 2.0 cm. The sediment mixing rate estimates from ^{7}Be range from 0.04 to 37.7 cm^2 y^{-1}, at the central part of lagoon and in the discharge area, respectively. The sediment mixing rates near shrimp farming areas were significantly elevated. Moreover, the average mixing rates in the discharge and non-discharge areas were significantly different. As a preliminary observation, the activities of shrimp farms influenced the redistribution of sediment at the water-sediment interface, as did the discharge flows.

* Corresponding author. Tel: +66-0-7428-8761; fax: +66-0-7455-8849.

E-mail address: tripop.b@psu.ac.th (T. Bhongsuwan).

Keywords: Songkhla lagoon, diffusion model, sediment mixing rates, bioturbation, ^{7}Be, ^{210}Pb, shrimp farming, river discharge

1. Introduction

The Songkhla lagoon is the largest lagoon in South-East Asia, located in southern Thailand on the east coast of the Malay Peninsula. It has three interconnected parts, namely the inner, the middle and the outer part. The outer part, known as Thale Sap Songkhla, is the southernmost part of the Songkhla lagoon. The outer Songkhla lagoon (**Fig. 1b**) is a shallow coastal lagoon with an average depth of ca. 2.0 m (1.5 m) in the rainy (summer) season. There is a narrow opening to the Gulf of Thailand allowing tides to propagate into the lagoon. The aquatic environment in the outer Songkhla lagoon is, therefore, a combination of seawater and freshwater, and the hydrodynamic complexity of this system is mainly controlled by tides, runoffs, winds and waves. The Songkhla lagoon is an important ecosystem with abundant fishery resources representing freshwater, brackish and marine animals. It also serves as an important nursery ground for many economically important species of fish, crab, and shrimp (Pornpinatepong et al., 2010). Moreover, aquatic animal husbandry is practiced both in and around this lagoon. Fish (sea bass) farming was introduced in 1971 and is localized in the outer Songkla lagoon around Koh Yo island. Culturing the black tiger shrimp (*Penaeus monodon*) was introduced by the government in the early 1980s to improve household incomes and to enhance employment opportunities of the local population. Shrimp farming dramatically insreased from 3,491 ha to 7,799 ha over the period from 1982 to 2000 (Tanavud et al., 2001; Pornpinatepong et al., 2010). Since the Songkla lagoon and its catchment are mostly within the Songkhla province, this provincial economy is heavily influenced by the natural and aquacultural production of the lagoon. Since 2002, the fishery production from wild and aquaculture populations has rapidly decreased, as seen in its contributions to the gross provincial product (GPP) which were 14,902, 13,270, 8,001 and 6,533 million bath per year (at the current market prices) in 2002, 2005, 2009 and 2013, respectively (NESDB, 2014). This despite the Department of Fisheries having restored economic aquatic animals in this lagoon and implemented many techniques to prevent diseases and to treat the shrimp in the farms. Shrimp farming has expanded to freshwater areas replacing paddy fields, causing the soil to acquire high salinity level and low organic content, while the wastewaters from shrimp farming are

discharged into the lagoon (Tanavud et al., 2001; Pornpinatepong et al., 2010). The Songkhla lagoon is impacted by a large watershed area with agriculture mainly of rice, rubber trees, and oil palm trees, and also with a large urban human population. The urban domestic wastewaters, fertilizers from agriculture, and the high suspended sediment load from erosion in the watersheds enter the lagoon through various canals and cause environmental degradation (e.g. Bhongsuwan and Bhongsuwan, 2002; Chittrakarn et al., 1998; Gyawali et al., 2013; Ladachart et al., 2011; Pornpinatepong et al., 2010; Pradit et al., 2013; Sirinawin et al., 1998; Sirinawin and Sompongchaiyakul, 2005). Furthermore, the hydrodynamics in this lagoon is mainly driven by winds and tidal responses. The wind-induced waves stir up the sediment easily and wind-induced currents distribute the suspended sediments because of the shallowness and the soft mud bottom. The water velocities are mostly low in the lagoon, but strong flows occur in the canal connecting to the Gulf of Thailand, to north and south of Koh Yo island, and affected by tidal chages (Ganasut et al., 2005; Pornpinatepong et al., 2006; Primo de Siqueira, 2011). These processes influence the distributions of chemical species in the interfacial zone that can deteriorate water quality and disturb the stratigraphic structure in the sediments (e.g. Bradshaw et al., 2006; Crusius et al., 2004; Lecroart et al., 2010; Schmidt et al., 2007).

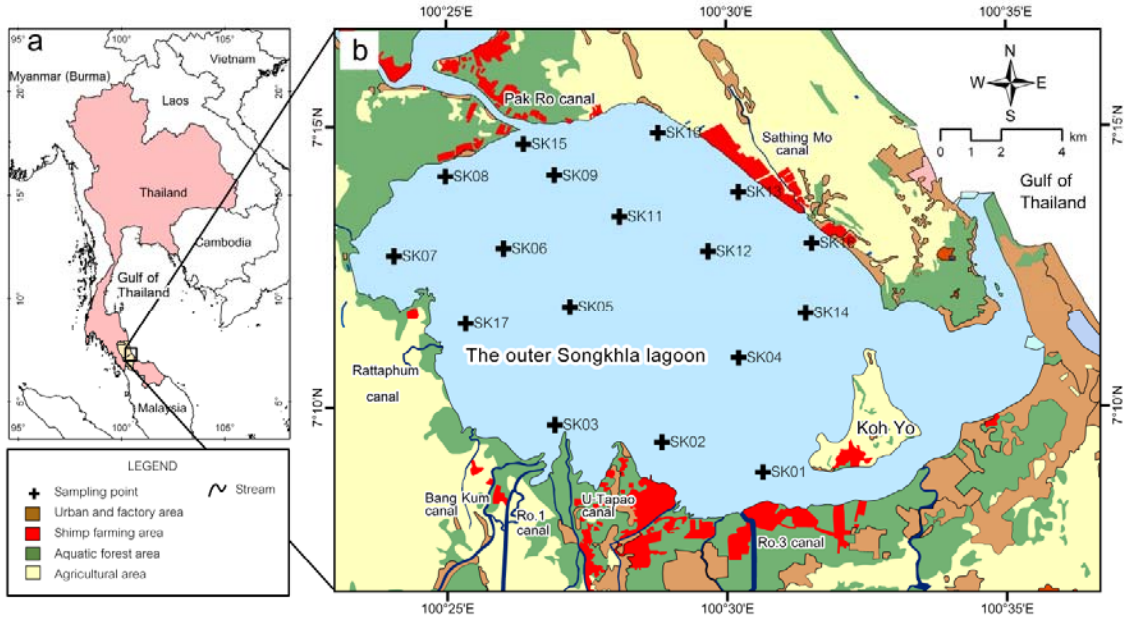

Fig.1 Location map of the study area, and sampling points shown in magnification of the study area.

These complications have been discussed in a large number of scientific studies aiming to find and mitigate environmental impacts. Studying the particle exchange processes at the sediment-water interface provides new insights into benthic processes. Therefore, quantitative sediment mixing rates in terms of diffusion coefficient (D_b) and penetration depth (L) are required for understanding the sedimentation processes and ecological activities at the water-sediment interface in the lagoon. The D_b represents the mixing intensity in the sediment column, and is estimated by fitting a diffusion model to depth profiles of tracers (e.g. Krishnaswami et al., 1980; Lecroart et al., 2007a; Lecroart et al., 2007b; Lecroart et al., 2010; Schmidt et al., 2007; Palinkas et al., 2005).

In this paper, we present an investigation of sediment mixing at the water-sediment interface on the outer Songkhla lagoon. Results are reported on detailed depth profiles of both short- and long-lived radionuclides, namely ^{7}Be and ^{210}Pb, in the bottom sediment cores. These radionuclides are assessed as tracers indicating short- and long-term sediment mixing rates (D_b). Moreover, this work shows impacts of shrimp farming and river discharge.

2. Methods

2.1 Sampling of the sediment cores

Totally 16 bottom sediment cores in the outer Songkhla lagoon were collected using a hand-operated corer equipped with PVC core tubes (8.5 cm internal diameter, 30 cm length), on December 25, 2013. Sediment core sampling locations in the lagoon are shown in **Fig. 1b**. All the cores were kept vertical, transported to the laboratory, and then sliced at 0.5 cm intervals in the depth direction, using the handheld extruder shown in **Fig. 2**. These specimens were dried at 105 °C for 24 hours in an electric oven, ground in a ceramic mortar, sieved to < 2 mm fraction, weighed, and stored in airtight sealed polyethylene bottles. The particle sizes of sediments were determined by sieve analysis. The ^{7}Be activities were measured by a gamma spectrometer with a HPGe detector (GC7020, Canberra Industries, USA) in a low-background cylindrical shield (Model 747, Canberra, USA) and coupled to a multichannel analyzer (DSA1000, Canberra, USA). The energy resolution was 0.88 keV (FWHM) at 122

keV (^{57}Co), and 1.77 keV (FWHM) at 1332 keV (^{60}Co). The minimum counting-time for each specimen was set at 40,000s. However, when a specimen had analytical error exceeding 1σ, we increased the counting-time up to 100,000s to reduce the analytical error to below 25% or 1σ. Gamma ray energy at 477.7 keV was analysed for ^{7}Be determination. The IAEA TEL 2011-03 WWOPT soil-04 sample with certified radionuclide activities was used to calculate the relative efficiency of ^{7}Be detection at 477.7 keV. The ^{7}Be activities were corrected for decay from the sampling time on December 25, 2013. The selected sediment samples were sent to a laboratory at the Faculty of Sciences, University of Novi Sad, Serbia, to measure the total ^{210}Pb activity by such gamma spectrometry systems that have good efficiency at the gamma energy 46.6 keV. The average ^{226}Ra activity, known to support ^{210}Pb, was determined via gamma rays emitted by the daughter isotopes, ^{214}Pb at energy levels 295 and 352 keV and ^{214}Bi at energy level 609 keV. All sediment samples were stored for at least 4 weeks in sealed polyethylene bottles to allow radioactive equilibration of ^{226}Ra with its daughter isotopes. The excess or unsupported ^{210}Pb (^{210}Pb$_{ex}$) activity was then calculated as the difference between total and supported ^{210}Pb.

Fig. 2 Photographs showing (a) scenery of the study lagoon during sediment core sampling, and (b) slicing of an 0.5 cm thick layer from extruded sediment core, using a metal blade in the laboratory.

2.2 Radionuclide Tracers and Diffusion Model Equation

Naturally occurring radionulides, such as ^{210}Pb and ^{7}Be that are good radionuclide tracers, are widely used to determine the mixing rates in estuarine, marine and lake sediments, in combination with a vertical diffusion model based on analogous eddy diffusion (e.g. Krishnaswami et al., 1980; Lecroart et al., 2007; Schmidt et al., 2007; Palinkas et al., 2005). The mixing rates are estimated by identifying a steady-state vertical diffusion model from the depth profiles of these radionuclides adsorbed in the fine sediments.

The naturally occurring radionuclide ^{210}Pb originates from the ^{238}U decay series, and has a half-life of 22.3 years. There are two components contributing to ^{210}Pb in aquatic sediments. First, supported ^{210}Pb is produced by the *in situ* decay of the parent radionuclides in the soil or sediment. Its activity is in equilibrium with its long-lived parent ^{226}Ra. The second component is contributed by natural fallout, and this is called 'unsupported' or 'excess' ^{210}Pb. This component is produced by the decay of the gaseous radionuclide radon-222 (^{222}Rn) in the atmosphere, which in turn is released by the ^{238}U decay series in rocks and soils. The ^{210}Pb is easily attached to airborne particulates and removed from the atmosphere by both wet and dry deposition onto catchment surfaces and into water bodies (lake, lagoon, estuary and ocean). The ^{210}Pb falling onto catchment surfaces will be eroded and transported to the water bodies through waterways, and the ^{210}Pb falling directly into the water bodies is readily adsorbed by suspended particulate matter in the water column, and may be deposited to the bottom sediments (e.g. Appleby, 2001; Krishnaswamy et al., 1971; Sommerfield et al., 1999; Schmidt et al., 2007).

The ^{7}Be, with a half-life of 53 days, is naturally produced by the spallation reactions of the cosmic particle rays (protons and neutrons) with the nuclei of light elements (carbon, oxygen and nitrogen), in stratosphere and troposphere (e.g. Papastefanou and Ioannidou, 1995). The produced cosmogenic ^{7}Be atoms are readily attached to airborne particulates and migrate to the ground level by precipitation and dry deposition (e.g. Feely et al., 1989; Papastefanou and Ioannidou, 1995; Schuller et al., 2010; Zhu and Olsen., 2009). Therefore, the ^{7}Be in a lake or a lagoon comprises two

components. First, what is directly deposited from the atmosphere into the water column and the lagoon bottom, and second, what is transported from the watershed by streams and overland flow (e.g. Appleby, 2001; Jweda et al., 2008; Matsunaga et al., 1995; Walling, 2004).

These radionuclides have been used in prior studies to examine particle dynamics, sediment deposition/erosion, and sediment mixing by biological and physical activities (e.g. Feng et al., 1999; Palinkas et al., 2005; Schmidt et al., 2014; Zhu and Olsen., 2009). To understand the sediment mixing in a water body, one-dimensional eddy diffusion is the most widely used model of the vertical mixing rates at the water-sediment interface, and is shown in **Eq. (1)** (e.g. Aller and DeMaster, 1984; DeMaster et al., 1985; Krishnaswami et al., 1980; Lecroart et al., 2007a; Lecroart et al., 2007b; Lecroart et al., 2010; Meysman et al., 2003; Osaki et al., 1997; Pope et al., 1996; Reed et al., 2006; Schmidt et al., 2007; Smith and Schafer, 1999; Wheatcroft, 2006).

$$\frac{\partial A}{\partial t} = D_b \frac{\partial^2 A}{\partial z^2} - S\frac{\partial A}{\partial z} - \lambda A \qquad (1)$$

where A refers to the activity (Bq cm^{-3}) of the selected radionuclide tracer in the sediment, at depth z corrected for sediment compaction. A is calculated by multiplying the *in situ* wet density of the sediment (mass of dry solids per unit volume of wet sediment, ρ in kg cm^{-3}) and activity concentration of radionuclide tracer at depth z in the sediment (C, in Bq kg^{-1}). D_b is the particle mixing coefficient (cm^2 y^{-1}), S is the sediment accumulation rate (cm y^{-1}), and λ is the radioactive decay constant (y^{-1}).

The assumptions made on using **Eq. (1)** to estimate D_b from the radionuclide tracer profiles include: i) the diffusion process is assumed to occur at constant intensity within a surface mixed layer under steady state ($\partial A/\partial t = 0$), and ii) the activity of radionuclide tracer is equal to $A(0)$ at the sediment-water interface and approaches 0 as the depth approaches infinity (e.g. Aller and DeMaster, 1984; Appleby, 2001; DeMaster et al., 1985; Krishnaswami et al., 1980; Lecroart et al., 2010; Pope et al., 1996; Schmidt et al., 2007). The steady-state solution with these assumptions is

$$A(z) = A(0)\exp\left(\frac{S - \sqrt{S^2 + 4\lambda D_b}}{2D_b} z\right) \qquad (2)$$

Now the observed depth profiles can be fit with this model by using least squares regression, to identify the mixing coefficient (D_b) when the sedimentation rate is known.

2.3 Estimating the sediment accumulation rate from ^{210}Pb observations

The excess or unsupported ^{210}Pb ($^{210}Pb_{ex}$) profile and the radioactive decay law can be applied to establish sediment accumulation rates (e.g. Bonotto and Garcia-Tenorio, 2014; Simsek and Cagatay, 2014). The simplest model, the Constant Initial Concentration (CIC) model, is also known as the constant specific activity model. An increased flux of sediment particles from the water column will proportionally increase the transfer of $^{210}Pb_{ex}$ from the water to the sediment. In addition, the $^{210}Pb_{ex}$ activity profile is exponentially decreasing with depth the z (cm), as observed in equation (3).

$$C(z) = C(0)\exp\left(-z\frac{\lambda}{S}\right) \qquad (3)$$

where C(z) and C(0) are the $^{210}Pb_{ex}$ activity at depth z and at the top layer, respectively. The mean sedimentation rate S (cm y^{-1}) can be determined from the slope of $^{210}Pb_{ex}$ activity vs. depth, estimated from a least-squares fit (e.g. Bonotto and Garcia-Tenorio, 2014; Simsek and Cagatay, 2014).

3. Results

3.1 Sediment characteristics

Grain-size data at the sediment surface (0 – 1.5 cm) revealed that the outer Songkhla lagoon sediments are composed of mostly fine to very fine sand with some sandy sediments found near the canal mouth. The clay content in cores increases with distance from the river or canal mouth. For instance, the clay content at site SK03 located adjacent the Ro.1 canal mouth is low (34.9%), and comparatively much

higher at the site SK05 located far from the Ro.1 canal mouth (71.1%) or at the site SK04 far from the Ro.3 canal mouth (65.4%). This effect is caused by the high water flow rate at the mouth, which decreases with distance from the mouth. Two sites near the canal mouth (SK03 and SK13) have sandy sediments with low clay content, instead they have high medium to fine sand contents as shown in **Table 1**.

3.2 ^{210}Pb profiles

The $^{210}Pb_{ex}$ depth profiles in the outer Songkhla lagoon are shown in **Fig.3**. The $^{210}Pb_{ex}$ profiles at sites SK02, SK08 and SK17 were well fit by linear regression of the logarithm of $^{210}Pb_{ex}$ activity (Bq cm^{-3}) to the depth (cm), corroborating use of the vertical diffusion model described in **Section 2.2**. The $^{210}Pb_{ex}$ profile at site SK15 was not well fit by the vertical diffusion model. The sediment mixing rates, D_b, estimated from **Eq. (2),** are 41.9, 38.2 and 8.7 cm y^{-1} at the sites SK02, SK08 and SK17, respectively. Moreover, the $^{210}Pb_{ex}$ profiles can be used to establish sediment accumulation rates. The simplest Constant Initial Concentration (CIC) model was applied to the $^{210}Pb_{ex}$ profiles and the sedimentation rates estimates are 0.81, 0.77 and 0.37 cm y^{-1} at the sites SK02, SK08 and SK17, respectively. The previously reported 0.57 cm y^{-1} sedimentation rate near the site SK08 was obtained by Chittrakarn et al. (1998) using the ^{137}Cs method. Moreover, the total sediment discharged into the outer Songkhla lagoon system in 2002 was estimated by the Universal Soil Loss Equation (USLE) model in GIS environment to be 6.89×10^9 kg, or on an average 8.14×10^5 kg km^{-2} across the basin. The prior 0.44 cm y^{-1} sedimentation rate estimate (Tanavud et al., 2006) is lower than our rates at SK02 and SK08, but a little higher than our rate at SK17.

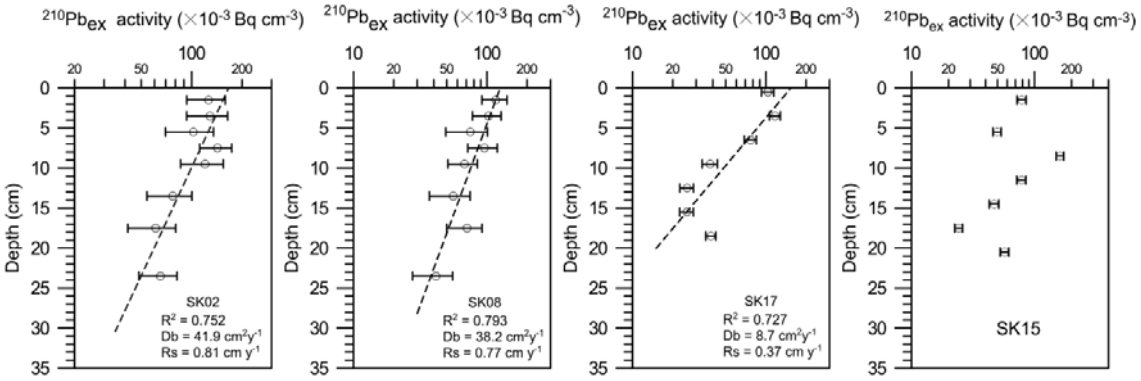

Fig. 3 $^{210}Pb_{ex}$ activity profiles from the Outer Songkhla lagoon. The straight line fits shown are used with **Eq. (2)** to estimate mixing coefficients.

3.3 ^{7}Be profiles

The depth profiles of ^{7}Be activity [Bq cm^{-3}] in each sediment core are presented in **Table 1** and **Fig. 4**. The maximum penetration depth at which ^{7}Be activity (or the thickness of mixed layer) was measurable in the cores ranged from 0.5 cm (sites SK06, SK14 and SK16) to 2.0 cm (sites SK02 and SK15). This result is comparable to that reported from a lake studied in western Yunnan and central Guizhou (Bai et al., 2002). In their study ^{7}Be was mainly distributed within a 2 cm top layer on the lake bottom. The maximum ^{7}Be depth penetration in another fresh water lake was between 1 cm and 3 cm (Krishnaswami et al., 1980). However, some studies have reported measurable ^{7}Be activities in sediment samples at depths up to 10 cm in river estuaries (Zhu and Olsen, 2009) and at 8 cm in a lagoon near shellfish farms in the summer (Schmidt et al., 2007). These prior studies of several areas show several penetration depths depending on the environment, on the atmospheric depositional flux of radionuclides, and on anthropogenic and biological activities (Palinkas et al., 2005; Zhu and Olsen, 2009). In the topmost sediment layer at 0 - 0.5 cm depth in the current study, the minimum and maximum activities of ^{7}Be were 10 ± 4 and 78 ± 10 mBq m^{-3}, found at sites SK03 and SK09. The fourteen ^{7}Be activity profiles in **Fig. 4** show decreasing activity with depth, and are well fit by linear regression of logarithmic activity to depth (cm). The sediment mixing coefficients estimated from the vertical diffusion model described in **Section 2.2** as **Eq. (2),** and using the sedimentation rate estimates from $^{210}Pb_{ex}$, range from 0.04 cm^2 y^{-1} at site SK06 to

37.7 cm^2 y^{-1} at site SK01, as shown in **Table 1.** However, the profiles from sites SK12, SK14 and SK16 are not well fit by linear regression of logarithmic activity to depth.

Table 1. The ^{7}Be activity, ^{7}Be inventory, clay-normalized ^{7}Be activity, ^{7}Be mixing coefficient, and constituent fractions in the sediment cores.

Cores	^{7}Be activity (mBq cm^{-3}) Depth (cm)				^{7}Be inventory[a]	Clay-normalized ^{7}Be	^{7}Be-D_b Eq.(2)	Locations		Percentage of classified sediment	
	0.0 - 0.5	0.5 - 1.0	1.0 - 1.5	1.5 - 2.0	(Bq m^{-2})	(Bq kg^{-1})	(cm^2 y^{-1})			medium to fine sand (0.1 – 0.3 mm)[b]	very fine sand to silt and clay (< 0.1 mm)[b]
SK01	44 ± 16	48 ± 14	31 ± 14		615 ± 135	81.9	37.7	DC	NSH	41.1	58.9
SK02	43 ± 13	21± 12	20 ± 12	11 ± 12	420 ± 141	90.1	6.6	DC	NSH	42.1	57.9
SK03	10 ± 4	8 ± 3	5 ± 3		114 ± 34	16.6	11.4	DC	FSH	65.1	34.9
SK04	45 ± 14	17 ± 14			308 ± 137	66.4	1.2	NDC	FSH	34.6	65.4
SK05	33 ± 9	18 ± 9	20 ± 9		358 ± 86	84.8	3.3	NDC	FSH	28.9	71.1
SK06	35± 11	3 ± 1			174 ± 57	91.6	0.04	NDC	FSH	16.9	83.1
SK07	35 ± 6	22 ± 6			284 ± 30	45.4	6.0	DC	FSH	18.5	81.5
SK08	22 ± 5	14 ± 6	11 ± 5	19 ± 7	237 ± 76	30.6	9.7	DC	NSH	29.3	70.7
SK09	78 ± 10	35 ± 10	31 ± 10		718 ± 105	130.2	5.7	DC	NSH	34.9	65.1
SK10	48 ± 10	27 ± 10	21 ± 11		482 ± 105	127.5	7.1	DC	NSH	25.8	74.2
SK11	40 ± 6	21 ± 6	7 ± 6		340 ± 98	123.1	1.5	NDC	FSH	49.2	50.8
SK13	45 ± 15	28 ± 14	21 ± 12		470 ± 132	61.7	8.2	NDC	NSH	66.3	33.7
SK15	44 ± 6	25 ± 4	33 ± 6	15 ± 7	587 ± 51	223.7	13.1	DC	NSH	48.4	51.6
SK12	16 ± 11	46 ± 10			307 ± 116	25.4	NA	NDC	FSH	46.2	53.8
SK14	37 ± 16				184 ± 81	30.9	NA	NDC	FSH	24.9	75.1
SK16	35 ± 14				175 ± 69	28.8	NA	DC	NSH	28.8	71.2

[a] The sediment inventories of ^{7}Be which were calculated by Raksawong et al.(2016)

[b] Particle size of sediment classified by sieve analysis

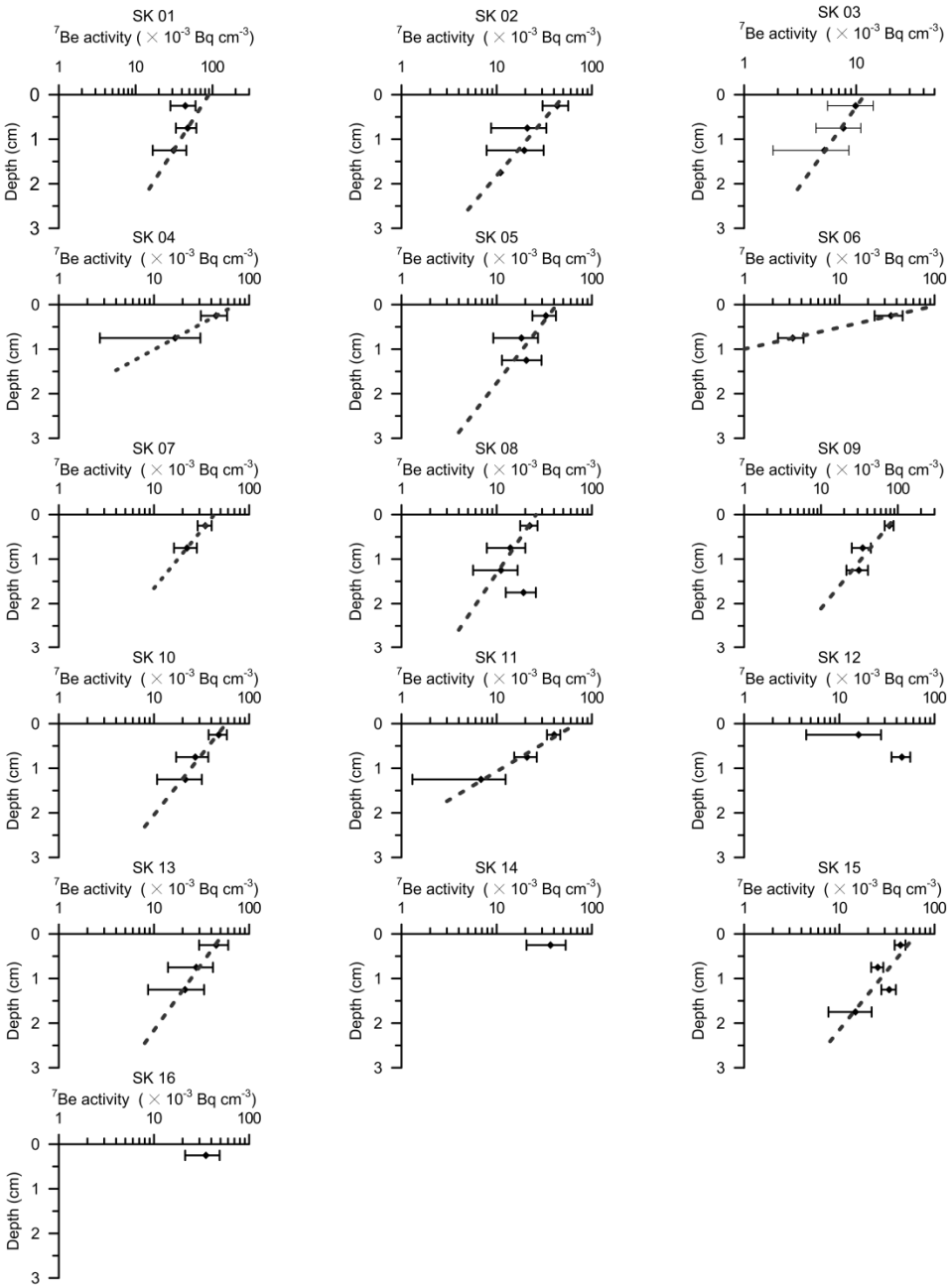

Fig. 4 ^{7}Be activity profiles from the Outer Songkhla lagoon. The linear fits according to **Eq. (2)** were used to estimate mixing rates.

4. Discussion

Generally, the diffusion model (**Eq.1**) can explain sediment mixing caused by ecological processes, called bioturbation rates, at the water-sediment interfaces in

estuarine, continental shelves, and deep-sea floor zones (e.g. Aller and DeMaster, 1984; Crusius et al., 2004; Feng et al., 1999; Lecroart et al., 2007; Osaki et al., 1997). There is less information on use of this model to approximate the sediment reworking processes in tropical monsoonal environments. The current results are an attempt to quantify the sediment reworking in the outer Songkhla lagoon by this particular approach.

The mixing depths obtainted from the penetration depths of ^{7}Be activity are high at the sites SK01, SK02, SK05, SK09, SK13 and SK15 (**Fig. 4**), and the sediment mixing coefficients are high at the sites SK01, SK03, SK08 and SK15 (**Table 1**), likely indicating a high vertical and spatial heterogeneity at the sediment-water interfaces of these sites. This is probably because high sediment mixing depth and rate are caused by bioturbation.

The sediment mixing coefficients by sediment type are plotted on the shaded color maps of the clay-normalized ^{7}Be activities (**Fig. 5a**), which removes any effects related to the particle size on the vertical activity and on the sediment inventory of ^{7}Be (**Fig. 5b**). The contour maps of the clay-normalized ^{7}Be activity (**Fig. 5a**) and sediment inventory of ^{7}Be (**Fig. 5b**) indicate the same two high activity zones, adjacent to the Pak Ro and Ro.3 canal mouths. These two zones probably indicate both high recent sediment deposition rate and high bioturbation, because the clay-normalized ^{7}Be activities affect via two pathways: 1) rapid transport and deposition during floods resulting in low activities, and 2) slow transport and deposition such that bioturbation rates exceed the burial rates resulting in high activities (e.g. Addington et al., 2007; Kniskern et al., 2010; Sommerfield et al., 1999). In the same way, the ^{7}Be inventories in the sediment are indicative of both the sediment deposition/erosion (e.g. Aller and DeMaster, 1984; Crusius et al., 2004; Fitzgerald et al., 2001; Krishnaswami et al., 1980; Neubauer et al., 2002; Palinkas et al., 2005; Sommerfield et al., 1999) and of the bioturbation (Osaki et al., 1997; Aller and DeMaster, 1984). Moreover, there is a high content of particle-reactive radionuclides in the sediment column, also indicating high sedimentation rate and strong bioturbation in these zones (Palinkas et al., 2005; Schmidt et al., 2007). The high sediment mixing coefficients (8.5 – 37.7 cm^2 y^{-1}) estimate for the sites SK01, SK02,

SK08, SK09, SK10 and SK15, using the sedimentation rates calculated from ^{210}Pb profiles, confirm strong bioturbation at the Pak Ro and Ro.3 canal mouths.

High sediment mixing coefficients are observed near the shoreline of the lagoon and by the canal mouths, as demonstrated by the sites SK01, SK03, SK08, SK09, SK10 and SK15, whereas low mixing coefficients (0.04 – 5.5 $cm^2\ y^{-1}$) prevail in the central lagoon area (sites SK04, SK05, SK06, and SK11). This indicates that bioturbation processes are strong near the shoreline of the lagoon and mouths of canals but weaker in the central lagoon area.

Based on the above discussion, rapid sediment mixing combined with slow sedimentation occurs near the mouth of Pak Ro canal zone (SK15) and near the mouth of Ro.3 canal (SK01). This is suggested by the mixing coefficients (13.1 and 37.7 $cm^2\ y^{-1}$ for sites SK15 and SK01, respectively) and the clay-normalized ^{7}Be activities that are high (223.7 and 81.9 Bq kg^{-1} for sites SK15 and SK01, respectively); however, both these zones had high sediment inventories of ^{7}Be. At the mouth of Ro.1 canal zone (SK03), both rapid sediment mixing and sedimentation are observed, since the sediment mixing coefficients are high (11.4 $cm^2\ y^{-1}$), and the clay-normalized ^{7}Be activity (16.6 Bq kg^{-1}) and sediment inventory of ^{7}Be (114 Bq m^{-2}) are low. The sediment mixing in this zone was probably affected by the high flow rates and turbulence. High sedimentation rate and less sediment mixing are observed at the site SK07 from the low clay-normalized ^{7}Be activity and low mixing coefficient (6.0 $cm^2\ y^{-1}$). We could not estimate the sediment mixing coefficients at north tip of Koh Yo island (sites SK12, SK14 and SK16), while low clay-normalized ^{7}Be activity and low sediment inventort of ^{7}Be were found in this area. These are caused by the large water flows with tidal currents that invade from the Gulf of Thailand (Raksawong et al., 2016; Pornpinatepong et al., 2006).

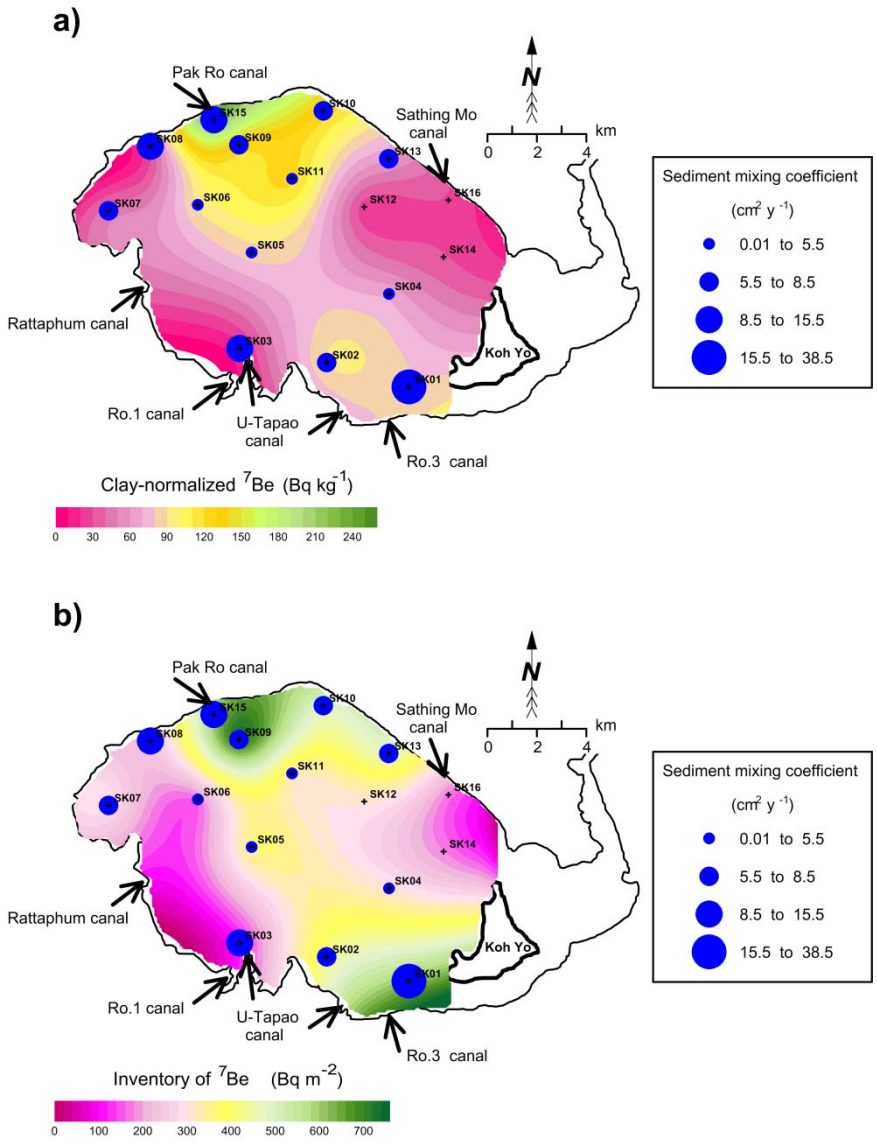

Fig. 5 Shaded color maps of **a**) clay-normalized ^{7}Be activity, and **b**) the inventory of ^{7}Be activity, including the sediment mixing coefficients in the outer Songkhla lagoon.

To assess the effects of bioturbation, we partitioned the sampled sediment cores to those from near shrimp farming (NSH) within 2.5 km from shrimp farms, and those far from shrimp farming (FSH), as well as discharge (DC) and non-discharge (NDC) groups (**Table 1**). The average sediment mixing rates by group were compared using the *Wilcoxon signed-rank test,* which is a non-parametric statistical hypothesis test for non-normal distributions. The sediment cores of NSH and FSH areas had average

sediment mixing coefficients 13.6 cm^2 y^{-1} and 4.4 cm^2 y^{-1}, respectively, (**Fig. 6a**) that are significantly different at $p < 0.05$. Therefore, the sediment mixing rates of NSH cases are higher than those of FSH cases. The excess feed and other effluents from shrimp farms are drained into the lagoon, where the benthic animals consume them. This current study indicates that high benthic activity in the NSH cases can greatly influence sediment mixing and sedimentation in the outer Songkhla lagoon.

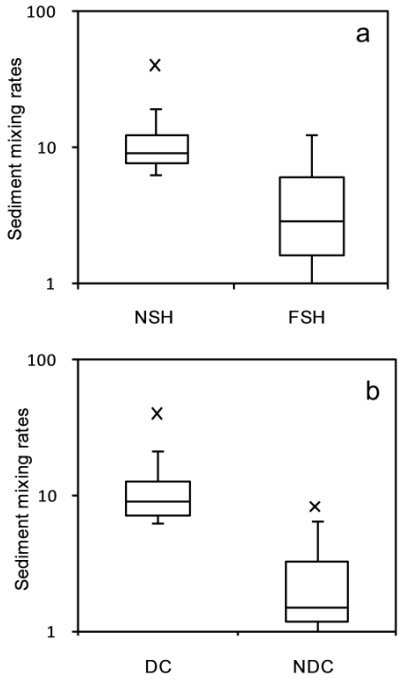

Fig. 6 Box plots of ^{7}Be activity grouped by **a)** near shrimp farming (NSH) and far from shrimp farming (FSH), and **b)** discharge (DC) and non-discharge (NDC) cases.

A comparison of the results between the discharge and the non-discharge areas shows that their average sediment mixing rates were 13.1 cm^2 y^{-1} and 2.8 cm^2 y^{-1}, respectively, as shown in **Fig. 6b**, this difference being significant at $p < 0.05$. This clearly indicates that discharge affects sediment mixing. In particular fine-sediments, fertilizers from agriculture, and a high load of suspended sediments from erosion are carried along by the runoff and flood waters from watersheds.

Particularly, the results for core SK01 show the highest 37.7 cm^2 y^{-1} sediment mixing rate (estimated from ^{7}Be) and 1.5 cm mixing depth. At site SK2, the sediment mixing rates estimated from ^{210}Pb and ^{7}Be are 41.9 and 7.4 cm^2 y^{-1}, respectively. The

different D_b values with estimated by long- and short-lived radionuclides for the same sites in coastal or estuarine environments was influenced from transient physical remobilization of the sediment-water interface by currents or intense sedimentation events (Lecroart et al., 2010). Thus, these two sites are must differ either in the physical or in the biological processes. Both are located near the mouth of Ro.3 cannel, with potential discharges and with fine sediments carried by runoff and flood waters from U-Tapao subcatchment. There are shrimp farms near the shoreline, and nutrient emissions enter the lagoon with drainage through the Ro-3. Hence, this zone possesses high benthic activity associated with high level of sediment reworking.

However, none of the ^{7}Be profiles in this study (**Fig. 4)** displayed a distinct subsurface activity peak, which could indicate physical mixing by winds and tides. Particularly, the ^{7}Be activity of the top layer at SK12 shows lower activity than the deeper layers, and SK14 profile shows effectively only one layer. These patterns probably reflect nonuniform deposition of sediment on the lagoon bottom due to resuspension of early deposited sediment, excess sediment deposited on the opposite sense, the horizontal dynamic movements such as the tidal variations and strong winds. While the winds are strong daily around 10.00 a.m. – 19.00 p.m. and induce strong waves and currents, the tidal stages (flood and ebb) can remove suspended sediments to the Gulf of Thailand.

5. Conclusions and Suggestions

In this preliminary study, the spatial distribution in the Outer Songkhla lagoon of sediment mixing coefficients estimated from ^{7}Be activity was investigated. The sediment mixing processes near shrimp farms and near discharge areas were stronger than far from shrimp farms or from discharge areas. Clearly, shrimp farms and discharge activities can significantly influence the redistribution of sediment at the water-sediment interface. For further work in this topical monsoonal environment, we suggest investigating the seasonal variations in short-term sediment mixing and deposition, in order to better understand the sedimentation processes and the impacts of anthropogenic activities. This sedimentological analysis of mixing precesses can facilitate the sustainable management of lagoon environments.

Acknowledgements

This research was financially supported by the Prince of Songkla University (project code: SCI550111S), the National Research Council of Thailand (project code: SCI560125S), the Nuclear Physics Research Laboratory, Physics Department, Faculty of Science, and the graduate fellowship from the Graduate School, Prince of Songkla University. We thank Associate Professor Seppo Karrila, Faculty of Science and Industrial Technology, Prince of Songkla University and the Research and Development Office of the Prince of Songkla University, for English proof reading service. In addition, the first author would like to thank Prince of Songkla University Graduate Studies Grant and the student exchange program between Prince of Songkla University and University of Novi Sad, Serbia. The Thai Meteorological Department is acknowledged for providing the meteorological data at the Songkhla station.

References

Addington, L. D., Kuehl, S. A., McNinch, J. E., 2007. Contrasting modes of shelf sediment dispersal off a high-yield river: Waiapu River, New Zealand. Mar. Geol. 243, 18–30.

Aller, R. C., DeMaster, D. J., 1984. Estimates of particle flux and reworking at the deep-sea floor using $^{234}Th/^{238}U$ disequilibrium. Earth Planet. Sci. Lett. 67, 308–318.

Appleby, P. G., 2001. Chronostratigraphic techniques inrecent sediments, in: Last, W. M., J. P. Smol (Eds.), Tracking environmental change using lake sediments. vollume 1: Basin analysis, coring, and chronological techniques. Kluwer Academic Publishers, Dordrecht, pp. 171–203.

Bai, Z. G., Wan, G. J., Huang, R. G., Liu, T. S., 2002. A comparison on the accumulation characteristics of ^{7}Be and ^{137}Cs in lake sediments and surface soils in western Yunnan and central Guizhou , China. Catena 49, 253–270.

Bhongsuwan, T., Bhongsuwan, D., 2002. Concentration of heavy metals Mn, Fe, Ni, Pb, Cr and Cd in bottom sediments of the Outer Songkhla Lake deposited between the year B.E. 2520-2538. Songklanakarin J. Sci. Technol. 24, 89–106.

Bonotto, D. M., García-Tenorio, R., 2014. A comparative evaluation of the CF:CS and CRS models in ^{210}Pb chronological studies applied to hydrographic basins in Brazil. Appl. Radiat. Isot. 92, 58–72.

Bradshaw, C., Kumblad, L., Fagrell, A., 2006. The use of tracers to evaluate the importance of bioturbation in remobilising contaminants in Baltic sediments. Estuar. Coast. Shelf Sci. 66, 123–134.

Chittrakarn, T., Pornpinatepong, S., Bhongsuwan, T., Nuannil, P., 1998. Mathematical model study for determination of sedimentation rate in Thalae Sap Songkhla. Final report, Songkhla: Dept. of Physics, Prince of Songkla University.

Crusius, J., Bothner, M. H., Sommerfield, C. K., 2004. Bioturbation depths, rates and processes in Massachusetts Bay sediments inferred from modeling of ^{210}Pb and $^{239+240}$Pu profiles. Estuar. Coast. Shelf Sci. 61, 643–655.

DeMaster, D. J., McKee, B. A., Nittrouer, C. A., Brewster, D. C., Biscaye, P. E., 1985. Rates of sediment reworking at the HEBBLE site Based on measurements of Th-234 , Cs-137 and Pb-210. Mar. Geol. 66, 133 – 148.

Feely, H. W., Larsen, R. J., Sanderson, C. G., 1989. Factors that cause seasonal variations in Beryllium-7 concentrations in surface air. J. Environ. Radioact. 9, 223–249.

Feng, H., Cochran, J. K., Hirschberg, D. J., 1999. ^{234}Th and ^{7}Be as tracers for the transport and dynamics of suspended particles in a partially mixed estuary. Geochim. Cosmochim. Acta 63, 2487–2505.

Fitzgerald, S. A., Klump, J. V., Swarzenski, P. W., Mackenzie, R. A., Richards, K. D., 2001. Beryllium-7 as a tracer of short-term sediment deposition and resuspension in the Fox River Wisconsin. Environ. Sci. Technol. 35, 300–305.

Ganasut, J., Weesakul, S., Vongvisessomjai, S., 2005. Hydrodynamic Modeling Thailand Lagoon, Thailand. Thammasat Int. J. Sci. Technol. 10, 32 – 46.

Gyawali, S., Techato, K., Yuangyai, C., Musikavong, C., 2013. Assessment of relationship between land uses of riparian zone and water quality of river for sustainable development of river basin, a case study of U-Tapao river basin, Thailand. Procedia Environ. Sci. 17, 291–297.

Jweda, J., Baskaran, M., van Hees, E., Schweitzer, L., 2008. Short-lived radionuclides (^{7}Be and ^{210}Pb) as tracers of particle dynamics in a river system in southeast Michigan. Limnol. Ocean. 53, 1934–1944.

Kniskern, T. A., Kuehl, S. A., Harris, C. K., Carter, L., 2010. Sediment accumulation patterns and fine-scale strata formation on the Waiapu River shelf, New Zealand. Mar. Geol. 270, 188–201.

Krishnaswami, S., Benninger, L. K., Aller, R. C., Von Damn, K. L., 1980. Atmospherically-derived radionuclides as tracers of sediment mixing and accumulation in near-shore marine and lake sediment: evidence from ^{7}Be, ^{210}Pb, and $^{239, 240}$Pu. Earth Planet. Sci. Lett. 47, 307–318.

Krishnaswamy, S., Lal, D., Martin, J. M., Meybeck, M., 1971. Geochronology of lake sediments. Earth Planet. Sci. Lett. 11, 407–414.

Ladachart, R., Suthirat, C., Hisada, K., Charusiri, P., 2011. Distribution of heavy metals in core sediments from the Middle part of Songkhla lake, Southern Thailand. J. Appl. Sci. 11, 3117–3129.

Lecroart, P., Maire, O., Schmidt, S., Grémare, A., Anschutz, P., Meysman, F. J. R., 2010. Bioturbation, short-lived radioisotopes, and the tracer-dependence of biodiffusion coefficients. Geochim. Cosmochim. Acta 74, 6049–6063.

Lecroart, P., Schmidt, S., Anschutz, P., Jouanneau, J.-M., 2007a. Modeling sensitivity of biodiffusion coefficient to seasonal bioturbation. J. Mar. Res. 65, 417–440.

Lecroart, P., Schmidt, S., Jouanneau, J. M., 2007b. Numerical estimation of the error of the biodiffusion coefficient in coastal sediments. Estuar. Coast. Shelf Sci. 72, 543–552.

Matsunaga, T., Amano, H., Ueno, T., Yanase, N., Kobayashi, Y., 1995. The role of suspended particles in the discharge of ^{210}Pb and ^{7}Be within the Kuji River watershed , Japan. J. Environ. Radioact. 26, 3–17.

Meysman, F. J. R., Boudreau, B. P., Middelburg, J. J., 2003. Relations between local, nonlocal, discrete and continuous models of bioturbation. J. Mar. Res. 61, 391–410.

NESDB (Office of the National Economic and Social Development Board), 2014. Gross regional and provincial product: chain volume measures 2014 edition. Bangkok.

Neubauer, S. C., Anderson, I. C., Constantine, J. A., Kuehl, S. A., 2002. Sediment deposition and accretion in a Mid-Atlantic (U.S.A.) tidal freshwater marsh. Estuar. Coast. Shelf Sci. 54, 713–727.

Osaki, S., Sugihara, S., Momoshima, N., Maeda, Y., 1997. Biodiffusion of ^{7}Be and ^{210}Pb in intertidal estuarine sediment. J. Environ. Radioact. 37, 55–71.

Palinkas, C. M., Nittrouer, C. A., Wheatcroft, R. A., Langone, L., 2005. The use of ^{7}Be to identify event and seasonal sedimentation near the Po River delta, Adriatic Sea. Mar. Geol. 222-223, 95–112.

Papastefanou, C., Ioannidou, A., 1995. Aerodynamic size association of ^{7}Be in ambient aerosols. J. Environ. Radioact. 26, 273–282.

Pope, R. H., Demaster, D. J., Smith, C. R., Seltmann, H., 1996. Rapid bioturbation in equatorial pacific sediments: Evidence from excess ^{234}Th measurements. Deep. Res. Part II Top. Stud. Oceanogr. 43, 1339–1364.

Pornpinatepong, K., Kiripat, S., Treewanchai, S., Chongwilaikasaem, S., Pornsawang, C., Chantarasap, P., Chandee, C., Jantrakul, P., 2010. Pollution conrol and sustainable Fisheries management in Songkhla Lake, Thailand. Research report. Songkhla: Dept. of Economics, Prince of Songkla University. Report No. 2010-RR5.

Pornpinatepong, S., Tanaka, H., Takasaki, M., 2006. Application of 2-D vertically averaged boundary-fitted coordinate model of tidal circulation in Thale Sap Songkhla, Thailand. Walailak J. Sci. Technol. 3, 105–118.

Pradit, S., Pattarathomrong, M. S., Panutrakul, S., 2013. Arsenic cadmium and lead concentrations in sediment and biota from Songkhla Lake: A review. Procedia - Soc. Behav. Sci. 91, 573–580.

Primo de Siqueira, B. V., 2011. Climate Change impacts no mixing and circulation at Songkhla Lagoon, Thailand. Msc Thesis. Delft University of Technology.

Raksawong, S., Krmar, M., Bhongsuwan, T., 2016. Measurement of ^{7}Be inventory in the outer Songkhla lagoon. J. Radioanal. Nucl. Chem. 310, 33–44.

Reed, D. C., Huang, K., Boudreau, B. P., Meysman, F. J. R., 2006. Steady-state tracer dynamics in a lattice-automaton model of bioturbation. Geochim. Cosmochim. Acta 70, 5855–5867.

Schmidt, S., Gonzalez, J.-L., Lecroart, P., Tronczyński, J., Billy, I., Jouanneau, J.-M., 2007. Bioturbation at the water-sediment interface of the Thau Lagoon: impact of shellfish farming. Aquat. Living Resour. 20, 163–169.

Schmidt, S., Howa, H., Diallo, A., Martín, J., Cremer, M., Duros, P., Fontanier, C., Deflandre, B., Metzger, E., Mulder, T., 2014. Recent sediment transport and deposition in the Cap-Ferret Canyon, South-East margin of Bay of Biscay. Deep. Res. Part II Top. Stud. Oceanogr. 104, 134–144.

Schuller, P., Walling, D. E., Iroumé, A., Castillo, A., 2010. Use of beryllium-7 to study the effectiveness of woody trash barriers in reducing sediment delivery to streams after forest clearcutting. Soil Tillage Res. 110, 143–153.

Simsek, F. B., Cagatay, M. N., 2014. Geochronology of lake sediments using ^{210}Pb with double energetic window method by LSC: an application to Lake Van. Appl. Radiat. Isot. 93, 126–33.

Sirinawin, W., Sompongchaiyakul, P., 2005. Nondetrital and total metal distribution in core sediments from the U-Tapao canal, Songkhla, Thailand. Mar. Chem. 94, 5–16.

Sirinawin, W., Turner, D. R., Westerlund, S., Kanatharana, P., 1998. Trace metals study in the Outer Songkla Lake , Thale Sap Songkla , a southern Thai estuary. Mar. Chem. 62, 175–183.

Smith, J. N., Schafer, C. T., 1999. Sedimentation, bioturbation, and Hg uptake in the sediments of the estuary and Gulf of St. Lawrence. Limnol. Oceanogr. 44, 207–219.

Sommerfield, C. K., Nittrouer, C. A., Alexander, C. R., 1999. ^{7}Be as a tracer of flood sedimentation on the northern California continental margin. Cont. Shelf Res. 19, 335–361.

Tanavud, C., Yongchalermchai, C., Sansena, T., 2006. Assessment of soil erosion and sediment deposition in Songkla Lake Basin. Thai J. Soil Fertil. 28, 42–57.

Tanavud, C., Yongchalermchai, C., Bennui, A., Densrisereekul, O., 2001. The expansion of inland shrimp farming and its environmental impacts in Songkla Lake Basin. Kasetsart J (Natural Sci). 35, 326 – 343.

Walling, D. E., 2004. Using environmental radionuclides to trace sediment mobilisation and delivery in river basins as an aid to catchment management. Proc. Ninth Int. Symp. River Sediment. October 18, 121–135.

Wheatcroft, R. A., 2006. Time-series measurements of macrobenthos abundance and sediment bioturbation intensity on a flood-dominated shelf. Prog. Oceanogr. 71, 88–122.

Zhu, J., Olsen, C. R., 2009. Beryllium-7 atmospheric deposition and sediment inventories in the Neponset River estuary , Massachusetts , USA. J. Environ. Radioact. 100, 192–197.

Paper V

SEDIMENTATION RATES IN THE U-TAPAO ESTUARY DEMONSTRATED BY ^{210}Pb-AND ^{137}Cs-DATING METHODS

Santi Raksawong[1], Miodrag Krmar[2], Tripob Bhongsuwan[1*]

[1]*Department of Physics, Faculty of Science, Prince of Songkla University, Thailand*
[2]*Department of Physics, Faculty of Science, University of Novi Sad, Serbia*

*E-mail: tripop.b@psu.ac.th

Published in Proceeding the 4th Academic Conference on Natural Science for Young Scientists, Master & PhD Students from Asean Countries. 15-18 December, 2015 - Bangkok, Thailand, pp.74 – 79 (Online).

Available URL: http://iop.vast.ac.vn/activities/conf_asean/2015/

SEDIMENTATION RATES IN THE U-TAPAO ESTUARY DEMONSTRATED BY ^{210}Pb-AND ^{137}Cs-DATING METHODS

Santi Raksawong[1], Miodrag Krmar[2], Tripob Bhongsuwan[1*]

[1]*Department of Physics, Faculty of Science, Prince of Songkla University, Thailand*
[2]*Department of Physics, Faculty of Science, University of Novi Sad, Serbia*
*E-mail: tripop.b@psu.ac.th

Abstract. The study of sediment dynamics will provide an understanding of the dynamics of pollutants, and aid in developing sustainable effective management. The ^{210}Pb and ^{137}Cs dating techniques have been widely used to reconstruct the sedimentation histories in the lake sediment. In this contribution, we present the preliminary analyses and results of sedimentation rates. One site from U-Tapao estuary located in the Outer Songkhla lagoon, southern Thailand was selected and the vertical profiles of excess ^{210}Pb and ^{137}Cs were used for analyses. The average accumulation rates determined by ^{137}Cs method are 5.7 and 6.5 kg m^{-2} year^{-1} from 1963 to 1986 and 1986 to sampling time, respectively. Moreover, the sediment accumulation rates between 8.8 and 3.3 kg m^{-2} year^{-1} during sampling time to 1954 were obtained by the CIC and CRS models. Two-marker events based on ^{137}Cs activity were used to validate age of sediment layers obtained by ^{210}Pb method.

Keywords. *Songkhla lagoon, ^{210}Pb-dating, ^{137}Cs- dating, Sedimentation rates*

I. INTRODUCTION

Nowadays, the Songkhla lagoon is facing the pollution problems as evidenced by several factors: overall low water quality, contamination by toxic pollutants/nutrients, and rapid sedimentation in some areas [1-9]. Especially, the unsanitary drainage from Hat Yai urban area, and the wastewater from large factories along the U-Tapao canal and its watershed drain into the U-Tapao estuary [6,8-9,10-13]. Therefore, studying the sedimentation dynamics in this area will provide an understanding of the dynamics of pollutants to develop effectively sustainable management. Over the past four decades in the sediment chronology, the ^{210}Pb and ^{137}Cs dating techniques have been widely used to reconstruct the sedimentation histories from a year up to 150 years [14-17].

^{210}Pb is naturally occurring radionuclide of the ^{238}U series. Its closed parent is ^{222}Rn, a noble gas having short half-life, 3.8 days. This gas escapes into the atmosphere from surface soil layers and provides ^{210}Pb with mobility in atmosphere. The ^{210}Pb is introduced into the estuarine environment through atmospheric precipitation, terrestrial runoff and in situ production from ^{226}Ra in the water column and soil or sediment. ^{210}Pb falling directly into the lake is removed quickly to sediments by adsorption process and deposited on the bottom of the lake together with the sediment [18]. Two simple models known as the CIC and CRS models are usually applied. For constant sedimentation rates, the CIC model is the simplest method based on the supply of ^{210}Pb to the sediments which is constant initial concentration [18,19]. Moreover, the CRS model is based on the assumption of the constant rate of supply unsupported ^{210}Pb or $^{210}Pb_{ex}$ to the sediment and insignificant mobility of ^{210}Pb in the sediment column [18]. Sometime, the chronological results provided by the ^{210}Pb-dating models could probably provide less reliable information on sediment accumulation rates. When the researchers need a high level of confidence in chronology, the ^{210}Pb-dating models must always be validated by the ^{137}Cs profile for identifying the peaks corresponding to sediment deposition in 1963 and 1986, or other records of known contaminant inputs [15,18,20].

In this paper, one selected core was taken from the U-Tapao estuary located in the Outer Songkhla lagoon. Results of sedimentation rates are estimated by the vertical profiles of excess ^{210}Pb and ^{137}Cs.

II. METHODOLOGY

Study area

The Outer Songkhla lagoon is located in southern Thailand between latitudes 7^{o} 05’ and 7^{o} 50’ N and longitudes 100^{o} 05’ and 100^{o} 37’ E, a part of the east coast of

the Malay Peninsula. The Outer Songkhla Lagoon is a shallow coastal lagoon with an average depth around 2.0 m in rainy season and 1.5 m in summer season.

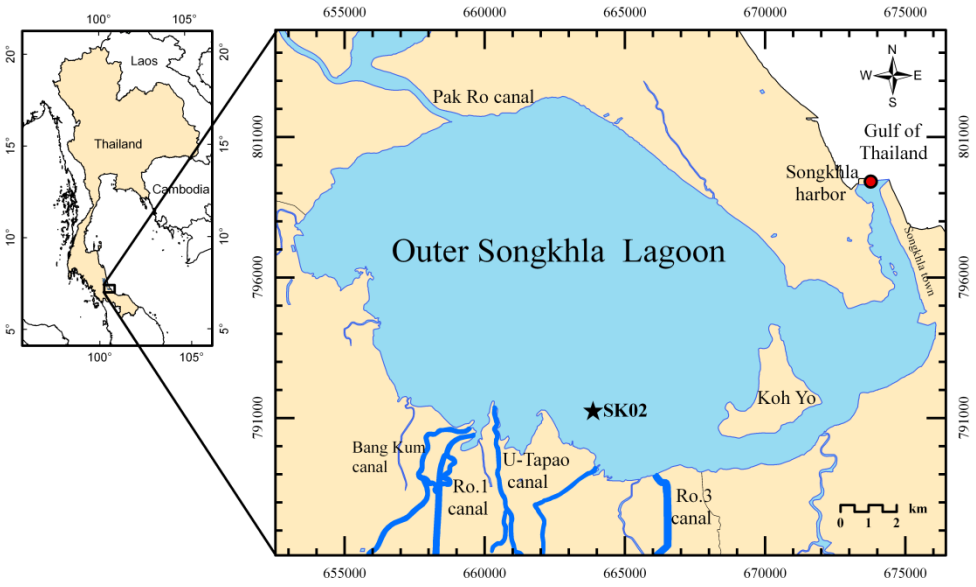

Fig. 1 *study area in the Outer Songkhla lagoon, black star (★) is the location of the collected sediment core*

At the lower east side near the Songkhla harbor and the Songkhla town, it has a deep channel (5 – 12 m depth) connecting the lagoon with the sea of the Gulf of Thailand and allowing the tides to propagate into the lagoon as shown in **Fig.1**. Therefore the aquatic environment in this lagoon is a combination of seawater and freshwater, and the hydrodynamic complexity of this system is mainly controlled by tide, runoff, wind and wave.

Sample preparation and measurements

The sediment core was collected using a hand-operated corer equipped with the PVC tube (8.5 cm internal diameter, 150 cm long). In the laboratory, the sediment core was sliced horizontally at 1.0 cm intervals through its depth using the handheld extruder. All the specimens were dried at 105 °C for 24 hours by electric oven, and grinded by ceramic mortar, and sieved to < 2 mm fraction, homogenized, weighed and put into a polyethylene containers of a similar geometry with the calibration source.

The selected sediment samples at depth layers (2, 4, 6, 8, 10, 14, 18, 24, and 30 cm) were sent to the nuclear laboratory of the Faculty of Sciences, University of Novi Sad, Serbia, to measure the ^{210}Pb activity usinga low background 100% relative efficiency gamma spectrometer at 46.5 keV gamma line. Other sediment samples were measured in the Nuclear Laboratory at the Prince of Songkla University,

Thailand, using a 80% relative efficiency gamma spectrometer coupled with a DSA 1000 multichannel analyzer. Due to a very low activity of ^{137}Cs in sediments, its gamma ray energy 661.6 keV was measured by counting-time periods of minimum 40,000s to maximum 100,000s to provide the lowest reasonable analytical error. The IAEA TEL 2011-03 WWOPT soil sample-04 with known radionuclide activities was used to calculate the relative efficiency of ^{137}Cs at gamma energy line 661.6 keV.

III. RESULTS AND DISCUSSIONS

This paper shows the results of sediment samples from a single core coded SK02 selected for interpretation of two different sedimentation processes. It can be seen that the ^{137}Cs time-markers correspond to the fallout from the Chernobyl nuclear accident in 1986 and the highest atmospheric thermonuclear weapon testing in 1963. Both chronologic markers can be identified as shown in **Fig.2**.

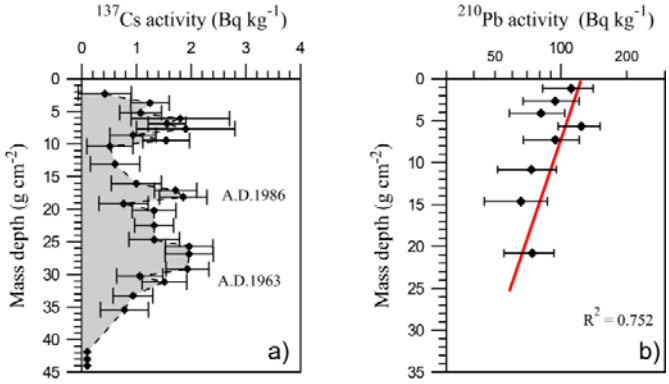

Fig. 2a) *^{137}Cs depth profile,* **b)** *^{210}Pb activity profiles from the Outer Songkhla lagoon. The curve corresponds to those used by the CIC model to estimate sedimentation rate.*

The ^{137}Cs activity in each sediment layers varied between the level of detection limit and 2.1 Bq kg^{-1}. The peak values of ^{137}Cs activity at the mass depths of 18.1 and 31.2 g cm^{-2} correspond to the sedimentation years of A.D.1986 and A.D.1963, respectively. The average accumulation rates calculated in the period from A.D.1963 to 1986 and A.D.1986 till the moment of sampling from those markers are 5.6 kg m^{-2} y^{-1} (linear sedimentation rate 0.52 cm y^{-1}), and 6.7 kg m^{-2} y^{-1} (linear sedimentation rate 0.78 cm y^{-1}), respectively. The previous sedimentation rate of 0.57 cm y^{-1}near the Pak Ro channel, reported by Chittrakarn et al [2] was the result of the ^{137}Cs method.

The ^{210}Pb dating method can be used to estimate the sedimentation rates in this site. The depth distribution of $^{210}Pb_{ex}$ activity shows some regular decreasing trend. It was supposed that the simplest CIC model can be applied in the estimation of sediment mass accumulation at this location. The mean sedimentation rate is 9.62 kg m^{-2} y^{-1}, calculated from the slope of the graph between the logarithmic scale of the $^{210}Pb_{ex}$ activity and mass depth. Moreover, the mass accumulation rates obtained by

the CRS model are between 8.3 and 3.3 kg m^{-2} y^{-1}. The CRS model provides the best result that the marker-peak values of ^{137}Cs are validated as shown in **Fig 3**.

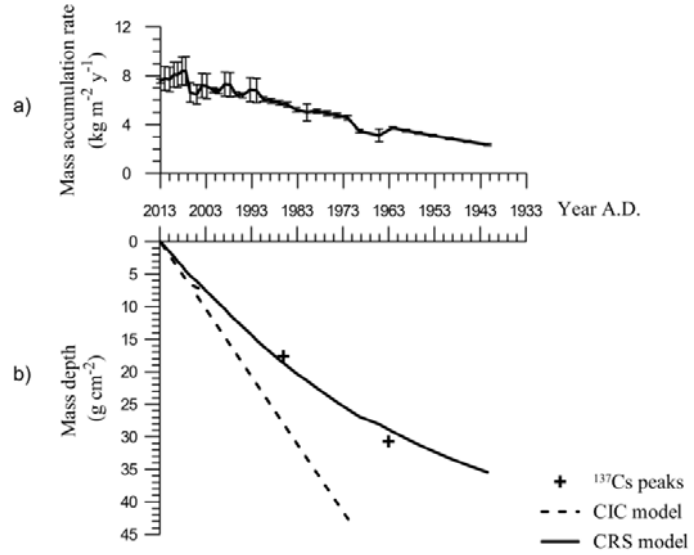

Fig. 3.a) *results obtained by estimating from CIC and CRS models and validated by ^{137}Cs markers,***b)** *comparison between mass accumulation rates obtained from CRS model and ^{137}Cs method*

The mass accumulation rate that provides from dating by CRS model in recent year is high value about 8.0 kg m^{-2} y^{-1} and it gradually decreases. So it indicates that in the past, before 1960s the Songkhla lagoon experienced a low sedimentation rate.

IV. CONCLUSIONS

The mass accumulation rates of the sediment at a selected location in the Outer Songkla lagoon were determined based on both vertical profiles of ^{137}Cs and ^{210}Pb in sediment core. Use of ^{210}Pb-dating models was validated by using fallout of artificial radionuclide ^{137}Cs, that showed a very good correlation between them. Also CRS model indicates that the sedimentation rates show a constant increasing trend with time.

V. ACKNOWLEDGEMENTS

This research was financially supported by the Prince of Songkla University (project code: SCI550111S), the National Research Council of Thailand (project code: SCI560125S), the Physics Department, Geophysics Research Center, Faculty of Science and the graduate fellowship from the Graduate School, Prince of Songkla University. In addition, the first author would like to thank Prince of Songkla University, Graduate Studies Grant and the student exchange program between Prince of Songkla University and University of Novi Sad.

REFERENCES

[1] T. Bhongsuwan and D. Bhongsuwan, *Songklanakarin J. Sci. Technol.*, Vol. **24**, 2002, pp. 89–106.

[2] T. Chittrakarn, T. Bhongsuwan, P. Nunnin, and T. Thong-jerm, "The determination of Sedimentation rate in Songkhla Lake Using Isotopic Technique," Songkhla:Prince of Songkhla University, 2539.

[3] S. Gyawali, K. Techato, S. Monprapussorn, and C. Yuangyai, *Procedia - Soc. Behav. Sci.*, Vol. **91**, 2013, pp. 556–563.

[4] K. Kitbamroong, P. Sompongchaiyaku, and G. Padmanabhan, *J. Appl. Sci.*, Vol. **9**, 2009, pp. 2519–2531.

[5] R. Ladachart, C. Suthirat, K. Hisada, and P. Charusiri, *J. Appl. Sci.*, Vol. **11**, 2011, pp. 3117–3129.

[6] K. Pornpinatepong, S. Kiripat, S. Treewanchai, S. Chongwilaikasaem, C. Pornsawang, P. Chantarasap, C. Chandee, and P. Jantrakul, "Pollution conrol and sustainable fisheries management in Songkhla Lake, Thailand," Songkhla:Prince of Songkhla University, 2010.

[7] S. Pradit, M. S. Pattarathomrong, and S. Panutrakul, *Procedia - Soc. Behav. Sci.*, Vol. **91**, 2013, pp. 573–580.

[8] W. Sirinawin, D. R. Turner, S. Westerlund, and P. Kanatharana, *Mar. Chem.*, Vol. **62**, 1998, pp. 175–183.

[9] W. Sirinawin and P. Sompongchaiyakul, *Mar. Chem.*, Vol. **94**, 2005, pp. 5–16.

[10] S. Angsupanich and R. Kuwabara, *Lakes Reserv. Res. Manag.*, Vol. **4**, 1999, pp. 1–13.

[11] P. Chevakidagarn, *Songklanakarin J. Sci. Technol.*, Vol. **28**, 2006, pp. 633–639.

[12] S. Maneepong, *SongklanakarinJ. Sci. Technol.*, Vol. **18**, 1996, pp. 87 – 97.

[13] S. Maneepong and S. Angsupanich, *Songklanakarin J. Sci. Technol.*, Vol. **21**, 1999, pp. 111 – 121.

[14] Y. S. Ahn, F. Nakamura, and K. W. Chun, *Geomorphology*, Vol. **114**, 2010, pp. 284–293.

[15] M. Baskaran, J. Nix, C. Kuyper, and N. Karunakara, *J. Environ. Radioact.*,Vol. **138**, 2014, pp. 355–363.

[16] J. O' Reilly, L. L. Vintró, P. I. Mitchell, I. Donohue, M. Leira, W. Hobbs, and K. Irvine, *J. Environ. Radioact.*, Vol. **102**, 2011, pp. 495–499.

[17] S. P. Rai, V. Kumar, and B. Kumar, *Hydrol. Sci. J.*, Vol. **52**, 2007, pp. 181–191.

[18] P. G. Appleby, "Chronostratigraphic techniques inrecent sediments," in *Tracking Environmental Change Using Lake Sediments. Vollume 1: Basin Analysis, Coring, and Chronological Techniques*, vol. 1, W. M. Last and J. P. Smol, Eds. Dordrecht, The Netherlands: Kluwer Academic Publishers, 2001, pp. 171–203.

[19] S. C. Yao, S. J. Li, and H. C. Zhang, *J. Radioanal. Nucl. Chem.*, Vol. **278**, 2008, pp. 55–58.

[20] J. M. Abril, *J. Paleolimnol.*, Vol. **30**, 2003, pp. 407–414.

CURRICULUM VITAE

Name **Mr. Santi Raksawong**

Student **5510230015**

Educational Attainment

Degree	Name of Institution	Year of Graduation
B.Sc (Physics)	Prince of Songkla University	2003
M.Sc (Physics)	Prince of Songkla University	2008

Scholarship Awards during Enrolment

1. Grant of the Prince of Songkla University Graduate Studies
2. Grant of the student exchange program between Prince of Songkla University and University of Novi Sad, Serbia
3. Teaching assistance in Department of Physics

List of Publication and Proceeding

Raksawong, S., Krmar, M., Bhongsuwan, T. (2016) Measurement of ^{7}Be inventory in the outer Songkhla lagoon, Thailand. Journal of Radioanalytical and Nuclear Chemistry. 310, 33-44.

Raksawong, S., Bhongsuwan, T. (2016) The ^{7}Be profile in the undisturbed soil used for reference site to estimate the soil erosion. Proceedings of the international Nuclear Science and Technology Conference (INST 2016), Bangkok.

Raksawong, S., Krmar, M., Bhongsuwan, T. (2015) Sedimentation rates in the U-Tapao estuary demonstrated by ^{210}Pb- and ^{137}Cs- dating methods. Proceedings of the 4th Academic Conference on Natural Science for Young Scientists, Master and Ph D students from ASEAN Countries, Bangkok, 74-79.

Raksawong, S., Krmar, M., Bhongsuwan, T. (2016) Using ^{210}Pb dating method to extrapolate sedimentary geochronology and sedimentation rates in the outer Songkhla lagoon. Abstract of the 7th international conference on Applied Geophysics, Bangkok.